Neutral Current Supernova Neutrino-Nucleus Scattering off ^{127}I and ^{133}Cs

Master's Thesis, 27.07.2020

Author:

Matti Hellgren

Supervisor:

Prof. Jouni Suhonen

JYVÄSKYLÄN YLIOPISTO
FYSIIKAN LAITOS

Preface

I would like to sincerely thank my supervisor, Professor Jouni Suhonen for not only providing an interesting and challenging topic for this thesis, but also for his guidance throughout the writing process. I would also like to extend my gratitude to Dr. Pekka Pirinen for his assistance related to the various computer programs utilized in this work, and for his patience for answering the many questions I had regarding them.

With that being said, there is little else for me to say about this thesis. While some might consider brevity uncharacteristic of me, I will keep at least one section of this document short and let the work speak for itself.

Matti Hellgren

Abstract

The scattering of astrophysical neutrinos off the stable Iodine and Caesium nuclei ^{127}I and ^{133}Cs was studied to explore the possibility of utilizing them in neutrino detection. The reactions considered in this work were elastic and inelastic weak neutral current neutrino-nucleus and antineutrino-nucleus scatterings. The neutrinos that were included were of the e-flavour and had their origin in supernova core collapse events. The theoretical formalism of semileptonic neutrino-nucleus processes was reviewed in great detail, and several key equations were derived meticulously. The primary quantity of interest was the scattering cross section.

The model used for the description of the two odd-A nuclei of interest was the MQPM, which is built upon the BCS model and QRPA. MQPM was thus applied to the odd-A nuclei by first performing the BCS and QRPA calculations on even-even reference nuclei (^{126}Te, ^{128}Xe, ^{132}Xe and ^{134}Ba) adjacent to the odd-A nuclei, and then using these results to run the MQPM calculations for the odd-A nuclei. The nuclear model provided the eigenfunctions and -energies of the nuclei and the reduced neutral current one-body transition densities which entered into the cross section calculations. The ultimate results of this thesis were the energy averaged total cross sections, which were obtained by integrating the double differential cross section over the angular coordinates, summing over all possible final nuclear states and folding the cross section with the neutrino energy spectrum. The neutrino energy spectrum used was a modified two-parameter thermal Fermi-Dirac distribution.

The resulting theoretical QRPA spectra were in decent agreement with experimental results, while the MQPM spectra had some discrepancies, particularly at the low-energy end. These had minimal effect on the cross sections, which were found to be in line with earlier similar calculations. Overall, the results were cautiously optimistic, but preliminary. Nothing in them outright implied that the nuclei considered would not be fit for neutrino detection, but further studies are needed for an exhaustive assessment of their suitability for such a role.

Tiivistelmä

Tutkielmassa tarkasteltiin astrofysikaalisten neutriinojen sirontaa stabiileista jodi- ja caesium ytimistä ^{127}I and ^{133}Cs, tarkoituksena arvioida kyseisten ytimien hyödyntämisen mahdollisuutta neutriinojen havaitsemisessa. Työssä käsiteltävät reaktiot koostuivat elastisista ja epäelastisista heikon neutraalin virran neutriino-ydin ja antineutriino-ydin sironnoista. Reaktioihin osallistuvina neutriinoina käytettiin supernovaräjähdyksissä alkunsa saaneita elektronin neutriinoja. Semileptonisten neutriino-ydin prosessien teoreettinen formalismi käytiin yksityiskohtaisesti läpi, ja keskeisimmät yhtälöt johdettiin tarkasti. Työn kannalta oleellisin suure oli sironnan vaikutusala.

Työssä tarkasteltujen parittoman massaluvun ytimien mallintamisessa käytetty malli oli MQPM, joka itsessään rakentuu BCS-mallin ja QRPA:n päälle. MQPM:n soveltaminen parittoman massaluvun ytimien mallintamiseen tapahtui siten tekemällä ensiksi BCS- ja QRPA-laskut parittomien ytimien vieressä oleville parillis-parillisille referenssiytimille (^{126}Te, ^{128}Xe, ^{132}Xe and ^{134}Ba), ja käyttämällä näistä saatuja tuloksia haluttujen MQPM-laskujen tekemiseen. Valitusta ydinmallista saatiin ytimien tilojen aaltofunktiot ja näitä vastaavat energiat, sekä redusoidut neutraalin virran yhden kappaleen siirtymätiheydet, joita käytettiin vaikutusalojen laskemisessa. Työn lopullisina tuloksina olivat energiakeskiarvoistetut kokonaisvaikutusalat, jotka saatiin integroimalla kaksoisdifferentiaalinen vaikutusala kulmakoordinaattien yli, summaamalla ytimen kaikkien mahdollisten lopputilojen yli, ja integroimalla lopuksi saatu vaikutusala ja neutriinojen energiaspektri energian yli. Neutriinojen energiaspektrille käytettiin muunnettua termistä kahden parametrin Fermi-Dirac jakaumaa.

Tuloksina saatujen QRPA-spektrien yhteensopivuus vastaavien kokeellisten spektrien kanssa oli kohtalainen, kun taas MQPM-spektreissä oli muutamia poikkeavuuksia, erityisesti spektrien matalaenergiapäässä. Näillä oli minimaalinen vaikutus vaikutusaloihin, joiden tulokset olivat verrattavissa aiempien vastaavanlaisten tutkimuksien tulosten kanssa. Kaiken kaikkiaan saatuihin tuloksiin voidaan suhtautua varovaisen optimistisesti, vaikka ne ovatkin tutkimuskysymyksen kannalta preliminäärisiä. Mikään tuloksissa ei suoranaisesti viitannut siihen, että tutkittuja ytimiä ei voitaisi

käyttää neutriinojen havaitsemisessa, mutta aiheeseen liityville jatkotutkimuksille on tarvetta, jotta kysymykseen voidaan vastata tyhjentävästi.

Contents

1 Introduction

A supernova event is the final stage in the stellar evolution of a massive star. Categorized as a cataclysmic variable, a supernova consists of a violent explosion that takes place after the silicon burning stage, leaving behind a neutron star or a black hole if the event does not destroy the star altogether[1]. Supernovae are some of the most notable astrophysical events that occur in the universe and an active area of research for a variety of reasons. While they are perhaps best known as a major contributor to the abundances of heavy elements in the universe, supernova explosions also release a considerable amount of energy, some in the form of visible light, which together with their transient nature has made them influential in the history of astronomy[1].

A considerable fraction of the energy released in a supernova is radiated in the form of neutrinos, that are created in the many nuclear reactions that occur during the explosion. As neutrinos have a mean free path in matter that is most conveniently measured in light years[3], most of them reach earth unobstructed. This creates an opportunity to study the conditions inside a star during a supernova explosion by measuring the properties of the emitted neutrinos. There are also a number of open questions regarding neutrinos themselves, such as the value of their rest mass[4], the details of CP violation in the lepton sector of the Standard Model[5] and their possible Majorana character[6], and research into astrophysical neutrinos can help shed light into them as well. The drawback of the neutrinos being hardly impeded by matter at all is that detecting them on earth is extremely difficult, requiring enormous facilities designed for this purpose that are capable of detecting only a tiny fraction of the total number of neutrinos passing through[7].

The detection of neutrinos is based on them interacting with matter via weak interaction. In particular, a neutrino scattering off a nucleus by the exchange of an intermediate vector boson can leave the nucleus in an excited state. The subsequent decay of this excited state can then be observed by the detection of the decay

[1] SN1572 and SN1604 provided counter-evidence against the static Aristotelian model of the universe[2].

products. Atomic nuclei can therefore be used to indirectly detect neutrinos through neutrino-nucleus scattering. The question of which nuclei would be fit for such use is then of high importance. Nuclei chosen for detectors should have a sufficiently high neutrino scattering cross sections to maximize the number of reactions. As the timescales in experiments where neutrinos are detected can be of the order of months, the nuclei should also be stable enough that their natural radioactive decay does not interfere with the measurements considerably and create false positives. While there are several other properties of the nuclei that need to be considered (such as price, availability of the desired isotopes and chemical properties of the elements), these are the most important from a nuclear physics perspective.

In this thesis we explore the possibility of using the only stable isotopes of Iodine and Caesium, namely ^{127}I and ^{133}Cs, in supernova neutrino detection by calculating the weak neutral current neutrino-nucleus scattering cross section. The nuclear model chosen to describe the nuclei of interest was the microscopic quasiparticle-phonon model (MQPM)[8], a model based on BCS quasiparticles[9] and QRPA phonons[10]. MQPM is applied to an odd-A nucleus by first selecting an adjacent even-even nucleus as a reference nucleus, and then performing the BCS and QRPA calculations on it. The generated BCS quasiparticles and QRPA phonons are then used to construct the quasiparticle-phonon states for the odd-A nucleus[8]. For the odd-A nuclei considered in this thesis, all adjacent even-even nuclei (^{126}Te, ^{128}Xe, ^{132}Xe and ^{134}Ba) were utilized as reference nuclei, i.e. both reference nuclei candidates for both odd-A nuclei were used. The details of these nuclear models are presented in section 2, along with a detailed review of the theory behind neutrino-nucleus scattering.

In section 3 we present the results of the calculations of this thesis. These include the QRPA spectra of the reference nuclei, the MQPM spectra of the odd-A nuclei and the energy averaged total cross sections of the scattering reactions. The acquired results are analyzed and, in the case of the energy spectra, their agreement with measurements assessed using experimental data, while the theoretical cross sections are merely compared with results of similar earlier calculations due to the absence of experimental results. In the same section we also provide a brief overview on the conditions inside a star undergoing a supernova explosion, focusing on the role of neutrinos and what reactions generate them. In particular, we are interested in the shape of their energy distribution as supernova neutrinos are emitted with a wide range of energies, which is a fact that needs to be taken into account when

computing the total cross sections of the scatterings. Finally, in section 4 we discuss the conclusions drawn from the results and suggestions of possible topics for further research on the subject.

2 Theory

In this section we will present the theoretical framework that was used to describe the phenomena relevant to this thesis. The theory could be divided into the particle physics part, focused mainly on semileptonic nuclear processes and the cross sections of the scattering reactions, and the nuclear physics part, composed of general nuclear theory and specific nuclear models that were used in this work. Despite this, we have divided this section into three subsections instead of two. In the first, our goal is to derive an equation for the double differential cross section of the scattering process. In the second, we will discuss the nuclear physics of this thesis and how it enters into the cross section calculations. In the third and final part we combine the results of the previous two parts for an expression for the aforementioned cross section in terms of parameters that we can input into the calculations, and quantities that arise from the nuclear model used to construct the eigenstates and -energies of the nuclei of interest.

2.1 Semileptonic neutrino reactions

We will first consider the general phenomenology of neutrino-nucleus scattering. Our starting point will be the couplings between the weak intermediate vector boson fields and the lepton and nuclear fields. We will build the Hamiltonian of the scattering process from these and utilize a standard formalism of semileptonic nuclear processes to arrive at an expression for the double differential reaction cross section in terms of spherical tensor multipole operators. Throughout this section, we will be working on the nuclear level. That is, the quark degrees of freedom inside nucleons will be omitted and the nucleons will be treated as point-like particles. Their internal structure is taken into account in later sections.

2.1.1 Reaction basics and lepton fields

In the following we will consider the scattering events due to weak interaction between low-energy astrophysical (anti)neutrinos and target nuclei. Both weak neutral- and charged-currents will be discussed. The processes of interest can be represented by

$$l + N(A,Z) \rightarrow l' + N'(A,Z'), \tag{1}$$

where l and l' are the incoming and outgoing leptons with four momenta k_μ and k'_μ, and $N(A,Z)$ and $N'(A,Z')$ the incoming and outgoing nuclei (with mass number A, proton numbers Z and Z' and four momenta K_μ and K'_μ) respectively. These type of processes are mediated by the exchange of intermediate vector bosons $W^\pm$ and Z^0. These gauge boson fields couple to charge changing ($\mathcal{J}_\mu^{(\pm)}$) and neutral ($\mathcal{J}_\mu^{(0)}$) weak lepton and nuclear fields through the interaction Lagrangian density[11, Chapter 42]

$$\mathcal{L}_I(x) = \frac{g}{2\sqrt{2}}\left[\mathcal{J}_\mu^{(-)}W_\mu^+ + \mathcal{J}_\mu^{(+)}W_\mu^-\right] + \frac{g}{2\cos\theta_W}\mathcal{J}_\mu^{(0)}Z_\mu^0 \quad (= -\mathcal{H}_I(x)), \tag{2}$$

where g is a dimensionless coupling constant and θ_W the Weinberg angle. The basic vertices associated with the couplings in the above Lagrangian density are illustrated in figure 1. These basic vertices can be used to construct the Feynman diagram of the second order process where a lepton and a nucleon interact through an exchange of an intermediate boson, which is presented in figure 2. The four momentum transfer associated with the reaction can be seen from the figure to be $q_\mu = k'_\mu - k_\mu = K_\mu - K'_\mu$. The S-matrix of the process, which consists of the lepton and hadron currents $j_\mu(\boldsymbol{x})$ and $\mathcal{J}_\mu(\boldsymbol{x})$ and the gauge boson propagator, can be derived from the above Lagrangian density together with the Feynman rules of the electroweak theory[12, Appendix B]. Instead of dealing with the gauge boson propagator, it is convenient to consider the case when $q_\mu q^\mu \ll M_B^2$, that is, when the transferred four-momentum is small compared to the gauge boson ($B = W,Z$) mass. In this case the gauge boson propagator reduces to[12, Page 507]

$$\frac{-i(g_{\mu\nu} - \frac{q_\nu q_\mu}{M_B^2})}{q_\mu q^\mu - M_B^2 + i\epsilon} \approx \frac{ig_{\mu\nu}}{M_B^2}, \tag{3}$$

and the exchange of a gauge boson reduces to a point-like current-current interaction between a lepton and a nucleon. We can now define an effective Hamiltonian density

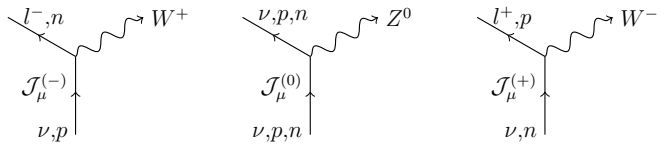

Figure 1. The basic vertices of the couplings associated with the Lagrangian density of equation 2 between the charge changing ($\mathcal{J}_\mu^{(\pm)}$) and neutral ($\mathcal{J}_\mu^{(0)}$) weak lepton and nuclear fields, and the intermediate vector bosons ($W^\pm$ and Z^0)[11, Chapter 42]. The nucleons (p and n) are taken to be point-like particles without internal structure. The quark degrees of freedom are taken into account later in the form of nuclear form factors.

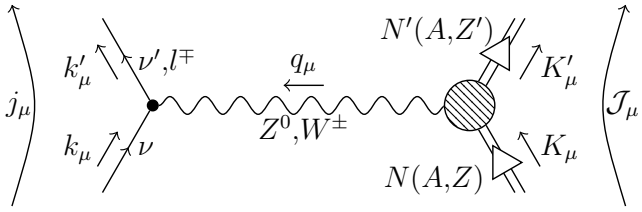

Figure 2. Feynman diagram illustrating the interaction between an uncharged lepton (ν) and an atomic nucleus ($N(A,Z)$) through the exchange of an intermediate vector boson (Z^0 or $W^\pm$). The outgoing lepton is uncharged in neutral current reactions and charged in charged current reactions, with a charge opposite to that of the exchanged vector boson. The lepton (j_μ) nuclear ($\mathcal{J}_\mu$) currents are also present to illustrate the connection to the effective current-current Hamiltonian of equation 6.

$$\mathcal{H}_{\text{eff}}(\boldsymbol{x}) = \frac{G}{\sqrt{2}} j_\mu(\boldsymbol{x}) \mathcal{J}^\mu(\boldsymbol{x}). \tag{4}$$

where

$$\frac{G}{\sqrt{2}} = \frac{g^2}{8M_W^2} = \frac{g^2}{8M_Z^2 \cos^2\theta_W}, \tag{5}$$

which reproduces the S-matrix of the process of figure 2 at the low momentum transfer limit when it is treated in the lowest order.

The effective Hamiltonian operator $\hat{H}_{\text{eff}}$ operating on the Hilbert spaces of the nucleus and the free lepton is acquired by integrating over the spatial coordinates

$$\hat{H}_{\text{eff}} = \int \mathcal{H}_{\text{eff}}(\boldsymbol{x}) \mathrm{d}^3\boldsymbol{x} = \frac{G}{\sqrt{2}} \int j_\mu(\boldsymbol{x}) \mathcal{J}^\mu(\boldsymbol{x}) \mathrm{d}^3\boldsymbol{x}. \tag{6}$$

Using this, we get for the Hamiltonian matrix elements between states

$$H_{fi} = \langle f| \hat{H}_{\text{eff}} |i\rangle = \int \langle f| \mathcal{H}_{\text{eff}} |i\rangle \, \mathrm{d}^3\boldsymbol{x} = \frac{G}{\sqrt{2}} \int \langle f| j_\mu(\boldsymbol{x}) |i\rangle \langle f| \mathcal{J}^\mu(\boldsymbol{x}) |i\rangle \, \mathrm{d}^3\boldsymbol{x}. \quad (7)$$

After specifying the interaction Hamiltonian matrix elements of the system, the rate of the reaction can be determined through Fermi's golden rule. The transition rate w from initial state i to final state f is given by[13, Chapter 5.7]

$$w(i \to f) = 2\pi |H_{fi}|^2 \delta(E_f - E_i), \quad (8)$$

where this expression is understood to be integrated over the density of states

$$\rho(E_f) = \frac{\mathrm{d}n}{\mathrm{d}E_f}. \quad (9)$$

The nucleus is extremely heavy compared to the incoming leptons and its recoil energy will be neglected. The density of states for a box-normalized plane wave in 3D k-space is known to be[14, Chapter 3]

$$\rho(\boldsymbol{k}') = V \frac{\mathrm{d}^3\boldsymbol{k}'}{(2\pi)^3} = \frac{V}{(2\pi)^3} (k')^2 \mathrm{d}k' \mathrm{d}\Omega, \quad (10)$$

where V is the volume of the box. The rightmost equality of equation 10 follows from approximating the variable $\boldsymbol{k}'$ as continuous and transforming to spherical coordinates in k-space. Now using the fact that $E_{k'} \mathrm{d}E_{k'} = k' \mathrm{d}k'$ we get

$$\rho(\boldsymbol{k}') = \frac{V}{(2\pi)^3} (k')^2 \mathrm{d}k' \mathrm{d}\Omega = \frac{V}{(2\pi)^3} k' E_{k'} \mathrm{d}E_{k'} \mathrm{d}\Omega = \rho(E_{k'}) = \rho(E_f). \quad (11)$$

Integrating the transition rate over this with respect to energy now yields

$$\begin{aligned} &w(i \to f) = \int_0^\infty 2\pi |H_{fi}|^2 \delta(E_f - E_i) \frac{V}{(2\pi)^3} k' E_{k'} \mathrm{d}E_{k'} \mathrm{d}\Omega = \\ &\frac{V}{(2\pi)^2} \int_0^\infty |H_{fi}|^2 \delta(E_{K'} + E_{k'} - E_K - E_k) k' E_{k'} \mathrm{d}E_{k'} \mathrm{d}\Omega = \frac{k' E_{k'}}{(2\pi)^2} V |H_{fi}|^2 \mathrm{d}\Omega. \end{aligned} \quad (12)$$

The scattering cross section σ in an experimental setting is defined as[15, Page 89]

$$\sigma = \frac{W_r(i \to f)}{J_\nu N_N} = \frac{\overline{w}(i \to f)}{J_\nu}, \quad (13)$$

where $W_r(i \to f)$ is the number of reactions/unit time, $\overline{w}$ is w integrated over the angular coordinates, N_N the number density of the target particles and J_ν the flux of the incoming particles. The flux is defined as the product of the velocity v_ν of the incoming particles and their number density N_ν. Now considering we have $v_\nu = c = 1$ and $N_\nu = 1/V$, we get $J_\nu = 1/V$. The differential of the cross section is thus

$$\mathrm{d}\sigma = \frac{w(i \to f)}{J_\nu} = \frac{k' E_{k'}}{(2\pi)^2} V |H_{fi}|^2 \frac{1}{1/V} \mathrm{d}\Omega = \frac{k' E_{k'}}{(2\pi)^2} V^2 |H_{fi}|^2 \mathrm{d}\Omega \tag{14}$$

and the differential cross section

$$\frac{\mathrm{d}\sigma}{\mathrm{d}\Omega} = \frac{k' E_{k'}}{(2\pi)^2} V^2 |H_{fi}|^2. \tag{15}$$

To actually apply the above equation, the matrix elements of the nuclear and lepton currents between the states need to be determined. We will next consider the lepton current first, as it is relatively simple, consisting of couplings between point-like Dirac particles that do not experience the often troublesome strong interaction.

Lepton fields can be treated mathematically as quantized Dirac fields normalized to a box of volume V. The field operator $\psi(x)$ is then given by[11, Page 431]

$$\psi(x) = \frac{1}{\sqrt{V}} \sum_{\boldsymbol{p}\lambda} \left[a_{\boldsymbol{p}\lambda} u(\boldsymbol{p}\lambda) e^{i\boldsymbol{p}\cdot\boldsymbol{x}} + b^\dagger_{\boldsymbol{p}\lambda} v(-\boldsymbol{p}\lambda) e^{-i\boldsymbol{p}\cdot\boldsymbol{x}} \right], \tag{16}$$

where $a_{\boldsymbol{p}\lambda}$ is the lepton annihilation and $b^\dagger_{\boldsymbol{p}\lambda}$ the antilepton creation operator, λ the helicity quantum number and u and v the Dirac spinors for a lepton and an antilepton respectively. Leptons in the weak Hamiltonian couple through the vector (γ_μ) and axial vector ($\gamma_\mu\gamma_5$) forms, which lead to the lepton current[11, Chapter 42]

$$j_\mu(\boldsymbol{x}) = \overline{\psi}_{l'} \gamma_\mu (1 - \gamma_5) \psi_l, \tag{17}$$

where the adjoint $\overline{\psi}$ is defined as $\overline{\psi} = \psi^\dagger \gamma^0$. The complete state s of the system consists of the nuclear state of a definite angular momentum quantum numbers J_s and M_s, and the free lepton state of momentum $\boldsymbol{k}_s$

$$|s\rangle = |n_s J_s M_s\rangle \, |\boldsymbol{k}_s \lambda_s\rangle \, . \tag{18}$$

The n_s in the above expression is used to denote the rest of the quantum numbers

required to completely specify the quantum state of the nucleus. The lepton current operator of equation 17 operates only on the lepton part of the state of the system so we can ignore the nuclear part of equation 18 for now. For the reaction of equation 1 involving neutrinos we now get

$$\langle f|\, j_\mu(\boldsymbol{x})\,|i\rangle = \langle \boldsymbol{k}'\sigma'|\,\overline{\psi}_{l'}\gamma_\mu(1-\gamma_5)\psi_l\,|\boldsymbol{k}\sigma\rangle = \frac{1}{V}\sum_{\substack{\boldsymbol{p}',\boldsymbol{p}\\ \lambda',\lambda}} \langle 0|\, a_{\boldsymbol{k}'\sigma'}\Big[a^\dagger_{\boldsymbol{p}'\lambda'}u^\dagger(\boldsymbol{p}'\lambda')e^{-i\boldsymbol{p}'\cdot\boldsymbol{x}} +$$
$$b_{\boldsymbol{p}'\lambda'}v^\dagger(-\boldsymbol{p}'\lambda')e^{i\boldsymbol{p}'\cdot\boldsymbol{x}}\Big]\gamma^0\gamma_\mu(1-\gamma_5)\Big[a_{\boldsymbol{p}\lambda}u(\boldsymbol{p}\lambda)e^{i\boldsymbol{p}\cdot\boldsymbol{x}} + b^\dagger_{\boldsymbol{p}\lambda}v(-\boldsymbol{p}\lambda)e^{-i\boldsymbol{p}\cdot\boldsymbol{x}}\Big]a^\dagger_{\boldsymbol{k}\sigma}\,|0\rangle\,. \tag{19}$$

The above expression essentially consists of four terms that are proportional to the vacuum expectation values of $a_{\boldsymbol{k}'\sigma'}a^\dagger_{\boldsymbol{p}'\lambda'}a_{\boldsymbol{p}\lambda}a^\dagger_{\boldsymbol{k}\sigma}$, $a_{\boldsymbol{k}'\sigma'}a^\dagger_{\boldsymbol{p}'\lambda'}b^\dagger_{\boldsymbol{p}\lambda}a^\dagger_{\boldsymbol{k}\sigma}$, $a_{\boldsymbol{k}'\sigma'}b_{\boldsymbol{p}'\lambda'}a_{\boldsymbol{p}\lambda}a^\dagger_{\boldsymbol{k}\sigma}$ and $a_{\boldsymbol{k}'\sigma'}b_{\boldsymbol{p}'\lambda'}b^\dagger_{\boldsymbol{p}\lambda}a^\dagger_{\boldsymbol{k}\sigma}$. The second and the third of these obviously vanish, as they have a different number of creation and annihilation operators for both types of particles. The fourth would lead to a delta function term of $\delta_{\boldsymbol{k}'\boldsymbol{k}}\delta_{\sigma'\sigma}$, which would correspond to the case where the lepton is in the same state both before and after the scattering, meaning that no scattering would take place. Thus only the first of these terms contribute and equation 19 reduces to

$$\langle f|\, j_\mu(\boldsymbol{x})\,|i\rangle = \frac{1}{V}\sum_{\substack{\boldsymbol{p}',\boldsymbol{p}\\ \lambda',\lambda}} \langle 0|\, a_{\boldsymbol{k}'\sigma'}\Big[a^\dagger_{\boldsymbol{p}'\lambda'}u^\dagger(\boldsymbol{p}'\lambda')e^{-i\boldsymbol{p}'\cdot\boldsymbol{x}}\Big]\gamma^0\gamma_\mu(1-\gamma_5)\Big[a_{\boldsymbol{p}\lambda}u(\boldsymbol{p}\lambda)e^{i\boldsymbol{p}\cdot\boldsymbol{x}}\Big]a^\dagger_{\boldsymbol{k}\sigma}\,|0\rangle$$
$$= \frac{1}{V}\sum_{\substack{\boldsymbol{p}',\boldsymbol{p}\\ \lambda',\lambda}} \overline{u}(\boldsymbol{p}'\lambda')\gamma_\mu(1-\gamma_5)u(\boldsymbol{p}\lambda)\,\langle 0|\, a_{\boldsymbol{k}'\sigma'}a^\dagger_{\boldsymbol{p}'\lambda'}a_{\boldsymbol{p}\lambda}a^\dagger_{\boldsymbol{k}\sigma}\,|0\rangle\, e^{-i(\boldsymbol{p}'-\boldsymbol{p})\cdot\boldsymbol{x}} = \frac{1}{V}\sum_{\substack{\boldsymbol{p}',\boldsymbol{p}\\ \lambda',\lambda}} \overline{u}(\boldsymbol{p}'\lambda')\gamma_\mu\cdot$$
$$(1-\gamma_5)u(\boldsymbol{p}\lambda)\delta_{\boldsymbol{k}'\boldsymbol{p}'}\delta_{\sigma'\lambda'}\delta_{\boldsymbol{k}\boldsymbol{p}}\delta_{\sigma\lambda}e^{-i(\boldsymbol{p}'-\boldsymbol{p})\cdot\boldsymbol{x}} = \frac{1}{V}\overline{u}(\boldsymbol{k}'\sigma')\gamma_\mu(1-\gamma_5)u(\boldsymbol{k}\sigma)e^{-i(\boldsymbol{k}'-\boldsymbol{k})\cdot\boldsymbol{x}} =$$
$$\frac{1}{V}\overline{u}(\boldsymbol{k}'\sigma')\gamma_\mu(1-\gamma_5)u(\boldsymbol{k}\sigma)e^{-i\boldsymbol{q}\cdot\boldsymbol{x}} \equiv \frac{1}{V}\overline{u}(\boldsymbol{k}')\gamma_\mu(1-\gamma_5)u(\boldsymbol{k})e^{-i\boldsymbol{q}\cdot\boldsymbol{x}}, \tag{20}$$

where we have dropped the spin quantum numbers σ' and σ, since they will be summed over later. In a similar manner, for the reaction involving antineutrinos we get

$$\langle f|\, j_\mu(\boldsymbol{x})\,|i\rangle = \frac{1}{V}\overline{v}(-\boldsymbol{k})\gamma_\mu(1-\gamma_5)v(\boldsymbol{k}')e^{-i\boldsymbol{q}\cdot\boldsymbol{x}}. \tag{21}$$

Based on these results, we can write the lepton current matrix elements as

$$\langle f|\, j_\mu(\boldsymbol{x})\,|i\rangle = l_\mu e^{-i\boldsymbol{q}\cdot\boldsymbol{x}} = (l_0, -\boldsymbol{l})e^{-i\boldsymbol{q}\cdot\boldsymbol{x}}, \tag{22}$$

where

$$l_\mu = \frac{1}{V}\cdot\begin{cases}\overline{u}(\boldsymbol{k}')\gamma_\mu(1-\gamma_5)u(\boldsymbol{k}), \text{ for neutrino reactions,}\\ \overline{v}(-\boldsymbol{k})\gamma_\mu(1-\gamma_5)v(\boldsymbol{k}'), \text{ for antineutrino reactions.}\end{cases} \tag{23}$$

The nuclear current can be written in a similar fashion

$$\begin{aligned}&\langle f|\,\mathcal{J}_\mu(\boldsymbol{x})\,|i\rangle = \langle f|\,(\mathcal{J}_0(\boldsymbol{x}), -\boldsymbol{\mathcal{J}}(\boldsymbol{x}))\,|i\rangle = (\langle f|\,\mathcal{J}_0(\boldsymbol{x})\,|i\rangle\,, -\langle f|\,\boldsymbol{\mathcal{J}}(\boldsymbol{x})\,|i\rangle) \equiv\\ &(\mathcal{J}_0(\boldsymbol{x})_{fi}, -\boldsymbol{\mathcal{J}}(\boldsymbol{x})_{fi})\end{aligned} \tag{24}$$

to express the effective Hamiltonian as

$$H_{fi} = \frac{G}{\sqrt{2}}\int l_\mu e^{-i\boldsymbol{q}\cdot\boldsymbol{x}}\begin{pmatrix}\mathcal{J}_0(\boldsymbol{x})_{fi}\\ \boldsymbol{\mathcal{J}}(\boldsymbol{x})_{fi}\end{pmatrix}\mathrm{d}^3\boldsymbol{x} = \frac{G}{\sqrt{2}}\int e^{-i\boldsymbol{q}\cdot\boldsymbol{x}}\left[l_0\mathcal{J}_0(\boldsymbol{x})_{fi} - \boldsymbol{l}\cdot\boldsymbol{\mathcal{J}}(\boldsymbol{x})_{fi}\right]\mathrm{d}^3\boldsymbol{x}. \tag{25}$$

2.1.2 Plane wave decomposition in vector spherical harmonics

To proceed further, it is convenient to first expand the plane wave factor in equation 25 in terms of spherical harmonics. For this, we will define a spherical basis[13, Chapter 3.11] by first defining a Cartesian basis with unit vectors $\mathbf{e}_{\boldsymbol{q}_1}$, $\mathbf{e}_{\boldsymbol{q}_2}$ and $\mathbf{e}_{\boldsymbol{q}_3}$ illustrated in figure 3 and given by

$$\mathbf{e}_{\boldsymbol{q}_3} \equiv \frac{\boldsymbol{q}}{|\boldsymbol{q}|}. \tag{26}$$

The unit vectors $\mathbf{e}_{\boldsymbol{q}_1}$ and $\mathbf{e}_{\boldsymbol{q}_2}$ are determined by requiring that the set of unit vectors be mutually orthonormal and that the coordinate system be right handed. We can then construct a spherical basis by defining the unit vectors

$$\mathbf{e}_0 \equiv \mathbf{e}_{\boldsymbol{q}_3} \tag{27}$$

and

$$\mathbf{e}_\pm \equiv \mp\frac{1}{\sqrt{2}}\left(\mathbf{e}_{\boldsymbol{q}_1} \pm i\mathbf{e}_{\boldsymbol{q}_2}\right). \tag{28}$$

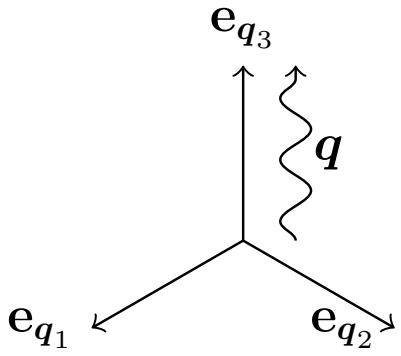

Figure 3. The Cartesian unit vectors used to define the spherical basis of equations 27 and 28. The vector $\mathbf{e}_{\boldsymbol{q}_3}$ is defined by equation 26, which guarantees that $\boldsymbol{q} \parallel \mathbf{e}_{\boldsymbol{q}_3}$.

In this basis any arbitrary three-vector $\mathbf{l}$ can be expanded as[10, Chapter 2.1.3]

$$\mathbf{l} = \sum_{\lambda=0,\pm1} l_\lambda \mathbf{e}_\lambda^\dagger = l_1\mathbf{e}_1^\dagger + l_{-1}\mathbf{e}_{-1}^\dagger + l_{\lambda=0}\mathbf{e}_0^\dagger = l_1\mathbf{e}_1^\dagger + l_{-1}\mathbf{e}_{-1}^\dagger + l_3\mathbf{e}_0^\dagger, \tag{29}$$

where we have adopted the notation $l_{\lambda=0} \equiv l_3$, since l_0 is already used to denote the time component of the four-vector l_μ.

Using the completeness of the spherical harmonics and spherical coordinates $(r,\Omega) = (r,\theta,\phi)$ we can write[16]

$$e^{i\boldsymbol{q}\cdot\boldsymbol{x}} = e^{iqr\cos\theta} = \sum_{l'} C_{l'}(r) Y_{l'}^0(\Omega), \tag{30}$$

where $q = |\boldsymbol{q}|$. By operating on the above expression with

$$\int Y_l^{0*}(\Omega)\mathrm{d}\Omega = \int Y_l^0(\Omega)\mathrm{d}\Omega \tag{31}$$

and utilizing the orthogonality of the spherical harmonics we get

$$\int Y_l^0(\Omega) e^{iqr\cos\theta}\mathrm{d}\Omega = \sum_{l'} C_{l'}(r) \int Y_l^{0*} Y_{l'}^0(\Omega)\mathrm{d}\Omega = \sum_{l'} C_{l'}(r)\delta_{ll'} = C_l(r). \tag{32}$$

Substituting the explicit form of the spherical harmonic[17, Page 128]

$$Y_l^0 = \sqrt{\frac{2l+1}{4\pi}} P_l(\cos\theta) = \frac{\hat{l}}{\sqrt{4\pi}} P_l(\cos\theta) \tag{33}$$

into the left side of equation 32, we can write C_l as

$$C_l(r) = \int \frac{\hat{l}}{\sqrt{4\pi}} P_l(\cos\theta) e^{iqr\cos\theta} \mathrm{d}\Omega = \frac{\hat{l}}{\sqrt{4\pi}} \int_{-1}^{1}\int_{0}^{2\pi} P_l(\cos\theta) e^{iqr\cos\theta} \mathrm{d}\phi \mathrm{d}(\cos\theta) = \frac{\hat{l}}{\sqrt{4\pi}} 2\pi \int_{-1}^{1} P_l(\cos\theta) e^{iqr\cos\theta} \mathrm{d}(\cos\theta) = \hat{l}\sqrt{\pi}\frac{2}{-i^l}\frac{-i^l}{2}\int_{-1}^{1} P_l(\cos\theta) e^{iqr\cos\theta} \mathrm{d}(\cos\theta) = \hat{l}\sqrt{\pi}\frac{2}{-i^l} j_l(qr) = \hat{l}\sqrt{4\pi} i^l j_l(qr), \tag{34}$$

where the second to last equality follows from the integral representation of the spherical Bessel function of the first kind $j_\alpha(x)$[18, Page 438]:

$$j_\alpha(x) = \frac{-i^\alpha}{2}\int_{-1}^{1} P_\alpha(\cos\theta) e^{ix\cos\theta} \mathrm{d}(\cos\theta). \tag{35}$$

The plane wave expansion in spherical harmonics is then

$$e^{i\boldsymbol{q}\cdot\boldsymbol{x}} = \sum_l i^l \sqrt{4\pi}\hat{l} j_l(qr) Y_l^0(\Omega) = \sum_l i^l \sqrt{4\pi}\hat{l} j_l(\rho) Y_l^0(\Omega), \tag{36}$$

where $\rho = qr$.

Next we will write the earlier result in terms of the vector spherical harmonics $\boldsymbol{\mathcal{Y}}_{Jl1}^M$ and use them to express the Hamiltonian matrix elements in terms of irreducible tensor operators. The vector spherical harmonics are defined by[11, Page 55]

$$\boldsymbol{\mathcal{Y}}_{Jl1}^M(\Omega) \equiv \sum_{m'\lambda'} (lm'1\lambda'|JM) Y_l^{m'}(\Omega)\mathbf{e}_{\lambda'}. \tag{37}$$

Multiplying both sides of this equation by $(lm1\lambda|JM)$ and summing over J and M we get

$$\sum_{JM}(lm1\lambda|JM)\boldsymbol{\mathcal{Y}}_{Jl1}^M(\Omega) = \sum_{JMm\lambda}(lm1\lambda|JM)(lm'1\lambda'|JM) Y_l^{m'}(\Omega)\mathbf{e}_{\lambda'} = \sum_{m\lambda}\delta_{mm'}\delta_{\lambda\lambda'} Y_l^{m'}(\Omega)\mathbf{e}_{\lambda'} = Y_l^m(\Omega)\mathbf{e}_\lambda. \tag{38}$$

Combining this result with equation 36 we get

$$e^{i\boldsymbol{q}\cdot\boldsymbol{x}}\mathbf{e}_\lambda = \sum_l i^l\sqrt{4\pi}\hat{l}j_l(\rho)Y_l^0(\Omega)\mathbf{e}_\lambda = \sum_l i^l\sqrt{4\pi}\hat{l}j_l(\rho)\sum_{JM}(l01\lambda|JM)\boldsymbol{\mathcal{Y}}^M_{Jl1}(\Omega) = \\ \sum_{JMl} i^l\sqrt{4\pi}\hat{l}j_l(\rho)(l01\lambda|JM)\boldsymbol{\mathcal{Y}}^M_{Jl1}(\Omega) = \sum_{Jl} i^l\sqrt{4\pi}\hat{l}j_l(\rho)(l01\lambda|J\lambda)\boldsymbol{\mathcal{Y}}^\lambda_{Jl1}(\Omega), \tag{39}$$

where in deriving the last equality we used the fact that for a Clebsch–Gordan coefficient not to vanish, it must fulfil the sum condition for the magnetic quantum numbers[10, Page 7]. In this case this leads to the equation $0 + \lambda = M$, so the sum over M contains only a single non-vanishing term. The sum over l can be similarly reduced to a small number of terms by utilizing the triangular condition of the Clebsch–Gordan coefficients[10, Page 7]. In this case the triangular condition leads to

$$|l-1| \leq J \leq l+1 \Rightarrow l = J-1,\, J,\, J+1, \tag{40}$$

so the sum over l reduces to only three terms. We will deal with the cases corresponding to different λ-values separately.

When $\lambda = 0$, we get from equation 39 and the above triangular condition

$$e^{i\boldsymbol{q}\cdot\boldsymbol{x}}\mathbf{e}_0 = \sqrt{4\pi}\sum_{J\geq 0}\Big[i^{J-1}\widehat{(J-1)}j_{J-1}(\rho)((J-1)010|J0)\boldsymbol{\mathcal{Y}}^0_{J(J-1)1}(\Omega) + \\ i^J\hat{J}j_J(\rho)(J010|J0)\boldsymbol{\mathcal{Y}}^0_{JJ1}(\Omega) + i^{J+1}\widehat{J+1}j_{J+1}(\rho)((J+1)010|J0)\boldsymbol{\mathcal{Y}}^0_{J(J+1)1}(\Omega)\Big]. \tag{41}$$

We will use the following identities for evaluating the Clebsch–Gordan coefficients in the above expression[19, Appendix B]:

$$(j_1m10|(j_1+1)m) = \sqrt{\frac{(j_1-m+1)(j_1+m+1)}{(2j_1+1)(j_1+1)}}, (j_1m10|j_1m) = \frac{m}{\sqrt{j_1(j_1+1)}} \text{ and} \\ (j_1m10|(j_1-1)m) = -\sqrt{\frac{(j_1-m)(j_1+m)}{j_1(2j_1+1)}}. \tag{42}$$

From these we get

$$((J-1)010|J0) = \sqrt{\frac{(J-1-0+1)(J-1+0+1)}{(2J-2+1)(J-1+1)}} = \sqrt{\frac{J^2}{(2J-1)J}} = \sqrt{\frac{J}{2J-1}}, \tag{43}$$

$$((J+1)010|J0) = -\sqrt{\frac{(J+1-0)(J+1+0)}{(J+1)(2J+2+1)}} = -\sqrt{\frac{(J+1)^2}{(J+1)(2J+3)}} = -\sqrt{\frac{J+1}{2J+3}} \tag{44}$$

and

$$(J010|J0) = 0. \tag{45}$$

With these, we get from equation 41

$$\begin{aligned} &e^{i\boldsymbol{q}\cdot\boldsymbol{x}}\mathbf{e}_0 = \sqrt{4\pi}\sum_{J\geq 0} i^J\Big[i^{-1}\widehat{(J-1)}\sqrt{\frac{J}{2J-1}}j_{J-1}(\rho)\boldsymbol{\mathcal{Y}}^0_{J(J-1)1}(\Omega) - \\ &i\widehat{J+1}\sqrt{\frac{J+1}{2J+3}}j_{J+1}(\rho)\boldsymbol{\mathcal{Y}}^0_{J(J+1)1}(\Omega)\Big] = -\sqrt{4\pi}\sum_{J\geq 0} i^J\Big[i\sqrt{J}j_{J-1}(\rho)\boldsymbol{\mathcal{Y}}^0_{J(J-1)1}(\Omega) + \\ &i\sqrt{J+1}j_{J+1}(\rho)\boldsymbol{\mathcal{Y}}^0_{J(J+1)1}(\Omega)\Big] = -i\sum_{J\geq 0}\sqrt{4\pi(2J+1)}i^J\Bigg[\sqrt{\frac{J}{2J+1}}j_{J-1}(\rho)\boldsymbol{\mathcal{Y}}^0_{J(J-1)1}(\Omega) \\ &+\sqrt{\frac{J+1}{2J+1}}j_{J+1}(\rho)\boldsymbol{\mathcal{Y}}^0_{J(J+1)1}(\Omega)\Bigg]. \end{aligned} \tag{46}$$

The above expression can be simplified by the identity[20, Chapter 5]

$$\nabla_r\left[j_l(r)Y^m_l(\Omega)\right] = \sqrt{\frac{l+1}{2l+1}}j_{l+1}(\rho)\boldsymbol{\mathcal{Y}}^m_{l(l+1)1}(\Omega) + \sqrt{\frac{l}{2l+1}}j_{l-1}(\rho)\boldsymbol{\mathcal{Y}}^m_{l(l-1)1}(\Omega), \tag{47}$$

where the three gradient is taken in the spherical coordinates. This results in

$$e^{i\boldsymbol{q}\cdot\boldsymbol{x}}\mathbf{e}_0 = -i\sum_{J\geq 0}\sqrt{4\pi(2J+1)}i^J\nabla_\rho\left[j_J(\rho)Y^0_J(\Omega)\right], \tag{48}$$

where the three gradient is now in spherical coordinates with $\rho = qr$ as the radial coordinate. The operators ∇_ρ and ∇_r are related by

$$\begin{aligned} &\rho = qr \Rightarrow \mathrm{d}\rho = q\mathrm{d}r \Rightarrow \nabla_\rho = \hat{\boldsymbol{\rho}}\frac{\partial}{\partial\rho} + \hat{\boldsymbol{\theta}}\frac{1}{\rho}\frac{\partial}{\partial\theta} + \hat{\boldsymbol{\phi}}\frac{1}{\rho\sin\theta}\frac{\partial}{\partial\phi} = \hat{\boldsymbol{r}}\frac{\partial}{q\partial r} + \hat{\boldsymbol{\theta}}\frac{1}{qr}\frac{\partial}{\partial\theta} + \\ &\hat{\boldsymbol{\phi}}\frac{1}{qr\sin\theta}\frac{\partial}{\partial\phi} = \frac{1}{q}\left(\hat{\boldsymbol{r}}\frac{\partial}{\partial r} + \hat{\boldsymbol{\theta}}\frac{1}{r}\frac{\partial}{\partial\theta} + \hat{\boldsymbol{\phi}}\frac{1}{r\sin\theta}\frac{\partial}{\partial\phi}\right) = \frac{1}{q}\nabla_r, \end{aligned} \tag{49}$$

where $\hat{\boldsymbol{\rho}}$, $\hat{\boldsymbol{r}}$, $\hat{\boldsymbol{\theta}}$ and $\hat{\boldsymbol{\phi}}$ are the unit vectors of the spherical coordinate systems. In the above derivation, we used the fact that

$$\hat{\boldsymbol{\rho}} = \frac{q\boldsymbol{r}}{|q\boldsymbol{r}|} = \frac{q\boldsymbol{r}}{q|\boldsymbol{r}|} = \frac{\boldsymbol{r}}{|\boldsymbol{r}|} = \hat{\boldsymbol{r}}. \tag{50}$$

We can now write equation 48 as

$$\begin{aligned} e^{i\boldsymbol{q}\cdot\boldsymbol{x}}\mathbf{e}_0 = -\frac{i}{q}\sum_{J\geq 0}\sqrt{4\pi(2J+1)}i^J\nabla_r\left[j_J(\rho)Y_J^0(\Omega)\right] = \\ -\frac{i}{q}\sum_{J\geq 0} i^J\sqrt{4\pi}\hat{J}\nabla\left[j_J(\rho)Y_J^0(\Omega)\right], \end{aligned} \tag{51}$$

where we have dropped the subscript r from the three gradient operator.

The cases $\lambda = \pm 1$ are similar and will be dealt together. In these cases, equation 39 leads to

$$\begin{aligned} e^{i\boldsymbol{q}\cdot\boldsymbol{x}}\mathbf{e}_\lambda = \sqrt{4\pi}\sum_{J\geq 1}\Big[i^{J-1}\widehat{(J-1)}j_{J-1}(\rho)((J-1)01\lambda|J\lambda)\boldsymbol{\mathcal{Y}}^\lambda_{J(J-1)1}(\Omega) + \\ i^J\hat{J}j_J(\rho)(J01\lambda|J\lambda)\boldsymbol{\mathcal{Y}}^\lambda_{JJ1}(\Omega) + i^{J+1}\widehat{(J+1)}j_{J+1}(\rho)((J+1)01\lambda|J\lambda)\boldsymbol{\mathcal{Y}}^\lambda_{J(J+1)1}(\Omega)\Big]. \end{aligned} \tag{52}$$

For the explicit form of the Clebsch–Gordan coefficients in the above equation we will use the following identities[19, Appendix B] for $\lambda = +1$:

$$(j_1(m-1)11|(j_1+1)m) = \sqrt{\frac{(j_1+m+1)(j_1+m)}{(2j_1+2)(2j_1+1)}}, \tag{53}$$

$$(j_1(m-1)11|j_1m) = -\sqrt{\frac{(j_1-m+1)(j_1+m)}{2j_1(j_1+1)}} \tag{54}$$

and

$$(j_1(m-1)11|(j_1-1)m) = \sqrt{\frac{(j_1-m+1)(j_1-m)}{2j_1(2j_1+1)}}, \tag{55}$$

and the following identities for $\lambda = -1$:

$$(j_1(m+1)1-1|(j_1+1)m) = \sqrt{\frac{(j_1-m+1)(j_1-m)}{(2j_1+2)(2j_1+1)}}, \tag{56}$$

$$(j_1(m+1)1-1|j_1m) = \sqrt{\frac{(j_1+m+1)(j_1-m)}{2j_1(j_1+1)}} \tag{57}$$

and

$$(j_1(m+1)1-1|(j_1-1)m) = \sqrt{\frac{(j_1+m+1)(j_1+m)}{2j_1(2j_1+1)}}. \tag{58}$$

Using these, we get

$$\begin{aligned}
&((J-1)011|J1) = \sqrt{\frac{(J-1+1+1)(J-1+1)}{(2J-2+2)(2J-2+1)}} = \sqrt{\frac{J(J+1)}{2J(2J-1)}} = \sqrt{\frac{J+1}{2(2J-1)}},\\
&(J011|J1) = -\sqrt{\frac{(J-1+1)(J+1)}{2J(J+1)}} = -\sqrt{\frac{J(J+1)}{2J(J+1)}} = -\sqrt{\frac{1}{2}} \text{ and}\\
&((J+1)011|J1) = \sqrt{\frac{(J+1)(J+1-1)}{2(J+1)(2J+2+1)}} = \sqrt{\frac{J(J+1)}{2(J+1)(2J+3)}} = \sqrt{\frac{J}{2(2J+3)}},
\end{aligned} \tag{59}$$

and

$$\begin{aligned}
&((J-1)01-1|J-1) = \sqrt{\frac{(J+1)(J-1+1)}{(2J-2+2)(2J-1)}} = \sqrt{\frac{J(J+1)}{2J(2J-1)}} = \sqrt{\frac{J+1}{2(2J-1)}},\\
&(J01-1|J-1) = \sqrt{\frac{(J-1+1)(J+1)}{2J(J+1)}} = \sqrt{\frac{J(J+1)}{2J(J+1)}} = \sqrt{\frac{1}{2}} \text{ and}\\
&((J+1)01-1|J-1) = \sqrt{\frac{(J+1-1+1)(J+1-1)}{2(J+1)(2J+2+1)}} = \sqrt{\frac{J(J+1)}{2(J+1)(2J+3)}} =\\
&\sqrt{\frac{J}{2(2J+3)}}.
\end{aligned} \tag{60}$$

As it turns out, aside from the signs of the $j_1 = J$ coefficients, the Clebsch–Gordan

coefficients are the same for both values of λ. Thus, for equation 52 we now get

$$e^{i\boldsymbol{q}\cdot\boldsymbol{x}}\mathbf{e}_\lambda = \sqrt{4\pi}\sum_{J\geq 1} i^J\Bigg[i^{-1}\widehat{(J-1)}\sqrt{\frac{J+1}{2(2J-1)}}j_{J-1}(\rho)\boldsymbol{\mathcal{Y}}^\lambda_{J(J-1)1}(\Omega)\mp$$
$$\hat{J}\sqrt{\frac{1}{2}}j_J(\rho)\boldsymbol{\mathcal{Y}}^\lambda_{JJ1}(\Omega) + i\widehat{(J+1)}\sqrt{\frac{J}{2(2J+3)}}j_{J+1}(\rho)\boldsymbol{\mathcal{Y}}^\lambda_{J(J+1)1}(\Omega)\Bigg] =$$
$$\sqrt{4\pi}\sum_{J\geq 1} i^J\Bigg[\mp\sqrt{\frac{2J+1}{2}}j_J(\rho)\boldsymbol{\mathcal{Y}}^\lambda_{JJ1}(\Omega) + i\sqrt{\frac{J(2J+3)}{2(2J+3)}}j_{J+1}(\rho)\boldsymbol{\mathcal{Y}}^\lambda_{J(J+1)1}(\Omega) -$$
$$i\sqrt{\frac{(J+1)(2J-1)}{2(2J-1)}}j_{J-1}(\rho)\boldsymbol{\mathcal{Y}}^\lambda_{J(J-1)1}(\Omega)\Bigg] = \sqrt{4\pi}\sum_{J\geq 1} i^J\Bigg[\mp\sqrt{\frac{2J+1}{2}}j_J(\rho)\boldsymbol{\mathcal{Y}}^\lambda_{JJ1}(\Omega) +$$
$$i\sqrt{\frac{J}{2}}j_{J+1}(\rho)\boldsymbol{\mathcal{Y}}^\lambda_{J(J+1)1}(\Omega) - i\sqrt{\frac{J+1}{2}}j_{J-1}(\rho)\boldsymbol{\mathcal{Y}}^\lambda_{J(J-1)1}(\Omega)\Bigg] = \sum_{J\geq 1}\sqrt{\frac{4\pi(2J+1)}{2}}i^J\Bigg\{$$
$$\mp j_J(\rho)\boldsymbol{\mathcal{Y}}^\lambda_{JJ1}(\Omega) - i\Bigg[\sqrt{\frac{J+1}{2J+1}}j_{J-1}(\rho)\boldsymbol{\mathcal{Y}}^\lambda_{J(J-1)1}(\Omega) - \sqrt{\frac{J}{2J+1}}j_{J+1}(\rho)\boldsymbol{\mathcal{Y}}^\lambda_{J(J+1)1}(\Omega)\Bigg]\Bigg\} \tag{61}$$

for both $\lambda = \pm 1$.

The different orders of spherical Bessel functions in equation 61 need to be dealt with in order to proceed. The following differential relations can be used to express spherical Bessel functions of a given order in terms of one with different order[19, Page 439]:

$$\left(\frac{1}{r}\frac{\mathrm{d}}{\mathrm{d}r}\right)^m\left(r^{J+1}j_J(r)\right) = r^{J-m+1}j_{J-m}(r) \tag{62}$$

and

$$\left(\frac{1}{r}\frac{\mathrm{d}}{\mathrm{d}r}\right)^m\left(r^{-J}j_J(r)\right) = (-1)^m r^{-J-m}j_{J+m}(r). \tag{63}$$

Choosing $m = 1$ we get

$$\left(\frac{1}{r}\frac{\mathrm{d}}{\mathrm{d}r}\right)\left(r^{J+1}j_J(r)\right) = r^J j_{J-1}(r) \Leftrightarrow \frac{1}{r}\left((J+1)r^J j_J(r) + r^{J+1}\frac{\mathrm{d}j_J}{\mathrm{d}r}(r)\right) = r^J j_{J-1}(r)$$
$$\Leftrightarrow \left(\frac{\mathrm{d}}{\mathrm{d}r} + \frac{J+1}{r}\right)j_J(r) = j_{J-1}(r) \Rightarrow \left(\frac{\mathrm{d}}{q\mathrm{d}r} + \frac{J+1}{qr}\right)j_J(qr) = j_{J-1}(qr) \Leftrightarrow$$
$$\frac{1}{q}\left(\frac{\mathrm{d}}{\mathrm{d}r} + \frac{J+1}{r}\right)j_J(qr) = j_{J-1}(qr) \tag{64}$$

and

$$\left(\frac{1}{r}\frac{\mathrm{d}}{\mathrm{d}r}\right)\left(r^{-J}j_J(r)\right) = -r^{-J-1}j_{J+1}(r) \Leftrightarrow r^J\left(Jr^{-J-1}j_J(r) - r^{-J}\frac{\mathrm{d}j_J(r)}{\mathrm{d}r}\right) = j_{J+1}(r)$$
$$\Leftrightarrow \left(\frac{J}{r} - \frac{\mathrm{d}}{\mathrm{d}r}\right)j_J(r) = j_{J+1}(r) \Rightarrow \left(\frac{J}{qr} - \frac{\mathrm{d}}{q\mathrm{d}r}\right)j_J(qr) = j_{J+1}(qr) \Leftrightarrow$$
$$\frac{1}{q}\left(\frac{J}{r} - \frac{\mathrm{d}}{\mathrm{d}r}\right)j_J(qr) = j_{J+1}(qr), \tag{65}$$

where we have used the transformation $r \to qr$. With these above results, equation 61 can be written as

$$e^{i\boldsymbol{q}\cdot\boldsymbol{x}}\mathbf{e}_\lambda = \sum_{J\geq 1}\sqrt{2\pi(2J+1)}i^J\Bigg\{\mp j_J(\rho)\boldsymbol{\mathcal{Y}}^\lambda_{JJ1}(\Omega) - i\Bigg[\sqrt{\frac{J+1}{2J+1}}j_{J-1}(\rho)\boldsymbol{\mathcal{Y}}^\lambda_{J(J-1)1}(\Omega) -$$
$$\sqrt{\frac{J}{2J+1}}j_{J+1}(\rho)\boldsymbol{\mathcal{Y}}^\lambda_{J(J+1)1}(\Omega)\Bigg]\Bigg\} = \sum_{J\geq 1}\sqrt{2\pi(2J+1)}i^J\Bigg\{\mp j_J(\rho)\boldsymbol{\mathcal{Y}}^\lambda_{JJ1}(\Omega) - \frac{i}{q}\Bigg[$$
$$\sqrt{\frac{J+1}{2J+1}}\left(\frac{\mathrm{d}}{\mathrm{d}r} + \frac{J+1}{r}\right)j_J(\rho)\boldsymbol{\mathcal{Y}}^\lambda_{JJ_-1}(\Omega) + \sqrt{\frac{J}{2J+1}}\left(\frac{\mathrm{d}}{\mathrm{d}r} - \frac{J}{r}\right)j_J(\rho)\boldsymbol{\mathcal{Y}}^\lambda_{JJ_+1}(\Omega)\Bigg]\Bigg\}, \tag{66}$$

where we have abbreviated $J+1 = J_+$ and $J_- = J-1$. We can use the following curl relation[20, Chapter 5] for the terms inside the square brackets in the above expression:

$$\nabla\times\left[j_J(qr)\boldsymbol{\mathcal{Y}}^\lambda_{JJ1}(\Omega)\right] = i\Bigg[\sqrt{\frac{J+1}{2J+1}}\left(\frac{\mathrm{d}}{\mathrm{d}r} + \frac{J+1}{r}\right)j_J(\rho)\boldsymbol{\mathcal{Y}}^\lambda_{JJ_-1}(\Omega) +$$
$$\sqrt{\frac{J}{2J+1}}\left(\frac{\mathrm{d}}{\mathrm{d}r} - \frac{J}{r}\right)j_J(\rho)\boldsymbol{\mathcal{Y}}^\lambda_{JJ_+1}(\Omega)\Bigg]. \tag{67}$$

With this we finally get for equation 66

$$e^{i\boldsymbol{q}\cdot\boldsymbol{x}}\mathbf{e}_\lambda = \sum_{J\geq 1}\sqrt{2\pi(2J+1)}i^J\Bigg\{\mp j_J(\rho)\boldsymbol{\mathcal{Y}}^\lambda_{JJ1}(\Omega) - \frac{1}{q}\nabla\times\left[j_J(qr)\boldsymbol{\mathcal{Y}}^\lambda_{JJ1}(\Omega)\right]\Bigg\} =$$
$$-\sum_{J\geq 1}\sqrt{2\pi(2J+1)}i^J\Bigg\{\lambda j_J(\rho)\boldsymbol{\mathcal{Y}}^\lambda_{JJ1}(\Omega) + \frac{1}{q}\nabla\times\left[j_J(qr)\boldsymbol{\mathcal{Y}}^\lambda_{JJ1}(\Omega)\right]\Bigg\}. \tag{68}$$

2.1.3 Spherical tensor multipole operators and reaction cross section

We can now use the Hermitian adjoints of equations 51 and 68 to write equation 25 in terms of irreducible tensors. For the aforementioned adjoints we get

$$\begin{aligned}&\left(e^{i\boldsymbol{q}\cdot\boldsymbol{x}}\mathbf{e}_0\right)^\dagger = e^{-i\boldsymbol{q}\cdot\boldsymbol{x}}\mathbf{e}_0^\dagger = \frac{i}{q}\sum_{J\geq 0}(-i)^J\sqrt{4\pi}\hat{J}\left\{\nabla\left[j_J(\rho)Y_J^0(\Omega)\right]\right\}^\dagger = \\ &\frac{i}{q}\sum_{J\geq 0}(-i)^J\sqrt{4\pi}\hat{J}\nabla\left[j_J(\rho)Y_J^0(\Omega)\right].\end{aligned} \tag{69}$$

and

$$\begin{aligned}&\left(e^{i\boldsymbol{q}\cdot\boldsymbol{x}}\mathbf{e}_\lambda\right)^\dagger = e^{-i\boldsymbol{q}\cdot\boldsymbol{x}}\mathbf{e}_\lambda^\dagger = -\sum_{J\geq 1}\sqrt{2\pi(2J+1)}(-i)^J\Bigg\{\lambda j_J(\rho)\left(\boldsymbol{\mathcal{Y}}_{JJ1}^\lambda(\Omega)\right)^\dagger + \\ &\frac{1}{q}\nabla\times\left[j_J(qr)\left(\boldsymbol{\mathcal{Y}}_{JJ1}^\lambda(\Omega)\right)^\dagger\right]\Bigg\} = -\sum_{J\geq 1}\sqrt{2\pi}\hat{J}(-i)^J\Bigg\{\lambda j_J(\rho)\boldsymbol{\mathcal{Y}}_{JJ1}^{-\lambda}(\Omega) + \\ &\frac{1}{q}\nabla\times\left[j_J(qr)\boldsymbol{\mathcal{Y}}_{JJ1}^{-\lambda}(\Omega)\right]\Bigg\},\end{aligned} \tag{70}$$

where we used

$$\begin{aligned}&\left(\boldsymbol{\mathcal{Y}}_{JJ1}^\lambda(\Omega)\right)^\dagger = \sum_{m\lambda'}(Jm1\lambda'|J\lambda)Y_J^{m\dagger}(\Omega)\mathbf{e}_{\lambda'}^\dagger = \sum_{m\lambda'}(Jm1\lambda'|J\lambda)(-1)^m Y_J^{-m}(\Omega)(-1)^{\lambda'}\mathbf{e}_{-\lambda'} \\ &= \sum_{m\lambda'}(-1)^{m+\lambda'}(Jm1\lambda'|J\lambda)Y_J^{-m}(\Omega)\mathbf{e}_{-\lambda'} = \sum_{m\lambda'}(-1)^\lambda(Jm1\lambda'|J\lambda)Y_J^{-m}(\Omega)\mathbf{e}_{-\lambda'} = \\ &\sum_{m\lambda'}(-1)^{\lambda+1}(J-m1-\lambda'|J-\lambda)Y_J^{-m}(\Omega)\mathbf{e}_{-\lambda'} = (-1)^{\lambda+1}\sum_{m\lambda'}(Jm1\lambda'|J-\lambda)Y_J^m(\Omega)\mathbf{e}_{\lambda'} \\ &= (-1)^{\lambda+1}\boldsymbol{\mathcal{Y}}_{JJ1}^{-\lambda}(\Omega) \Rightarrow \left(\boldsymbol{\mathcal{Y}}_{JJ1}^\lambda(\Omega)\right)^\dagger = \boldsymbol{\mathcal{Y}}_{JJ1}^{-\lambda}(\Omega), \text{ for } \lambda = \pm 1.\end{aligned} \tag{71}$$

By defining operators[21]

$$M_{LM}(q) \equiv j_L(\rho)Y_M^L \text{ and } \boldsymbol{M}_{JL}^M(q) \equiv j_L(\rho)\boldsymbol{\mathcal{Y}}_{JL1}^M \tag{72}$$

we can write the adjoints above as

$$e^{-i\boldsymbol{q}\cdot\boldsymbol{x}}\mathbf{e}_0^\dagger = \frac{i}{q}\sum_{J\geq 0}(-i)^J\sqrt{4\pi}\hat{J}\nabla\left[M_{J0}(q)\right] \tag{73}$$

and

$$e^{-i\boldsymbol{q}\cdot\boldsymbol{x}}\mathbf{e}_\lambda^\dagger = -\sum_{J\geq 1}\sqrt{2\pi}\hat{J}(-i)^J\left[\lambda\boldsymbol{M}_{JJ}^{-\lambda}(q)+\frac{1}{q}\nabla\times\boldsymbol{M}_{JJ}^{-\lambda}(q)\right]. \tag{74}$$

Next we will expand the $\boldsymbol{l}$-vector from equation 25 in the spherical basis by

$$\boldsymbol{l} = \sum_{\lambda=\pm1,0} l_\lambda \boldsymbol{e}_\lambda^\dagger, \tag{75}$$

where we will use the notation $l_{\lambda=0} = l_3$ to avoid confusion with the time component of the l_μ vector. We will also use the adjoint of the expansion of the plane wave in spherical harmonics of equation 36:

$$\left(e^{i\boldsymbol{q}\cdot\boldsymbol{x}}\right)^\dagger = e^{-i\boldsymbol{q}\cdot\boldsymbol{x}} = \sum_l (-i)^l\sqrt{4\pi}\hat{l}j_l(\rho)Y_l^0(\Omega) = \sum_l (-i)^l\sqrt{4\pi}\hat{l}M_{L0}(q). \tag{76}$$

Using the above results, we can finally express the Hamiltonian of equation 6 as

$$\begin{aligned}
&\hat{H}_{\text{eff}} = \frac{G}{\sqrt{2}}\int\left[l_0 e^{-i\boldsymbol{q}\cdot\boldsymbol{x}}\mathcal{J}_0(\boldsymbol{x})_{fi} - e^{-i\boldsymbol{q}\cdot\boldsymbol{x}}\boldsymbol{l}\cdot\boldsymbol{\mathcal{J}}(\boldsymbol{x})_{fi}\right]\mathrm{d}^3\boldsymbol{x} = \frac{G}{\sqrt{2}}\int\Bigg[l_0 e^{-i\boldsymbol{q}\cdot\boldsymbol{x}}\mathcal{J}_0(\boldsymbol{x})_{fi} - \\
&\sum_{\lambda=\pm1,0}\left(l_\lambda e^{-i\boldsymbol{q}\cdot\boldsymbol{x}}\mathbf{e}_\lambda^\dagger\right)\cdot\boldsymbol{\mathcal{J}}(\boldsymbol{x})_{fi}\Bigg]\mathrm{d}^3\boldsymbol{x} = \frac{G}{\sqrt{2}}\int\Bigg\{l_0\sum_{J\geq0}(-i)^J\sqrt{4\pi}\hat{J}M_{J0}(q)\mathcal{J}_0(\boldsymbol{x})_{fi} - \\
&l_3\frac{i}{q}\sum_{J\geq0}(-i)^J\sqrt{4\pi}\hat{J}\nabla\left[M_{J0}(q)\right]\cdot\boldsymbol{\mathcal{J}}(\boldsymbol{x})_{fi} + \sum_{\lambda=\pm1}l_\lambda\sum_{J\geq1}\sqrt{2\pi}\hat{J}(-i)^J\Bigg[\lambda\boldsymbol{M}_{JJ}^{-\lambda}(q) + \\
&\frac{1}{q}\nabla\times\boldsymbol{M}_{JJ}^{-\lambda}(q)\Bigg]\cdot\boldsymbol{\mathcal{J}}(\boldsymbol{x})_{fi}\Bigg\}\mathrm{d}^3\boldsymbol{x} = \frac{G}{\sqrt{2}}\int\Bigg\{\sum_{J\geq0}(-i)^J\sqrt{4\pi}\hat{J}\Bigg[l_0 M_{J0}(q)\mathcal{J}_0(\boldsymbol{x})_{fi} - \\
&\frac{i}{q}l_3\nabla\left[M_{J0}(q)\right]\cdot\boldsymbol{\mathcal{J}}(\boldsymbol{x})_{fi}\Bigg] + \sum_{\lambda=\pm1}l_\lambda\sum_{J\geq1}\sqrt{2\pi}\hat{J}(-i)^J\left[\lambda\boldsymbol{M}_{JJ}^{-\lambda}(q)+\frac{1}{q}\nabla\times\boldsymbol{M}_{JJ}^{-\lambda}(q)\right]\cdot \\
&\boldsymbol{\mathcal{J}}(\boldsymbol{x})_{fi}\Bigg\}\mathrm{d}^3\boldsymbol{x} = \frac{G}{\sqrt{2}}\Bigg\{\sum_{J\geq0}(-i)^J\sqrt{4\pi}\hat{J}\Bigg[l_0\int M_{J0}(q)\mathcal{J}_0(\boldsymbol{x})\mathrm{d}^3\boldsymbol{x} - \frac{i}{q}l_3\int\nabla\left[M_{J0}(q)\right]\cdot \\
&\boldsymbol{\mathcal{J}}(\boldsymbol{x})\mathrm{d}^3\boldsymbol{x}\Bigg] + \sum_{\lambda=\pm1}l_\lambda\sum_{J\geq1}\sqrt{2\pi}\hat{J}(-i)^J\Bigg[\frac{1}{q}\int\left[\nabla\times\boldsymbol{M}_{JJ}^{-\lambda}(q)\right]\cdot\boldsymbol{\mathcal{J}}(\boldsymbol{x})\mathrm{d}^3\boldsymbol{x} + \\
&\lambda\int\left[\boldsymbol{M}_{JJ}^{-\lambda}(q)\right]\cdot\boldsymbol{\mathcal{J}}(\boldsymbol{x})\mathrm{d}^3\boldsymbol{x}\Bigg]\Bigg\} = \frac{G}{\sqrt{2}}\Bigg\{\sum_{J\geq0}(-i)^J\sqrt{4\pi}\hat{J}\Bigg[l_0\mathcal{M}_{J0}(q) - l_3\mathcal{L}_{J0}(q)\Bigg] + \\
&\sum_{\lambda=\pm1}\sum_{J\geq1}\sqrt{2\pi}\hat{J}(-i)^J l_\lambda\Bigg[\mathcal{T}_{J-\lambda}^{\text{el}}(q) + \lambda\mathcal{T}_{J-\lambda}^{\text{mag}}(q)\Bigg]\Bigg\},
\end{aligned} \tag{77}$$

where we have defined the multipole operators[21]

$$\begin{aligned}
\mathcal{M}_{JM}(q) &= \int M_{JM}(q)\mathcal{J}_0(\boldsymbol{x})\mathrm{d}^3\boldsymbol{x}, \\
\mathcal{L}_{JM}(q) &= \frac{i}{q}\int \nabla\left[M_{JM}(q)\right]\cdot\boldsymbol{\mathcal{J}}(\boldsymbol{x})\mathrm{d}^3\boldsymbol{x}, \\
\mathcal{T}^{\mathrm{el}}_{JM}(q) &= \frac{1}{q}\int \left[\nabla\times\boldsymbol{M}^M_{JJ}(q)\right]\cdot\boldsymbol{\mathcal{J}}(\boldsymbol{x})\mathrm{d}^3\boldsymbol{x} \text{ and} \\
\mathcal{T}^{\mathrm{mag}}_{JM}(q) &= \int \left[\boldsymbol{M}^M_{JJ}(q)\right]\cdot\boldsymbol{\mathcal{J}}(\boldsymbol{x})\mathrm{d}^3\boldsymbol{x}.
\end{aligned} \tag{78}$$

It is worth mentioning that all of the above operators $\mathcal{O}_{JM}$ have both vector (V) and axial vector pieces and can be expressed as $\mathcal{O}_{JM} = O^V_{JM} - O^A_{JM}$. The Hamiltonian matrix elements are given by equation 25 and they are

$$\begin{aligned}
H_{fi} = \frac{G}{\sqrt{2}}\langle f|\Bigg\{ &\sum_{J\geq 0}(-i)^J\sqrt{4\pi}\hat{J}\Big[l_0\mathcal{M}_{J0}(q) - l_3\mathcal{L}_{J0}(q)\Big] + \\
&\sum_{\lambda=\pm1}\sum_{J\geq 1}\sqrt{2\pi}\hat{J}(-i)^J l_\lambda\Big[\mathcal{T}^{\mathrm{el}}_{J-\lambda}(q) + \lambda\mathcal{T}^{\mathrm{mag}}_{J-\lambda}(q)\Big]\Bigg\}|i\rangle\,.
\end{aligned} \tag{79}$$

The above equation holds generally for all nuclear wave functions and local nuclear weak currents provided that the matrix elements of the multipole operators are expressed in terms of their corresponding reduced matrix elements by using the Wigner-Eckart theorem[11, Chapter 45]. This will be done shortly, but we will first concentrate on the special case that is of interest here, namely the case of unobserved and unoriented nuclear targets.

Equation 15 is a valid expression for the differential cross section when the quantum numbers of the initial and final state are known. This isn't the case in practice as the magnetic quantum numbers of the nuclei involved in the reactions aren't usually known. When the nuclear targets are assumed unoriented and unobserved, we will sum over all the initial and final state magnetic quantum numbers and average over the initial states. We will also consider the sums over the spins of the leptons involved in the reactions later. Taking these two factors into consideration, the differential cross section can be written as[11, Page 480]

$$\frac{\mathrm{d}\sigma}{\mathrm{d}\Omega} = \frac{2k'E_{k'}}{(2\pi)^2}\left(\frac{V^2}{2}\sum_{\text{lepton spins}}\frac{1}{2J_i+1}\sum_{M_iM_f}|H_{fi}|^2\right). \tag{80}$$

It is worth pointing out that we will not average over the initial lepton spins since

as far as the massless (anti)neutrinos of the present case are considered, there are only left-handed neutrinos and right-handed antineutrinos. We do sum over their initial and final state spins, however, as the $1-\gamma_5$ coupling of equation 23 projects the correct type of lepton handedness and eliminates forbidden couplings[11, Page Chapter 42].

We will first consider the sums over the magnetic quantum numbers of the nucleus, i.e. we want to find an expression for

$$\frac{1}{2J_i+1}\sum_{M_iM_f}|H_{fi}|^2=\frac{1}{2J_i+1}\sum_{M_iM_f}|\langle f|H_{\text{eff}}|i\rangle|^2. \tag{81}$$

For the factor $|\langle f|H_{\text{eff}}|i\rangle|^2=\langle f|H_{\text{eff}}|i\rangle^*\langle f|H_{\text{eff}}|i\rangle$ we get using equation 79

$$\begin{aligned}
&|\langle f|H_{\text{eff}}|i\rangle|^2=\frac{G}{\sqrt{2}}\Bigg\{\sum_{I\geq 0}i^I\sqrt{4\pi}\hat{I}\Big[l_0^*\langle f|\mathcal{M}_{I0}(q)|i\rangle^*-l_3^*\langle f|\mathcal{L}_{I0}(q)|i\rangle^*\Big]+\sum_{\kappa=\pm1}\sum_{I\geq1}\sqrt{2\pi}\cdot\\
&\hat{I}i^Il_\kappa^*\Big[\langle f|\mathcal{T}^{\text{el}}_{I-\kappa}(q)|i\rangle^*+\kappa\langle f|\mathcal{T}^{\text{mag}}_{I-\kappa}(q)|i\rangle^*\Big]\Bigg\}\frac{G}{\sqrt{2}}\Bigg\{\sum_{J\geq0}(-i)^J\sqrt{4\pi}\hat{J}\Big[l_0\langle f|\mathcal{M}_{J0}(q)|i\rangle-\\
&l_3\langle f|\mathcal{L}_{J0}(q)|i\rangle\Big]+\sum_{\lambda=\pm1}\sum_{J\geq1}\sqrt{2\pi}\hat{J}(-i)^Jl_\lambda\Big[\langle f|\mathcal{T}^{\text{el}}_{J-\lambda}(q)|i\rangle+\lambda\langle f|\mathcal{T}^{\text{mag}}_{J-\lambda}(q)|i\rangle\Big]\Bigg\}=4\pi\cdot\\
&\frac{G^2}{2}\Bigg\{\sum_{I,J\geq0}\frac{i^I}{i^J}\hat{I}\hat{J}\Big[l_0^*\langle f|\mathcal{M}_{I0}(q)|i\rangle^*-l_3^*\langle f|\mathcal{L}_{I0}(q)|i\rangle^*\Big]\Big[l_0\langle f|\mathcal{M}_{J0}(q)|i\rangle-\\
&l_3\langle f|\mathcal{L}_{J0}(q)|i\rangle\Big]+\sum_{\kappa,\lambda=\pm1}\sum_{I,J\geq1}\frac{i^I}{2i^J}\hat{I}\hat{J}l_\kappa^*l_\lambda\Big[\langle f|\mathcal{T}^{\text{el}}_{I-\kappa}(q)|i\rangle^*+\kappa\langle f|\mathcal{T}^{\text{mag}}_{I-\kappa}(q)|i\rangle^*\Big]\cdot\\
&\Big[\langle f|\mathcal{T}^{\text{el}}_{J-\lambda}(q)|i\rangle+\lambda\langle f|\mathcal{T}^{\text{mag}}_{J-\lambda}(q)|i\rangle\Big]+\sum_{\lambda=\pm1}\sum_{I\geq0,J\geq1}\frac{i^I}{i^J}\frac{\sqrt{2}}{2}\hat{I}\hat{J}l_\lambda\Big[l_0^*\langle f|\mathcal{M}_{I0}(q)|i\rangle^*-\\
&l_3^*\langle f|\mathcal{L}_{I0}(q)|i\rangle^*\Big]\Big[\langle f|\mathcal{T}^{\text{el}}_{J-\lambda}(q)|i\rangle+\lambda\langle f|\mathcal{T}^{\text{mag}}_{J-\lambda}(q)|i\rangle\Big]+\sum_{\kappa=\pm1}\sum_{I\geq1,J\geq0}\frac{i^I}{i^J}\frac{\sqrt{2}}{2}\hat{I}\hat{J}l_\kappa^*\cdot\\
&\Big[\langle f|\mathcal{T}^{\text{el}}_{I-\kappa}(q)|i\rangle^*+\kappa\langle f|\mathcal{T}^{\text{mag}}_{I-\kappa}(q)|i\rangle^*\Big]\Big[l_0\langle f|\mathcal{M}_{J0}(q)|i\rangle-l_3\langle f|\mathcal{L}_{J0}(q)|i\rangle\Big]\Bigg\}.
\end{aligned} \tag{82}$$

By first considering only the latter two sums in the above expression, the terms resulting from expanding the square brackets are all proportional to factors of the form $\langle f|\mathcal{O}_{J0}(q)|i\rangle^*\langle f|\mathcal{O'}_{J'\mu}(q)|i\rangle$ and $\langle f|\mathcal{O}_{J0}(q)|i\rangle\langle f|\mathcal{O'}_{J'\mu}(q)|i\rangle^*$, where $\mathcal{O}_{J0}(q)=\mathcal{M}_{J0}(q)$ or $\mathcal{L}_{J0}(q)$ and $\mathcal{O'}_{J'\mu}(q)=\mathcal{T}^{\text{el}}_{J'-\mu}(q)$ or $\mathcal{T}^{\text{mag}}_{J'-\mu}(q)$. We will now apply the Wigner-Eckart

theorem[10, Page 29]

$$\langle n_f J_f M_f|\mathcal{O}_{JM}|n_i J_i M_i\rangle = (-1)^{J_f-M_f}\begin{pmatrix} J_f & J & J_i \\ -M_f & M & M_i\end{pmatrix}(n_f J_f||\mathcal{O}_J||n_i J_i). \tag{83}$$

By applying the theorem on the aforementioned factors, summing over the initial and final states and averaging over the initial states, we get

$$\frac{1}{2J_i+1}\sum_{M_i M_f}\langle f|\mathcal{O}_{J0}(q)|i\rangle^*\langle f|\mathcal{O'}_{J'\mu}(q)|i\rangle = \frac{1}{2J_i+1}\sum_{M_i M_f}(-1)^{J_f-M_f}\begin{pmatrix} J_f & J & J_i \\ -M_f & 0 & M_i\end{pmatrix}$$
$$(J_f||\mathcal{O}_J(q)||J_i)^*(-1)^{J_f-M_f}\begin{pmatrix} J_f & J' & J_i \\ -M_f & \mu & M_i\end{pmatrix}(J_f||\mathcal{O}_{J'}||J_i) = \frac{1}{2J_i+1}(J_f||\mathcal{O}_J(q)||J_i)^*\cdot$$
$$(J_f||\mathcal{O}_{J'}||J_i)\sum_{M_i M_f}\begin{pmatrix} J_f & J & J_i \\ -M_f & 0 & M_i\end{pmatrix}\begin{pmatrix} J_f & J' & J_i \\ -M_f & \mu & M_i\end{pmatrix} = \frac{1}{2J_i+1}(J_f||\mathcal{O}_J(q)||J_i)^*\cdot$$
$$(J_f||\mathcal{O}_{J'}||J_i)\frac{1}{2J+1}\delta_{JJ'}\delta_{0\mu} = 0, \tag{84}$$

due to $\mu = \pm 1 \neq 0$. In the above derivation, we have used the identity[19, Appendix B][10, Chapter 1]

$$\frac{1}{2J_i+1}\sum_{M_i M_f}\begin{pmatrix} J_f & J & J_i \\ -M_f & M & M_i\end{pmatrix}\begin{pmatrix} J_f & J' & J_i \\ -M_f & M' & M_i\end{pmatrix} = \frac{1}{(2J+1)(2J_i+1)}\delta_{JJ'}\delta_{MM'} \tag{85}$$

and omitted the quantum numbers n_f and n_i for the sake of brevity. Thus the last two sum terms of equation 82 do not contribute in the present case.

We will next consider the first two sum terms on the right side of equation 82. Expanding the square brackets we get

$$\frac{4\pi G^2}{2}\Bigg\{\sum_{I,J\geq 0}\frac{i^I}{i^J}\hat{I}\hat{J}\Big[l_0^*\langle f|\mathcal{M}_{I0}(q)|i\rangle^* - l_3^*\langle f|\mathcal{L}_{I0}(q)|i\rangle^*\Big]\Big[l_0\langle f|\mathcal{M}_{J0}(q)|i\rangle - l_3\cdot$$
$$\langle f|\mathcal{L}_{J0}|i\rangle\Big] + \sum_{\kappa,\lambda=\pm 1}\sum_{I,J\geq 1}\frac{i^I l_\kappa^* l_\lambda}{2i^J}\hat{I}\hat{J}\Big[\langle f|\mathcal{T}^{\rm el}_{I-\kappa}(q)|i\rangle^* + \kappa\langle f|\mathcal{T}^{\rm mag}_{I-\kappa}(q)|i\rangle^*\Big]\Big[\langle f|\mathcal{T}^{\rm el}_{J-\lambda}(q)|i\rangle$$
$$+\lambda\langle f|\mathcal{T}^{\rm mag}_{J-\lambda}(q)|i\rangle\Big]\Bigg\} =$$

$$\frac{4\pi G^2}{2}\Bigg\{\sum_{I,J\geq 0}\frac{i^I}{i^J}\hat{I}\hat{J}\Bigg[l_0 l_0^*|\langle f|\mathcal{M}_{I0}(q)|i\rangle|^2 - l_0^* l_3\langle f|\mathcal{M}_{J0}(q)|i\rangle^*\langle f|\mathcal{L}_{I0}(q)|i\rangle - l_0 l_3^*\langle f|\mathcal{L}_{I0}(q)|i\rangle^*\langle f|\mathcal{M}_{J0}(q)|i\rangle + l_3 l_3^*|\langle f|\mathcal{L}_{J0}(q)|i\rangle|^2\Bigg] + \sum_{\kappa,\lambda=\pm 1}\sum_{I,J\geq 1}\frac{i^I l_\kappa^* l_\lambda}{2i^J}\hat{I}\hat{J}\cdot \Bigg[\langle f|\mathcal{T}^{\rm el}_{I-\kappa}(q)|i\rangle^*\langle f|\mathcal{T}^{\rm el}_{J-\lambda}(q)|i\rangle + \lambda\langle f|\mathcal{T}^{\rm el}_{I-\kappa}(q)|i\rangle^*\langle f|\mathcal{T}^{\rm mag}_{J-\lambda}(q)|i\rangle + \kappa\langle f|\mathcal{T}^{\rm mag}_{I-\kappa}(q)|i\rangle^*\langle f|\mathcal{T}^{\rm el}_{J-\lambda}(q)|i\rangle + \lambda\kappa\langle f|\mathcal{T}^{\rm mag}_{I-\kappa}(q)|i\rangle^*\langle f|\mathcal{T}^{\rm mag}_{J-\lambda}(q)|i\rangle\Bigg]\Bigg\}. \tag{86}$$

The terms in the first sum above are all proportional to factors of the form $\langle f|\mathcal{O}_{J0}|i\rangle^*\langle f|\mathcal{O'}_{J'0}(q)|i\rangle$, where $\mathcal{O}_{J0}(q)$, $\mathcal{O'}_{J0}(q) = \mathcal{M}_{J0}(q)$ or $\mathcal{L}_{J0}(q)$. Applying the Wigner-Eckart theorem, summing over all initial and final states and averaging over the initial states just like before we get

$$\frac{1}{2J_i+1}\sum_{M_i M_f}\langle f|\mathcal{O}_{J0}|i\rangle^*\langle f|\mathcal{O'}_{J'0}(q)|i\rangle = \frac{\delta_{JJ'}}{(2J+1)(2J_i+1)}(J_f||\mathcal{O}_J||J_i)^*(J_f||\mathcal{O'}_J||J_i) = \frac{\delta_{JJ'}}{\hat{J}^2(2J_i+1)}(J_f||\mathcal{O}_J||J_i)^*(J_f||\mathcal{O'}_J||J_i). \tag{87}$$

The terms in the second sum above are similarly all proportional to factors of the form $\langle f|\mathcal{O}_{J\lambda}|i\rangle^*\langle f|\mathcal{O'}_{J'\mu}(q)|i\rangle$, where $\mathcal{O}_{J\lambda}(q)$, $\mathcal{O'}_{J\lambda}(q) = \mathcal{T}^{\rm el}_{J-\lambda}(q)$ or $\mathcal{T}^{\rm mag}_{J-\lambda}(q)$. Proceeding in the same manner as above, we get

$$\frac{1}{2J_i+1}\sum_{M_i M_f}\langle f|\mathcal{O}_{J\lambda}|i\rangle^*\langle f|\mathcal{O'}_{J'\mu}(q)|i\rangle = \frac{\delta_{JJ'}\delta_{\lambda\mu}}{(2J+1)(2J_i+1)}(J_f||\mathcal{O}_J||J_i)^*(J_f||\mathcal{O'}_J||J_i) = \frac{\delta_{JJ'}\delta_{\lambda\mu}}{\hat{J}^2(2J_i+1)}(J_f||\mathcal{O}_J||J_i)^*(J_f||\mathcal{O'}_J||J_i). \tag{88}$$

Combining the results derived above, we finally get

$$\frac{1}{2J_i+1}\sum_{M_i M_f}|\langle f|H_{\rm eff}|i\rangle|^2 = \frac{4\pi}{2J_i+1}\frac{G^2}{2}\Bigg\{\sum_{I,J\geq 0}\frac{i^I}{i^J}\frac{\hat{I}\hat{J}}{\hat{J}^2}\delta_{IJ}\Bigg[l_0 l_0^*|(J_f||\mathcal{M}_J||J_i)|^2 - l_0^* l_3(J_f||\mathcal{M}_J(q)||J_i)^*(J_f||\mathcal{L}_J(q)||J_i) - l_0 l_3^*(J_f|\mathcal{L}_J(q)||J_i)^*(J_f||\mathcal{M}_J(q)||J_i) +$$

$$l_3 l_3^* |(J_f||\mathcal{L}_J(q)||J_i)|^2\Big] + \sum_{\kappa,\lambda=\pm1}\sum_{I,J\geq 1}\frac{i^I l_\kappa^* l_\lambda}{2i^J}\frac{\hat{I}\hat{J}}{\hat{J}^2}\delta_{IJ}\delta_{\kappa\lambda}\Big[(J_f||\mathcal{T}_J^{\rm el}(q)||J_i)^*(J_f||\mathcal{T}_J^{\rm el}(q)||J_i)+$$
$$\lambda(J_f||\mathcal{T}_J^{\rm el}(q)||J_i)^*(J_f||\mathcal{T}_J^{\rm mag}(q)||J_i) + \kappa(J_f||\mathcal{T}_J^{\rm mag}(q)||J_i)^*(J_f||\mathcal{T}_J^{\rm el}(q)||J_i)+$$
$$\lambda\kappa(J_f||\mathcal{T}_J^{\rm mag}(q)||J_i)^*(J_f||\mathcal{T}_J^{\rm mag}(q)||J_i)\Big]\Big\} = \frac{4\pi}{2J_i+1}\frac{G^2}{2}\Big\{\sum_{J\geq 0}\Big[l_0 l_0^*|(J_f||\mathcal{M}_J||J_i)|^2+$$
$$l_3 l_3^*|(J_f||\mathcal{L}_J(q)||J_i)|^2 - l_0^* l_3(J_f||\mathcal{M}_J(q)||J_i)^*(J_f||\mathcal{L}_J(q)||J_i) - l_0 l_3^*(J_f|\mathcal{L}_J(q)||J_i)^*\cdot$$
$$(J_f||\mathcal{M}_J(q)||J_i)\Big] + \sum_{\lambda=\pm1}\sum_{J\geq 1}\frac{l_\lambda^* l_\lambda}{2}\Big[|(J_f||\mathcal{T}_J^{\rm el}(q)||J_i)|^2 + |(J_f||\mathcal{T}_J^{\rm mag}(q)||J_i)|^2+$$
$$\lambda(J_f||\mathcal{T}_J^{\rm el}(q)||J_i)^*(J_f||\mathcal{T}_J^{\rm mag}(q)||J_i) + \lambda(J_f||\mathcal{T}_J^{\rm mag}(q)||J_i)^*(J_f||\mathcal{T}_J^{\rm el}(q)||J_i)\Big]\Big\}. \tag{89}$$

The above expression can be simplified by exploiting the properties of complex numbers and relations involving vectors in the spherical basis defined earlier.

For all $z \in \mathbb{C}$, we can define $\mathrm{Re} : \mathbb{C} \to \mathbb{R}$ by[22, Chapter 1]

$$\mathrm{Re}(z) = \frac{1}{2}(z + z^*). \tag{90}$$

Now, by choosing $z = l_0^* l_3(J_f||\mathcal{M}_J(q)||J_i)^*(J_f||\mathcal{L}_J(q)||J_i)$ we can write

$$\begin{aligned} &- l_0^* l_3(J_f||\mathcal{M}_J(q)||J_i)^*(J_f||\mathcal{L}_J(q)||J_i) - l_0 l_3^*(J_f|\mathcal{L}_J(q)||J_i)^*(J_f||\mathcal{M}_J(q)||J_i) = \\ &- 2\mathrm{Re}\Big(l_0^* l_3(J_f||\mathcal{M}_J(q)||J_i)^*(J_f||\mathcal{L}_J(q)||J_i)\Big), \end{aligned} \tag{91}$$

and similarly with $z = (J_f||\mathcal{T}_J^{\rm el}(q)||J_i)^*(J_f||\mathcal{T}_J^{\rm mag}(q)||J_i)$ we get

$$\begin{aligned} &\lambda(J_f||\mathcal{T}_J^{\rm el}(q)||J_i)^*(J_f||\mathcal{T}_J^{\rm mag}(q)||J_i) + \lambda(J_f||\mathcal{T}_J^{\rm mag}(q)||J_i)^*(J_f||\mathcal{T}_J^{\rm el}(q)||J_i) = \\ &2\lambda\mathrm{Re}\Big((J_f||\mathcal{T}_J^{\rm el}(q)||J_i)^*(J_f||\mathcal{T}_J^{\rm mag}(q)||J_i)\Big). \end{aligned} \tag{92}$$

Next consider the scalar and vector products of vectors in the spherical basis. The scalar product of an arbitrary vector $\mathbf{l}$ with itself is

$$\begin{aligned} &\langle \mathbf{l}|\mathbf{l}\rangle = \mathbf{l}\cdot\mathbf{l}^* = \sum_\lambda l_\lambda \mathbf{e}_\lambda^\dagger \cdot \sum_\kappa l_\kappa^* \mathbf{e}_\kappa = \sum_{\kappa,\lambda} l_\lambda l_\kappa^* \mathbf{e}_\lambda^\dagger\cdot\mathbf{e}_\kappa = \sum_{\kappa,\lambda} l_\lambda l_\kappa^* \delta_{\lambda\kappa} = \sum_\lambda l_\lambda l_\lambda^* = \\ &l_+ l_+^* + l_- l_-^* + l_3 l_3^* \Rightarrow l_+ l_+^* + l_- l_-^* = \sum_{\lambda=\pm1} l_\lambda l_\lambda^* = \mathbf{l}\cdot\mathbf{l}^* - l_3 l_3^*, \end{aligned} \tag{93}$$

where the dot product between the basis vectors follow from the orthonormality of the basis. For vector products between the basis vectors, we utilize the relations defining the spherical basis presented in equations 27 and 28. We get

$$\mathbf{e}_0^\dagger \times \mathbf{e}_0 = \mathbf{e}_{q_3} \times \mathbf{e}_{q_3} = 0, \tag{94}$$

$$\mathbf{e}_\pm^\dagger \times \mathbf{e}_0 = \mp\frac{1}{\sqrt{2}}\left(\mathbf{e}_{q_1} \mp i\mathbf{e}_{q_2}\right) \times \mathbf{e}_{q_3} = \mp\frac{1}{\sqrt{2}}\left(\mathbf{e}_{q_1} \times \mathbf{e}_{q_3} \mp i\mathbf{e}_{q_2} \times \mathbf{e}_{q_3}\right) = \\ \mp\frac{1}{\sqrt{2}}\left(-\mathbf{e}_{q_2} \mp i\mathbf{e}_{q_1}\right) = \mp i\frac{1}{\sqrt{2}}\left(\mp\mathbf{e}_{q_1} + i\mathbf{e}_{q_2}\right) = \pm i\left(\pm\frac{1}{\sqrt{2}}\left(\mathbf{e}_{q_1} \mp i\mathbf{e}_{q_2}\right)\right) = \pm i\mathbf{e}_\mp \tag{95}$$

$$\mathbf{e}_\pm^\dagger \times \mathbf{e}_\pm = \frac{1}{2}\left(\mathbf{e}_{q_1} \mp i\mathbf{e}_{q_2}\right) \times \left(\mathbf{e}_{q_1} \pm i\mathbf{e}_{q_2}\right) = \frac{1}{2}(\mathbf{e}_{q_1} \times \mathbf{e}_{q_1} \pm i\mathbf{e}_{q_1} \times \mathbf{e}_{q_2} \mp i\mathbf{e}_{q_2} \times \mathbf{e}_{q_1} + \\ \mathbf{e}_{q_2} \times \mathbf{e}_{q_2}) = \frac{1}{2}(\pm i\mathbf{e}_{q_1} \times \mathbf{e}_{q_2} \mp i\mathbf{e}_{q_2} \times \mathbf{e}_{q_1}) = \frac{1}{2}(\pm i\mathbf{e}_{q_3} \pm i\mathbf{e}_{q_3}) = \pm i\mathbf{e}_{q_3} = \pm i\mathbf{e}_0, \tag{96}$$

$$\mathbf{e}_\pm^\dagger \times \mathbf{e}_\mp = -\frac{1}{2}\left(\mathbf{e}_{q_1} \mp i\mathbf{e}_{q_2}\right) \times \left(\mathbf{e}_{q_1} \mp i\mathbf{e}_{q_2}\right) = -\frac{1}{2}(\mathbf{e}_{q_1} \times \mathbf{e}_{q_1} \mp i\mathbf{e}_{q_1} \times \mathbf{e}_{q_2} \mp i\mathbf{e}_{q_2} \times \mathbf{e}_{q_1} \\ - \mathbf{e}_{q_2} \times \mathbf{e}_{q_2}) = \frac{1}{2}(\mp i\mathbf{e}_{q_1} \times \mathbf{e}_{q_2} \mp i\mathbf{e}_{q_2} \times \mathbf{e}_{q_1}) = \frac{1}{2}(\mp i\mathbf{e}_{q_3} \pm i\mathbf{e}_{q_3}) = 0, \tag{97}$$

and

$$\mathbf{e}_0^\dagger \times \mathbf{e}_\pm = -\mathbf{e}_0 \times \mathbf{e}_\mp^\dagger = \mathbf{e}_\mp^\dagger \times \mathbf{e}_0 = \mp i\mathbf{e}_\pm, \tag{98}$$

where in deriving the final product we used the antisymmetricity of the vector product and the relation

$$\mathbf{e}_\lambda^\dagger = (-1)^\lambda \mathbf{e}_{-\lambda}. \tag{99}$$

Using the results above, the vector product $\mathbf{l} \times \mathbf{l}^*$ takes the form

$$\mathbf{l} \times \mathbf{l}^* = (l_{-1}\mathbf{e}_-^\dagger + l_3\mathbf{e}_0^\dagger + l_1\mathbf{e}_+^\dagger) \times (l_{-1}^*\mathbf{e}_- + l_3^*\mathbf{e}_0 + l_1^*\mathbf{e}_+) = -il_{-1}l_{-1}^*\mathbf{e}_0 - \\ il_{-1}l_3^*\mathbf{e}_+ + il_3l_{-1}^*\mathbf{e}_- - il_3l_1^*\mathbf{e}_+ + il_1l_3^*\mathbf{e}_- + il_1l_1^*\mathbf{e}_0 = i\Big[(l_1l_3^* + l_3l_{-1}^*)\mathbf{e}_- + \\ (l_1l_1^* - l_{-1}l_{-1}^*)\mathbf{e}_0 - (l_{-1}l_3^* + l_3l_1^*)\mathbf{e}_+\Big]. \tag{100}$$

We denote

$$(\mathbf{l}\times\mathbf{l}^*)_3 = (\mathbf{l}\times\mathbf{l}^*)\cdot\mathbf{e}_0^\dagger = i(l_1 l_1^* - l_{-1}l_{-1}^*). \tag{101}$$

These results can then be used to simplify equation 89. Consider first the first summand on the right side of equation 89. Using the equations above we can write

$$\begin{aligned}
&l_0 l_0^*|(J_f||\mathcal{M}_J||J_i)|^2 + l_3 l_3^*|(J_f||\mathcal{L}_J(q)||J_i)|^2 - l_0^* l_3 (J_f||\mathcal{M}_J(q)||J_i)^*(J_f||\mathcal{L}_J(q)||J_i)\\
&- l_0 l_3^*(J_f|\mathcal{L}_J(q)||J_i)^*(J_f||\mathcal{M}_J(q)||J_i) = l_0 l_0^*|(J_f||\mathcal{M}_J||J_i)|^2 + l_3 l_3^*|(J_f||\mathcal{L}_J(q)||J_i)|^2 -\\
&2\mathrm{Re}(l_0^* l_3 (J_f||\mathcal{M}_J(q)||J_i)^*(J_f||\mathcal{L}_J(q)||J_i)).
\end{aligned} \tag{102}$$

For the second sum of equation 89 we get

$$\begin{aligned}
&\sum_{\lambda=\pm1}\sum_{J\geq1}\frac{l_\lambda^* l_\lambda}{2}\Big[|(J_f||\mathcal{T}_J^{\mathrm{el}}(q)||J_i)|^2 + |(J_f||\mathcal{T}_J^{\mathrm{mag}}(q)||J_i)|^2 + \lambda(J_f||\mathcal{T}_J^{\mathrm{el}}(q)||J_i)^*\cdot\\
&(J_f||\mathcal{T}_J^{\mathrm{mag}}(q)||J_i) + \lambda(J_f||\mathcal{T}_J^{\mathrm{mag}}(q)||J_i)^*(J_f||\mathcal{T}_J^{\mathrm{el}}(q)||J_i)\Big] = \sum_{\lambda=\pm1}\sum_{J\geq1}\frac{l_\lambda^* l_\lambda}{2}\Big[\\
&|(J_f||\mathcal{T}_J^{\mathrm{el}}(q)||J_i)|^2 + |(J_f||\mathcal{T}_J^{\mathrm{mag}}(q)||J_i)|^2 + 2\lambda\mathrm{Re}((J_f||\mathcal{T}_J^{\mathrm{el}}(q)||J_i)^*(J_f||\mathcal{T}_J^{\mathrm{mag}}(q)||J_i))\Big]\\
&= \sum_{J\geq1}\Big[\frac{1}{2}\left(l_{-1}^* l_{-1} + l_1^* l_1\right)\left(|(J_f||\mathcal{T}_J^{\mathrm{el}}(q)||J_i)|^2 + |(J_f||\mathcal{T}_J^{\mathrm{mag}}(q)||J_i)|^2\right) + (l_1^* l_1 - l_{-1}^* l_{-1})\cdot\\
&\mathrm{Re}((J_f||\mathcal{T}_J^{\mathrm{el}}(q)||J_i)^*(J_f||\mathcal{T}_J^{\mathrm{mag}}(q)||J_i))\Big] = \sum_{J\geq1}\Big[\frac{1}{2}\left(\mathbf{l}\cdot\mathbf{l}^* - l_3^* l_3\right)\Big(|(J_f||\mathcal{T}_J^{\mathrm{el}}(q)||J_i)|^2 +\\
&|(J_f||\mathcal{T}_J^{\mathrm{mag}}(q)||J_i)|^2\Big) - i(\mathbf{l}\times\mathbf{l}^*)_3\mathrm{Re}((J_f||\mathcal{T}_J^{\mathrm{el}}(q)||J_i)^*(J_f||\mathcal{T}_J^{\mathrm{mag}}(q)||J_i))\Big].
\end{aligned} \tag{103}$$

Combining these we finally arrive at the result

$$\begin{aligned}
&\frac{1}{2J_i+1}\sum_{M_i M_f}|\,\langle f|H_{\mathrm{eff}}|i\rangle\,|^2 = \frac{4\pi}{2J_i+1}\frac{G^2}{2}\Big\{\sum_{J\geq0}\Big[l_0 l_0^*|(J_f||\mathcal{M}_J||J_i)|^2 +\\
&l_3 l_3^*|(J_f||\mathcal{L}_J(q)||J_i)|^2 - 2\mathrm{Re}(l_3 l_0^*(J_f||\mathcal{L}_J(q)||J_i)(J_f||\mathcal{M}_J(q)||J_i)^*)\Big] +\\
&\sum_{J\geq1}\Big[\frac{1}{2}\left(\mathbf{l}\cdot\mathbf{l}^* - l_3^* l_3\right)\Big(|(J_f||\mathcal{T}_J^{\mathrm{el}}(q)||J_i)|^2 + |(J_f||\mathcal{T}_J^{\mathrm{mag}}(q)||J_i)|^2\Big) -\\
&i(\mathbf{l}\times\mathbf{l}^*)_3\mathrm{Re}((J_f||\mathcal{T}_J^{\mathrm{mag}}(q)||J_i)(J_f||\mathcal{T}_J^{\mathrm{el}}(q)||J_i)^*)\Big]\Big\}.
\end{aligned} \tag{104}$$

2.1.4 Lepton matrix elements

Equation 104 contains a number of factors of the form $l_\mu l_\nu^*$ which are functions of the lepton spins. Thus they contribute to the sums over the lepton spins in equation 80. Before proceeding with the diracology of the lepton matrix elements, the normalization of the Dirac-spinors appearing in equation 23 needs to be fixed. This has actually been already done implicitly while deriving equation 15 when the lepton flux was taken to be $1/V$, which is equivalent to requiring that the Dirac-spinors obey the relation[15, Chapter 5.5]

$$u^\dagger(\boldsymbol{k})u(\boldsymbol{k}) = 1, \quad v^\dagger(\boldsymbol{k})v(\boldsymbol{k}) = 1. \tag{105}$$

Substituting the explicit expressions[15, Page 105]

$$u(\boldsymbol{k}) = N(\boldsymbol{k}) \begin{pmatrix} \chi_\pm \\ \frac{\boldsymbol{\sigma}\cdot\boldsymbol{k}}{E_k+m}\chi_\pm \end{pmatrix}, \quad v(\boldsymbol{k}) = N(-\boldsymbol{k}) \begin{pmatrix} \frac{\boldsymbol{\sigma}\cdot\boldsymbol{k}}{E_k+m}\chi_\pm \\ \chi_\pm \end{pmatrix} \tag{106}$$

for the spinors u and v, we get for particles

$$\begin{aligned} &u^\dagger(\boldsymbol{k})u(\boldsymbol{k}) = |N(\boldsymbol{k})|^2 \left(\chi_\pm^\dagger \quad \tfrac{\boldsymbol{\sigma}^\dagger\cdot\boldsymbol{k}}{E_k+m}\chi_\pm^\dagger\right) \begin{pmatrix} \chi_\pm \\ \frac{\boldsymbol{\sigma}\cdot\boldsymbol{k}}{E_k+m}\chi_\pm \end{pmatrix} = |N(\boldsymbol{k})|^2 \chi_\pm^\dagger\chi_\pm \left(1 + \frac{(\boldsymbol{\sigma}\cdot\boldsymbol{k})^2}{(E_k+m)^2}\right) \\ &= |N(\boldsymbol{k})|^2 \left(1 + \frac{\boldsymbol{k}^2}{(E_k+m)^2}\right) = |N(\boldsymbol{k})|^2 \left(1 + \frac{E_k^2 - m^2}{(E_k+m)^2}\right) = |N(\boldsymbol{k})|^2 \cdot \\ &\left(\frac{(E_k+m)^2 + E_k^2 - m^2}{(E_k+m)^2}\right) = |N(\boldsymbol{k})|^2 \left(\frac{2E_k^2 + 2E_k m}{(E_k+m)^2}\right) = 2E_k|N(\boldsymbol{k})|^2 \left(\frac{E_k+m}{(E_k+m)^2}\right) \\ &= |N(\boldsymbol{k})|^2 \left(\frac{2E_k}{E_k+m}\right) \Rightarrow N(\boldsymbol{k}) = \frac{\sqrt{E_k+m}}{\sqrt{2E_k}} \text{ up to a phase.} \end{aligned} \tag{107}$$

The same result is acquired in the same manner for antiparticles. In deriving the above result we used the properties[23, Appendix D]

$$(\boldsymbol{\sigma}\cdot\boldsymbol{a})^2 = \boldsymbol{a}^2 \text{ and } \sigma_i^\dagger = \sigma_i, \tag{108}$$

for all three-vectors $\boldsymbol{a}$ and all Pauli matrices σ_i, $i \in \{1,2,3\}$.

The spin sums of factors of the form $l_\mu l_\nu^*$ contain factors of

$$\sum_{\text{spins}} u(\boldsymbol{k})\overline{u}(\boldsymbol{k}) \text{ and } \sum_{\text{spins}} v(-\boldsymbol{k})\overline{v}(-\boldsymbol{k}). \tag{109}$$

Before finding expressions for these, we will compute

$$\not{k} = \gamma^\mu k_\mu = \gamma^0 E_k - \gamma^i k_i = \begin{pmatrix} E_k \mathbb{1}_2 & 0 \\ 0 & -E_k \mathbb{1}_2 \end{pmatrix} - \begin{pmatrix} 0 & \sigma^i k_i \\ -\sigma^i k_i & 0 \end{pmatrix} = \begin{pmatrix} E_k \mathbb{1}_2 & -\boldsymbol{\sigma}\cdot\boldsymbol{k} \\ \boldsymbol{\sigma}\cdot\boldsymbol{k} & -E_k \mathbb{1}_2 \end{pmatrix}. \tag{110}$$

We now get

$$\begin{aligned}
&\sum_{\text{spins}} u(\boldsymbol{k})\overline{u}(\boldsymbol{k}) = \sum_{\text{spins}} |N(\boldsymbol{k})|^2 \begin{pmatrix} \chi \\ \frac{\boldsymbol{\sigma}\cdot\boldsymbol{k}}{E_k+m}\chi \end{pmatrix} \begin{pmatrix} \chi^\dagger & \frac{\boldsymbol{\sigma}\cdot\boldsymbol{k}}{E_k+m}\chi^\dagger \end{pmatrix} \gamma^0 = \sum_{\text{spins}} |N(\boldsymbol{k})|^2 \begin{pmatrix} \chi \\ \frac{\boldsymbol{\sigma}\cdot\boldsymbol{k}}{E_k+m}\chi \end{pmatrix} \cdot \\
&\begin{pmatrix} \chi^\dagger & -\frac{\boldsymbol{\sigma}\cdot\boldsymbol{k}}{E_k+m}\chi^\dagger \end{pmatrix} = \frac{E_k+m}{2E_k} \sum_{\text{spins}} \begin{pmatrix} \chi\chi^\dagger & -\frac{\boldsymbol{\sigma}\cdot\boldsymbol{k}}{E_k+m}\chi\chi^\dagger \\ \frac{\boldsymbol{\sigma}\cdot\boldsymbol{k}}{E_k+m}\chi\chi^\dagger & -\frac{\boldsymbol{k}^2}{(E_k+m)^2}\chi\chi^\dagger \end{pmatrix} = \frac{1}{2E_k}\cdot \\
&\begin{pmatrix} (E_k+m)\mathbb{1}_2 & -\boldsymbol{\sigma}\cdot\boldsymbol{k} \\ \boldsymbol{\sigma}\cdot\boldsymbol{k} & -\frac{E_k^2-m^2}{E_k+m}\mathbb{1}_2 \end{pmatrix} = \frac{1}{2E_k} \begin{pmatrix} (E_k+m)\mathbb{1}_2 & -\boldsymbol{\sigma}\cdot\boldsymbol{k} \\ \boldsymbol{\sigma}\cdot\boldsymbol{k} & -\frac{(E_k-m)(E_k+m)}{E_k+m}\mathbb{1}_2 \end{pmatrix} = \frac{1}{2E_k}\cdot \\
&\begin{pmatrix} (E_k+m)\mathbb{1}_2 & -\boldsymbol{\sigma}\cdot\boldsymbol{k} \\ \boldsymbol{\sigma}\cdot\boldsymbol{k} & -(E_k-m)\mathbb{1}_2 \end{pmatrix} = \frac{1}{2E_k} \begin{pmatrix} E_k\mathbb{1}_2 & -\boldsymbol{\sigma}\cdot\boldsymbol{k} \\ \boldsymbol{\sigma}\cdot\boldsymbol{k} & -E_k\mathbb{1}_2 \end{pmatrix} + \frac{1}{2E_k} \begin{pmatrix} m\mathbb{1}_2 & 0 \\ 0 & m\mathbb{1}_2 \end{pmatrix} = \\
&\frac{1}{2E_k}(\not{k}+m),
\end{aligned} \tag{111}$$

where we used

$$\sum_{\text{spins}} \chi\chi^\dagger = \chi_+\chi_+^\dagger + \chi_-\chi_-^\dagger = \begin{pmatrix} 1 & 0 \\ 0 & 0 \end{pmatrix} + \begin{pmatrix} 0 & 0 \\ 0 & 1 \end{pmatrix} = \begin{pmatrix} 1 & 0 \\ 0 & 1 \end{pmatrix} \equiv \mathbb{1}_2. \tag{112}$$

Again, we get for the antiparticle spinors $\overline{v}$ and v in a completely similar manner

$$\sum_{\text{spins}} v(\boldsymbol{k})\overline{v}(\boldsymbol{k}) = \frac{1}{2E_k}(\not{k}-m) \Rightarrow \sum_{\text{spins}} v(-\boldsymbol{k})\overline{v}(-\boldsymbol{k}) = -\frac{1}{2E_k}(\not{k}+m). \tag{113}$$

The above identities can be used to calculate the spin sums over the $l_\mu l_\nu^*$ factors. For

$l_0 l_0^*$ we get in the case of a charged current particle reaction[11, Chapter 46]

$$\frac{V^2}{2}\sum_{\text{lepton spins}} l_0 l_0^* = \frac{V^2}{2}\sum_{\text{lepton spins}} \frac{1}{V}\overline{u}(\boldsymbol{k}')\gamma_0(1-\gamma_5)u(\boldsymbol{k})\frac{1}{V}\left(\overline{u}(\boldsymbol{k}')\gamma_0(1-\gamma_5)u(\boldsymbol{k})\right)^* =$$
$$\frac{1}{2}\sum_{\text{lepton spins}} \overline{u}(\boldsymbol{k}')\gamma_0(1-\gamma_5)u(\boldsymbol{k})\left(\overline{u}(\boldsymbol{k}')\gamma_0(1-\gamma_5)u(\boldsymbol{k})\right)^\dagger = \frac{1}{2}\sum_{\text{lepton spins}} \overline{u}(\boldsymbol{k}')\gamma_0(1-$$
$$\gamma_5)u(\boldsymbol{k})u^\dagger(\boldsymbol{k})(1-\gamma_5^\dagger)\gamma_0^\dagger(u^\dagger(\boldsymbol{k}')\gamma^0)^\dagger = \frac{1}{2}\sum_{\text{lepton spins}} \overline{u}(\boldsymbol{k}')\gamma_0(1-\gamma_5)u(\boldsymbol{k})u^\dagger(\boldsymbol{k})\gamma^0\gamma^0(1-$$
$$\gamma_5)\gamma_0\gamma^0 u(\boldsymbol{k}') = \frac{1}{2}\sum_{\text{lepton spins}} \overline{u}(\boldsymbol{k}')\gamma_0(1-\gamma_5)u(\boldsymbol{k})\overline{u}(\boldsymbol{k})\gamma^0(1-\gamma_5)u(\boldsymbol{k}'),$$

(114)

where we used a number of properties of the gamma matrices and the fact that for complex numbers such as $\overline{u}(\boldsymbol{k}')\gamma_0(1-\gamma_5)u(\boldsymbol{k})$, we have $* = \dagger$. Next we will consider the right side of the above expression componentwise, move the factor $u(\boldsymbol{k}')$ in front of the factor $\overline{u}(\boldsymbol{k}')$, apply equation 111 and write the resulting expression as a trace of a product of matrices[15, Chapter 6]. We thus get

$$\frac{V^2}{2}\sum_{\text{lepton spins}} l_0 l_0^* = \frac{1}{2}\sum_{\text{lepton spins}} \overline{u}(\boldsymbol{k}')\gamma_0(1-\gamma_5)u(\boldsymbol{k})\overline{u}(\boldsymbol{k})\gamma^0(1-\gamma_5)u(\boldsymbol{k}') =$$
$$\frac{1}{2}\mathrm{Tr}\Big[\frac{\not{k}'+m}{2E_{k'}}\gamma_0(1-\gamma_5)\frac{\not{k}}{2E_k}\gamma^0(1-\gamma_5)\Big] = \frac{1}{8E_{k'}E_k}\Big\{\mathrm{Tr}\Big[\not{k}'\gamma_0(1-\gamma_5)\not{k}\gamma^0(1-\gamma_5)\Big]+$$
$$\mathrm{Tr}\Big[m\gamma_0(1-\gamma_5)\not{k}\gamma^0(1-\gamma_5)\Big]\Big\} = \frac{1}{8E_{k'}E_k}\Big\{\mathrm{Tr}\Big[\not{k}'\gamma_0\not{k}\gamma^0(1-\gamma_5)(1-\gamma_5)\Big]+$$
$$\mathrm{Tr}\Big[\not{k}\gamma^0(1-\gamma_5)m\gamma_0(1-\gamma_5)\Big]\Big\} = \frac{1}{8E_{k'}E_k}\Big\{2\mathrm{Tr}\Big[\not{k}'\gamma_0\not{k}\gamma^0(1-\gamma_5)\Big]+$$
$$\mathrm{Tr}\Big[\not{k}\gamma^0(1-\gamma_5)(1+\gamma_5)m\gamma_0\Big]\Big\} = \frac{1}{4E_{k'}E_k}\Big\{\mathrm{Tr}\Big[\not{k}'\gamma_0\not{k}\gamma^0\Big] - \mathrm{Tr}\Big[\not{k}'\gamma_0\not{k}\gamma^0\gamma_5\Big]\Big\} =$$
$$\frac{1}{4E_{k'}E_k}4((k')^0k^0 + (k')^0k^0 - k'_\mu k^\mu) = \frac{1}{E_{k'}E_k}(k'_0k^0 + \boldsymbol{k}'\cdot\boldsymbol{k}) = \frac{1}{E_{k'}E_k}(E_{k'}E_k + \boldsymbol{k}'\cdot\boldsymbol{k})$$
$$= 1 + \hat{\boldsymbol{k}}'\cdot\hat{\boldsymbol{k}},$$

(115)

Where we have defined the vectors $\hat{\boldsymbol{k}} = \boldsymbol{k}/(E_k)$ and $\hat{\boldsymbol{k}}' = \boldsymbol{k}'/(E_{k'})$. For neutral current particle reactions we have $\not{k}'$ instead of $\not{k}' + m$, which eventually leads to the same result as for charged current particle reactions, since the outgoing lepton mass m cancelled out in the derivation above. The derivation is done similarly for charged

and neutral current antiparticle reactions and the result is again the same as the one above.

The rest of the lepton spin sums are done in a similar manner as the one above, and the results are[11, Page 482]

$$\frac{V^2}{2}\sum_{\text{lepton spins}} l_3 l_3^* = 1 - \hat{\boldsymbol{k}}' \cdot \hat{\boldsymbol{k}} + 2\frac{1}{E_{k'}E_k q^2}(\boldsymbol{k}\cdot\boldsymbol{q})(\boldsymbol{k}'\cdot\boldsymbol{q}), \tag{116}$$

$$\frac{V^2}{2}\sum_{\text{lepton spins}} l_3 l_0^* = \frac{\boldsymbol{q}}{q}\cdot\left(\frac{\boldsymbol{k}}{E_k} + \frac{\boldsymbol{k}'}{E_{k'}}\right), \tag{117}$$

$$\frac{V^2}{2}\sum_{\text{lepton spins}} \frac{1}{2}\left(\mathbf{l}\cdot\mathbf{l}^* - l_3 l_3^*\right) = 1 - \frac{1}{E_{k'}E_k q^2}(\boldsymbol{k}\cdot\boldsymbol{q})(\boldsymbol{k}'\cdot\boldsymbol{q}) \tag{118}$$

and

$$-\frac{i}{2}\frac{V^2}{2}\sum_{\text{lepton spins}} (\mathbf{l}\times\mathbf{l}^*)_3 = \pm\frac{\boldsymbol{q}}{q}\cdot\left(\frac{\boldsymbol{k}}{E_k} - \frac{\boldsymbol{k}'}{E_{k'}}\right), \tag{119}$$

where in the last one the upper sign is used for neutrino, and the lower sign for antineutrino reactions respectively. These equations, together with earlier results, can then be used to finally arrive at an expression for the double differential cross section. By defining the Coulomb-longitudinal (CL) and transverse (T) contributions as[24]

$$\begin{aligned}&\sigma_{CL}^J \equiv (1+\cos\theta)|(J_f||\mathcal{M}_J(q)||J_i)|^2 + (1+\cos\theta - 2b\sin^2\theta)|(J_f||\mathcal{L}_J(q)||J_i)|^2 + \\ &qE_{\text{exc}}(1+\cos\theta)2\text{Re}\left[(J_f||\mathcal{M}_J(q)||J_i)(J_f||\mathcal{L}_J(q)||J_i)^*\right]\end{aligned} \tag{120}$$

and

$$\begin{aligned}&\sigma_T^J \equiv (1-\cos\theta + b\sin^2\theta)\left[|(J_f||\mathcal{T}_J^{\text{mag}}(q)||J_i)|^2 + |(J_f||\mathcal{T}_J^{\text{el}}(q)||J_i)|^2\right] \mp \\ &\frac{E_{k'}+E_k}{q}(1-\cos\theta)2\text{Re}\left[(J_f||\mathcal{T}_J^{\text{mag}}(q)||J_i)(J_f||\mathcal{T}_J^{\text{el}}(q)||J_i)^*\right],\end{aligned} \tag{121}$$

where $E_{\text{exc}} = E_{k'} - E_k$ and $q = |\boldsymbol{q}|$, we can write the double-differential cross section as

$$\frac{\mathrm{d}^2\sigma_{i\to f}}{\mathrm{d}\Omega\mathrm{d}E_{\text{exc}}} = \frac{G^2 k' E_{k'}}{\pi(2J_i+1)}\left(\sum_{J\geq 0}\sigma_{CL}^J + \sum_{J\geq 1}\sigma_T^J\right). \tag{122}$$

In the above expressions, θ is the angle between incoming and outgoing neutrinos

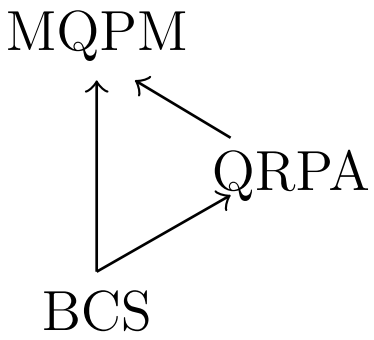

Figure 4. The hierarchy of the nuclear models used in this thesis. An arrow from one model to another indicates that the results of that model were used as inputs for the other.

and $b = E_k E_{k'}/q^2$.

2.2 Nuclear models

In this section we will present the theoretical nuclear physics relevant to this thesis. We will first discuss the concepts and ideas of nuclear theory in general and later use them to review the theory behind the nuclear models used in this work. The nuclear model that actually produced inputs for the scattering cross section calculations (MQPM) is built upon other, more simple models (BCS and QRPA) and uses their results as inputs for certain parameters. This hierarchy between these models is illustrated in figure 4. We will discuss each of these models at varying levels of detail by utilizing a powerful and widely used standard approach to deriving nuclear models, namely the equations-of-motion method.

2.2.1 The nuclear mean-field

The atomic nucleus is a quantum mechanical many-body system composed of strongly interacting protons and neutrons. When the nuclear force is assumed to act only between pairs of nucleons and they are taken to be point-like particles without an internal structure, the nuclear Hamiltonian of a nucleus with mass and neutron numbers A and N can be written as[10, Chapter 3]

$$H = T + V = \sum_{i=1}^{A} t(\boldsymbol{x}_i) + \frac{1}{2}\sum_{i\neq j}^{A} v(\boldsymbol{x}_i,\boldsymbol{x}_j), \tag{123}$$

where $t(\boldsymbol{x}_i)$ is the single-nucleon kinetic energy operator and $v(\boldsymbol{x}_i,\boldsymbol{x}_j)$ the potential energy operator for a pair of nucleons. Solving the resulting Schrödinger equation

$$H\Psi(\boldsymbol{x}_1,\boldsymbol{x}_2,...,\boldsymbol{x}_A) = E\Psi(\boldsymbol{x}_1,\boldsymbol{x}_2,...,\boldsymbol{x}_A) \tag{124}$$

is an immensely difficult task not only due to the complicated form of the nuclear force, but also due to the general difficulty of interacting quantum mechanical many-body problems, for which analytical solutions are known for only the simplest of special cases. A number of approaches to make the problem more tractable by approximating certain aspects of the system and simplifying it have been developed. They usually involve solving the stationary state wave functions and the corresponding energies numerically, often through the means of diagonalizing the Hamiltonian matrix of the system. In the following we will do just that by introducing the concept of a nuclear mean field, express the problem in terms of particle creation and annihilation operators of second quantization and finally transform the particle operators into quasiparticle operators, arriving at the BCS model for atomic nuclei.

The Hamiltonian of equation 123 can be split into a non-interacting quasiparticle part and residual interaction part by adding and subtracting a mean field term on the right side of this equation[10, Page 40]. The mean field term is composed of single-particle potentials summed over the number of nucleons. Formally the mean field experienced by a single nucleon can be thought of as resulting from the interactions of the nucleon with the other $A-1$ nucleons during some small interval of time $\Delta t = t_f - t_i$, averaged over the length of the interval[10, Page 41]. The idea of the mean field as a time averaged potential between the nucleons is not applicable in practice and serves only as a formal definition and to provide intuitive understanding for the concept, with the practical mean field being determined in other ways. Nevertheless, we may write

$$v(\boldsymbol{x}_i) = \frac{1}{\Delta t}\int_{t_i}^{t_f}\sum_{j\neq i}^{A} v(\boldsymbol{x}_i,\boldsymbol{x}_j)\mathrm{d}t, \quad V_{\text{mean field}} = \sum_{i=1}^{A} v(\boldsymbol{x}_i), \tag{125}$$

where in the former $v(\boldsymbol{x}_i,\boldsymbol{x}_j) = v(\boldsymbol{x}_i(t),\boldsymbol{x}_j(t))$. It should also be noted that the mean field we consider here is spherically symmetric, and all nuclear models discussed in this thesis are applicable to spherical (or in practice, nearly spherical) nuclei. Deformed mean fields and nuclei will not be considered.

Adding and subtracting the mean field potential to the nuclear Hamiltonian, we can write it as

$$H = \sum_{i=1}^{A} t(\boldsymbol{x}_i) + \sum_{i=1}^{A} v(\boldsymbol{x}_i) + \frac{1}{2}\sum_{i\neq j}^{A} v(\boldsymbol{x}_i,\boldsymbol{x}_j) - \sum_{i=1}^{A} v(\boldsymbol{x}_i) = H_0 + V_{\text{RES}}, \tag{126}$$

where we have defined[10, Page 40]

$$H_0 = \sum_{i=1}^{A} t(\boldsymbol{x}_i) + \sum_{i=1}^{A} v(\boldsymbol{x}_i) \text{ and } V_{\text{RES}} = \frac{1}{2}\sum_{i\neq j}^{A} v(\boldsymbol{x}_i,\boldsymbol{x}_j) - \sum_{i=1}^{A} v(\boldsymbol{x}_i). \tag{127}$$

We assume that V_{RES} is considerably smaller than V and neglect it for now. The Schrödinger equation for the non-interacting system is then

$$H_0\Psi(\boldsymbol{x}_1,\boldsymbol{x}_2,...,\boldsymbol{x}_A) = \left(\sum_{i=1}^{A} t(\boldsymbol{x}_i) + \sum_{i=1}^{A} v(\boldsymbol{x}_i)\right)\Psi(\boldsymbol{x}_1,\boldsymbol{x}_2,...,\boldsymbol{x}_A) = E\Psi(\boldsymbol{x}_1,\boldsymbol{x}_2,...,\boldsymbol{x}_A), \tag{128}$$

which separates into A identical single-quasiparticle Schrödinger equations

$$\left(t(\boldsymbol{x}) + v(\boldsymbol{x})\right)\psi_\alpha(\boldsymbol{x}) = h(\boldsymbol{x})\psi_\alpha(\boldsymbol{x}) = \epsilon_\alpha\psi_\alpha(\boldsymbol{x}), \quad h(\boldsymbol{x}) = t(\boldsymbol{x}) + v(\boldsymbol{x}), \tag{129}$$

with the ansatz

$$\Psi(\boldsymbol{x}_1,\boldsymbol{x}_2,...,\boldsymbol{x}_A) = \psi_{\alpha_1}(\boldsymbol{x}_1)\psi_{\alpha_2}(\boldsymbol{x}_2)\cdots\psi_{\alpha_A}(\boldsymbol{x}_A), \text{ with } \sum_{i=1}^{A}\epsilon_{\alpha_i} = E, \tag{130}$$

where we have adopted the so called Baranger notation[25]

$$|n_a l_a j_a m_\alpha\rangle \equiv |a m_\alpha\rangle \equiv |\alpha\rangle \tag{131}$$

for the quantum numbers of the single-quasiparticle states. Of these quantum numbers, l_a and j_a denote the orbital and total angular momentum of the state respectively, while m_α is the projection of j_a onto the z-axis and is known as the magnetic quantum number. The n_a is a quantum number that counts the states with a particular l_a value. We will still choose refer to these single-quasiparticle states as particles instead of quasiparticles, as we will reserve that term to the context of the BCS model. Equation 129 can then be solved for the eigenstates and -energies of the non-interacting system after the mean-field $v(\boldsymbol{x})$ is specified. There exists a number

of methods for determining the mean-field, ranging from treating the minimization of the residual interaction between the particles as a variational problem in the set of single-particle eigenstates $\{\psi_\alpha\}$ and solving the resulting non-linear equation iteratively for self-consistency, to descriptions based on realistic bare nucleon-nucleon interaction and meson exchange potentials, to simply picking a mathematically convenient phenomenological potential that exhibits the essential features of a more rigorously determined mean-field. In this thesis we will take the latter approach and choose the Coulomb-corrected Woods-Saxon potential with spin-orbit coupling as a phenomenological mean-field.

The Woods-Saxon mean-field is a spherically symmetric single-particle potential given as a function of the radial distance r by[26]

$$v_{WS}(r) = \frac{-V_0^{(WS)}}{1 + e^{\frac{r-R}{a}}}, \tag{132}$$

where $V_0^{(WS)}$, R and a are parameters that characterize the depth, radius and thickness of the potential respectively. A plot of the potential with typical parameter values is presented in figure 5. The essential features of the mean-field that arise due to the nuclear strong force are captured by the Woods-Saxon potential. In addition to the strong interaction, the protons in the nucleus as charged particles also experience the electromagnetic interaction. In order to take this into account, the mean-field potential experienced by protons is supplemented with a term of[10, Page 46]

$$v_C(r) = \frac{Ze^2}{4\pi\epsilon_0} \cdot \begin{cases} \frac{3-(r/R)^2}{2R}, r \leq R \\ \frac{1}{r}, r > R \end{cases}, \tag{133}$$

i.e. the electrostatic potential of a charged sphere of radius R. The final piece that we will add to the phenomenological potential is the so called spin-orbit term[3, Chapter 5]. It is proportional to $\boldsymbol{L} \cdot \boldsymbol{S}$, that is, the scalar product of the particle orbital ($\boldsymbol{L}$) and spin ($\boldsymbol{S}$) angular momentum operators. The historical motivation behind the inclusion of the spin-orbit term in the mean-field is related to the mean-field shell model of the atomic nucleus[3, Chapter 5], a theory where nucleon configurations are taken to correspond to specific ways of placing the nucleons on independent single-particle orbitals characterized by their total angular momentum j, orbital angular momentum l and the quantum number n which indicates the relative order

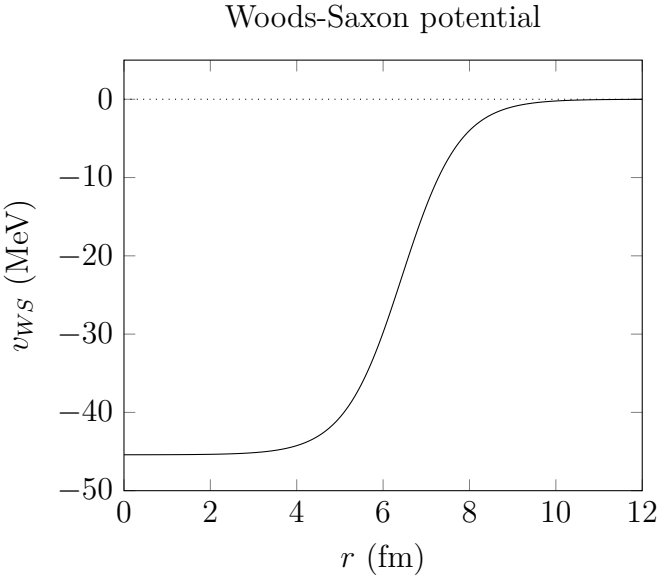

Figure 5. Illustration of a typical neutron Woods-Saxon potential for a nucleus in the mass range of the nuclei ^{127}I and ^{133}Cs that were considered in this thesis. The parameters V_0, R and a were chosen according to their defining equations in appendix A. Values of $A = 130$, $N = 76$ and $Z = 54$, which are intermediate to the two nuclei considered, were used.

of the orbitals with the same l, with higher n values corresponding to orbitals with higher energy (analogous to the principal quantum number of atomic physics). The explicit form of the spin-orbit interaction used in this thesis is[10, Chapter 3.2]

$$v_{SO}(r)\boldsymbol{L}\cdot\boldsymbol{S} = V_0^{(SO)}\frac{r_0^2}{r}\left(\frac{\mathrm{d}}{\mathrm{d}r}\frac{1}{1+e^{\frac{r-R}{a}}}\right)\boldsymbol{L}\cdot\boldsymbol{S} = -\frac{V_0^{(SO)}}{V_0^{(WS)}}\frac{r_0^2}{r}\left(\frac{\mathrm{d}}{\mathrm{d}r}v_{WS}(r)\right)\boldsymbol{L}\cdot\boldsymbol{S}, \quad (134)$$

where the derivative $\mathrm{d}/\mathrm{d}r$ is taken to operate only on the function inside the parenthesis, that is, $v_{WS}(r)$.

Assembling the different parts of the potential together, we finally arrive at an expression for the Hamiltonian of the single-particle Schrödinger equation:

$$h(\boldsymbol{x}) = h(r) = -\frac{1}{2m}\nabla^2 + v_{WS}(r) + v_C(r) + v_{SO}(r)\boldsymbol{L}\cdot\boldsymbol{S}. \quad (135)$$

The Laplacian expressed in spherical coordinates is

$$\nabla^2 = \frac{1}{r^2}\left[\frac{\partial}{\partial r}\left(r^2\frac{\partial}{\partial r}\right) + \frac{1}{\sin\theta}\frac{\partial}{\partial\theta}\left(\sin\theta\frac{\partial}{\partial\theta}\right) + \frac{1}{\sin^2\theta}\frac{\partial^2}{\partial\phi^2}\right] = \nabla_r^2 + \frac{\nabla_\Omega^2}{r^2}, \quad (136)$$

where we have defined

$$\nabla_r^2 = \frac{1}{r^2}\frac{\partial}{\partial r}\left(r^2\frac{\partial}{\partial r}\right) \text{ and } \nabla_\Omega^2 = \frac{1}{\sin\theta}\frac{\partial}{\partial\theta}\left(\sin\theta\frac{\partial}{\partial\theta}\right) + \frac{1}{\sin^2\theta}\frac{\partial^2}{\partial\phi^2}. \tag{137}$$

By starting from the definition of the angular momentum as the generator of rotations, it can be shown that the Cartesian components of $\boldsymbol{L}$ expressed in spherical coordinates are[13, Chapter 3.6]

$$\begin{aligned} L_x &= i\left(\sin\phi\frac{\partial}{\partial\theta} + \cot\theta\cos\phi\frac{\partial}{\partial\phi}\right), \\ L_y &= i\left(-\cos\phi\frac{\partial}{\partial\theta} + \cot\theta\sin\phi\frac{\partial}{\partial\phi}\right) \text{ and} \\ L_z &= -i\frac{\partial}{\partial\phi}. \end{aligned} \tag{138}$$

From these it follows straightforwardly that

$$\boldsymbol{L}^2 = L_x^2 + L_y^2 + L_z^2 = -\frac{1}{\sin\theta}\frac{\partial}{\partial\theta}\left(\sin\theta\frac{\partial}{\partial\theta}\right) - \frac{1}{\sin^2\theta}\frac{\partial^2}{\partial\phi^2} = -\nabla_\Omega^2. \tag{139}$$

The Laplacian can thus be written as

$$\nabla^2 = \nabla_r^2 - \frac{\boldsymbol{L}^2}{r^2} \tag{140}$$

and the single-particle Hamiltonian as

$$h(r) = -\frac{1}{2m}\left(\nabla_r^2 - \frac{\boldsymbol{L}^2}{r^2}\right) + v_{WS}(r) + v_C(r) + v_{SO}(r)\boldsymbol{L}\cdot\boldsymbol{S}. \tag{141}$$

After specifying $h(r)$, the states ψ_α and their energies ϵ_α can be solved, which in the case of the Woods-Saxon potential will be done numerically.

After the set of single-particle states $\{\psi_\alpha\}$ has been acquired, the complete solutions of equation 129 can be constructed as products of these single-particle states. As the system consists of multiple identical fermions, the complete solution wave functions Ψ must be antisymmetric with respect to the interchange of any two nucleons of the same species[17, Chapter 5]. This is achieved by forming Slater determinants of the single-particle states[10, Pages 42 and 57]. Slater determinants are, however, mathematically and notationally cumbersome to manipulate, as the

number of single-particle product terms in the wave function is equal to the product of the number of ways in which N neutrons and Z protons can be arranged, which is $N! \cdot Z!$. This results in an infeasibly large number of terms for all but the lightest of nuclei. To avert this problem, we will adopt the standard formalism of many-body quantum mechanics known as the occupation number representation.

2.2.2 Second quantization and the EoM method

To approach the problem of representing the Slater determinants of the wave functions of nuclei, we will first consider the set of single-particle states $\{|\alpha\rangle\}$ that were acquired as solutions of equation 129 ($\psi_\alpha(\boldsymbol{x}) = \langle \boldsymbol{x}|\alpha\rangle$). From these we can construct any N-particle Slater determinant $|\alpha_1\alpha_2...\alpha_N\rangle$, from which in turn we can construct the set of all N-particle Slater determinants $\{|\alpha_1\alpha_2...\alpha_N\rangle\}$ in the single-particle states. The set of Slater determinants spans (in the single-particle basis) the entire Hilbert space for N-identical particles which we will denote by $\mathcal{H}_N$. In particular, we have the vacuum state $|0\rangle$, which is the only element of $\mathcal{H}_0$. We can now define the Fock space $\mathcal{H}_F$ as[13, Chapter 7.5]

$$\mathcal{H}_F = \mathcal{H}_0 \oplus \mathcal{H}_1 \oplus \mathcal{H}_2 \oplus \cdots . \tag{142}$$

The advantage of the Fock space is that N-particle Slater determinants, which are Fock space vectors, can be represented by their occupation numbers n_1,n_2,...,n_N of the single-particle states which specify a Slater determinant completely. We thus adopt the notation[13, Page 460]

$$|\alpha_1\alpha_2...\alpha_N\rangle \equiv |n_1,n_2,...\rangle . \tag{143}$$

The states of this occupation number representation are conveniently understood in terms of creation and annihilation operators that provide mappings from the Hilbert spaces of N-identical particles to Hilbert spaces of $N+1$ and $N-1$ particles.

We define the creation $c_\alpha^\dagger$ and annihilation c_α operators based on their action on Fock space vectors. We have[13, Page 461]

$$c_\alpha^\dagger \, |n_1,n_2,...,n_\alpha,...\rangle = \eta_\alpha \, |n_1,n_2,...,n_\alpha + 1,...\rangle \text{ , when } n_\alpha = 0, \tag{144}$$

$$c_\alpha \left|n_1,n_2,...,n_\alpha,...\right\rangle = \eta_\alpha \left|n_1,n_2,...,n_\alpha - 1,...\right\rangle, \text{ when } n_\alpha = 1 \tag{145}$$

and

$$c_\alpha^\dagger \left|n_1,n_2,...,n_\alpha,...\right\rangle = c_\alpha \left|n_1,n_2,...,n_\alpha,...\right\rangle = 0, \text{ otherwise.} \tag{146}$$

In other words, the creation and annihilation operators change the particle number of the system by adding and removing particles respectively. Specifying the phase factor η_α as -1 raised to the power of the sum of all occupation numbers on the left of n_α specifies also the standard order of which the operators are to be written when constructing many-body states, which is

$$\left|n_1,n_2,...\right\rangle = \left|\alpha_1\alpha_2...\alpha_N\right\rangle = c_{\alpha_1}^\dagger c_{\alpha_2}^\dagger \cdots c_{\alpha_N}^\dagger \left|0\right\rangle. \tag{147}$$

The operators satisfy the standard fermionic anticommutation relations[13, Page 463]

$$\{c_\alpha,c_\beta^\dagger\} = \delta_{\alpha\beta}, \quad \{c_\alpha^\dagger,c_\beta^\dagger\} = \{c_\alpha,c_\beta\} = 0. \tag{148}$$

This formalism of representing the problem of a quantum many-body system in terms of the creation and annihilation operators is known as second quantization, which is a central topic of this section. We will next consider the construction of nuclear operators in second quantization.

It can be shown that a general one-body operator O in coordinate representation

$$O = \sum_{i=1}^{A} o(\boldsymbol{x}_i) \tag{149}$$

can be expressed in a second quantized form[10, Page 67]

$$O = \sum_{\alpha\beta} o_{\alpha\beta} c_\alpha^\dagger c_\beta, \tag{150}$$

where

$$o_{\alpha\beta} = \langle\alpha|O|\beta\rangle = \int \psi_\alpha^\dagger(\boldsymbol{x}) o(\boldsymbol{x}) \psi_\beta(\boldsymbol{x}) \mathrm{d}^3\boldsymbol{x}. \tag{151}$$

In particular, we have for spherical tensor operators $\mathcal{O}_{\lambda\mu}$ (such as the multipole

operators of equation 78)

$$\mathcal{O}_{\lambda\mu} = \sum_{\alpha\beta} \langle\alpha|O_{\lambda\mu}|\beta\rangle\, c^\dagger_\alpha c_\beta = \sum_{\alpha\beta} \hat{j}_\alpha^{-1}(a||O_\lambda||b)(j_\beta m_\beta \lambda\mu|j_\alpha m_\alpha) c^\dagger_\alpha c_\beta =$$
$$\sum_{\alpha\beta} \hat{j}_\alpha^{-1}(a||O_\lambda||b)(-1)^{j_\beta - m_\beta} \frac{\hat{j}_\alpha}{\hat{\lambda}} (j_\alpha m_\alpha j_\beta - m_\beta|\lambda\mu) c^\dagger_\alpha c_\beta = \hat{\lambda}^{-1} \sum_{ab} (a||O_\lambda||b) \Bigg[$$
$$\sum_{m_\alpha m_\beta} (j_\alpha m_\alpha j_\beta - m_\beta|\lambda\mu) c^\dagger_\alpha (-1)^{j_\beta - m_\beta} c_\beta \Bigg] = \hat{\lambda}^{-1} \sum_{ab} (a||O_\lambda||b) \Bigg[$$
$$\sum_{m_\alpha m_\beta} (j_\alpha m_\alpha j_\beta - m_\beta|\lambda\mu) c^\dagger_\alpha \tilde{c}_{-\beta} \Bigg] = \hat{\lambda}^{-1} \sum_{ab} (a||O_\lambda||b) \Bigg[\sum_{m_\alpha m_\beta} (j_\alpha m_\alpha j_\beta m_\beta|\lambda\mu) c^\dagger_\alpha \tilde{c}_\beta \Bigg] =$$
$$\hat{\lambda}^{-1} \sum_{ab} (a||O_\lambda||b) \left[c^\dagger_\alpha \tilde{c}_\beta \right]_{\lambda\mu}, \tag{152}$$

where we have used the Wigner-Eckart theorem, the cyclic property[10, Page 9]

$$(j_1 m_1 j_2 m_2|jm) = (-1)^{j_1 - m_1} \frac{\hat{j}}{\hat{j}_2} (j m j_1 - m_1|j_2 m_2) \tag{153}$$

of Clebsch–Gordan coefficients, defined the operator

$$\tilde{c}_\beta = (-1)^{j_\beta + m_\beta} c_{-\beta} = (-1)^{j_\beta + m_\beta} c_{b,-m_\beta} \tag{154}$$

and finally used the fact that both $c^\dagger_\alpha$ and $\tilde{c}_\beta$ are spherical tensor operators[10, Page 68], so the sum over the magnetic quantum numbers m_α and m_β can be written as a tensor product after making a change of index $-m_\beta \to m_\beta$. Two-body operators can be shown to have second quantized forms similar to the ones of one-body operators of equation 149. In particular we have for the potential[10, Page 69]

$$V = \frac{1}{2} \sum_{\alpha\beta\gamma\delta} \langle\alpha\beta|\, V\, |\gamma\delta\rangle\, c^\dagger_\alpha c^\dagger_\beta c_\delta c_\gamma = \frac{1}{2} \sum_{\alpha\beta\gamma\delta} v_{\alpha\beta\gamma\delta} c^\dagger_\alpha c^\dagger_\beta c_\delta c_\gamma = \frac{1}{4} \sum_{\alpha\beta\gamma\delta} \overline{v}_{\alpha\beta\gamma\delta} c^\dagger_\alpha c^\dagger_\beta c_\delta c_\gamma, \tag{155}$$

where the antisymmetrized two-nucleon interaction matrix element $\overline{v}_{\alpha\beta\gamma\delta}$ is defined as

$$\overline{v}_{\alpha\beta\gamma\delta} = v_{\alpha\beta\gamma\delta} - v_{\alpha\beta\delta\gamma}. \tag{156}$$

The full nuclear Hamiltonian of equation 126 could now be expressed as a matrix in the single-particle basis (which in practice would be truncated) and the energies and

wave functions of the ground state and the excited states solved by diagonalization of said matrix. Alternatively, we can treat nuclear configuration mixing as a variational problem and derive the related equations by an approach known as the equations of motion method, which we will employ below.

The equations of motion (EoM) method[10, Chapter 11] is a powerful approach to the nuclear many-body problem that can be employed to derive a number of sophisticated nuclear models. The idea behind EoM is to define an operator $Q^\dagger_\omega$, that creates an excitation $|\omega\rangle$ when operated upon the vacuum state $|0\rangle$, in terms of products of creation and annihilation operators. We require that $|\omega\rangle$ fulfils the Schrödinger equation

$$H\,|\omega\rangle = E_\omega\,|\omega\rangle \tag{157}$$

and construct the equation of motion for the excitation creation operator $Q^\dagger_\omega$[10, Chapter 11.1.1]:

$$\begin{aligned}&[H,Q^\dagger_\omega]\,|0\rangle = HQ^\dagger_\omega\,|0\rangle - Q^\dagger_\omega H\,|0\rangle = H\,|\omega\rangle - Q^\dagger_\omega E_0\,|0\rangle = E_\omega\,|\omega\rangle - E_0\,|\omega\rangle = \\ &(E_\omega - E_0)\,|\omega\rangle = (E_\omega - E_0)Q^\dagger_\omega\,|0\rangle \Leftrightarrow [H,Q^\dagger_\omega]\,|0\rangle = (E_\omega - E_0)Q^\dagger_\omega\,|0\rangle\,,\end{aligned} \tag{158}$$

where E_0 is the ground state energy $H\,|0\rangle = E_0\,|0\rangle$. The notation can be simplified by $E_\omega - E_0 \to E_\omega$, that is, by using E_ω to denote the excitation energy instead of the energy of the excited state. For a variational treatment, we first note that the operator $Q^\dagger_\omega$ consists of terms of the form[27, Chapter 8.4]

$$C_{\beta_1\beta_2\ldots\beta_j\gamma_1\gamma_2\ldots\gamma_k}\Pi(c^\dagger_{\beta_1},c^\dagger_{\beta_2},\ldots,c^\dagger_{\beta_j},c_{\gamma_1},c_{\gamma_2},\ldots,c_{\gamma_k}), \tag{159}$$

where $C_{\beta_1\beta_2\ldots\beta_j\gamma_1\gamma_2\ldots\gamma_k}$ is a coefficient and $\Pi(c^\dagger_{\beta_1},c^\dagger_{\beta_2},\ldots,c^\dagger_{\beta_j},c_{\gamma_1},c_{\gamma_2},\ldots,c_{\gamma_k})$ denotes a product of j creation operators $c^\dagger_\beta$ and k annihilation operators c_γ so that each individual operator is chosen from the set $\{c^\dagger_{\alpha_1},c^\dagger_{\alpha_2},\ldots,c^\dagger_{\alpha_i},c_{\alpha_1},c_{\alpha_2},\ldots,c_{\alpha_i}\}$, with the requirement $j + k = i$. We require also that

$$\left[\Pi(c^\dagger_{\beta_1},c^\dagger_{\beta_2},\ldots,c^\dagger_{\beta_j},c_{\gamma_1},c_{\gamma_2},\ldots,c_{\gamma_k})\right]^\dagger|0\rangle = 0. \tag{160}$$

The variations $\delta Q^\dagger$ are then given by[27, Page 302]

$$\delta Q^\dagger = \frac{\partial Q^\dagger_\omega}{\partial C}\delta C \Rightarrow \delta Q\,|0\rangle = 0, \tag{161}$$

where δC is an arbitrary variation.

The equation 158 can now be written as

$$\langle 0|\,\delta Q[H,Q_\omega^\dagger]\,|0\rangle = E_\omega\,\langle 0|\,\delta Q Q_\omega^\dagger\,|0\rangle \Rightarrow \langle 0|\,[\delta Q,[H,Q_\omega^\dagger]]\,|0\rangle = E_\omega\,\langle 0|\,[\delta Q,Q_\omega^\dagger]\,|0\rangle\,. \tag{162}$$

So far the treatment has been exact with the equation above arising from a genuine variational principle. In practice, however, it may often be necessary to replace the unknown exact vacuum state $|0\rangle$ with an approximate vacuum $|\Psi_0\rangle$. To do this, we first place yet another requirement on the form of the excitation operator $Q_\omega^\dagger$, namely that in the terms of equation 159, the products of creation and annihilation operators all consist of either an even or an odd number of these operators. These two different types of basic excitations are known as Bose-like (even) and Fermi-like (odd) excitations[10, Page 307]. With this in mind, equation 162 with the substitution $|0\rangle \to |\Psi_0\rangle$ can be written as

$$\langle \Psi_0|\,[\delta Q,H,Q_\omega^\dagger]_\pm\,|\Psi_0\rangle = E_\omega\,\langle \Psi_0|\,[\delta Q,Q_\omega^\dagger]_\pm\,|\Psi_0\rangle\,, \tag{163}$$

where

$$[\delta Q,H,Q_\omega^\dagger]_\pm = \frac{1}{2}\left(\left[[\delta Q,H],Q_\omega^\dagger\right]_\pm + \left[\delta Q,[H,Q_\omega^\dagger]\right]_\pm\right) \text{ and } [A,B]_\pm = AB \pm BA. \tag{164}$$

In the above equation, we choose the upper signs (anticommutators) for Fermi-like excitations and lower signs (commutators) for Bose-like excitation. It is also worth noting that equation 163 guarantees $\langle \Psi_0|\,Q_\alpha Q_\beta^\dagger\,|\Psi_0\rangle = \delta_{\alpha\beta}$.

2.2.3 The BCS model

We now have the formalism needed to derive the equations of the BCS model. We still need to specify the BCS vacuum $|\text{BCS}\rangle$ and the excitation operator $Q_\omega^\dagger$ (from which the variations δQ follow) to actually derive the equations. To do this, we will introduce the BCS quasiparticle creation and annihilation operators $a_\alpha^\dagger$ and a_α in terms of the particle creation and annihilation operators $c_\alpha^\dagger$ and c_α through what is known as the Bogoliubov-Valatin transformation[10, Page 393]

$$a_\alpha^\dagger = u_a c_\alpha^\dagger + v_a \tilde{c}_\alpha, \quad a_\alpha = u_a c_\alpha + v_a \tilde{c}_\alpha^\dagger. \tag{165}$$

The quasiparticle operators fulfil the same anticommutation rules of equation 148 as the particle operators. The quasiparticle annihilation operator also annihilates the BCS vacuum. In practice we are usually more interested in the spherical tensor form of the annihilation operator a_α, given by[10, Page 393]

$$\tilde{a}_\alpha = u_a \tilde{c}_\alpha - v_a c_\alpha^\dagger. \tag{166}$$

The basic excitation of the BCS model is now simply $Q_\omega^\dagger = a_\omega^\dagger$ with variations $\delta Q = c_\omega$ and $\tilde{c}_\omega^\dagger$. The variational parameters u_a and v_a are given more meaning after defining the BCS ground state, which will also be the vacuum for the EoM calculation, as[10, Page 392]

$$|\text{BCS}\rangle = \prod_{\alpha>0} (u_a - v_a c_\alpha^\dagger \tilde{c}_\alpha^\dagger) \, |0\rangle \,, \tag{167}$$

where $|0\rangle$ denotes the particle vacuum. From the above equation we can see that a particular single-particle orbital α is unoccupied with an associated probability amplitude of u_a and occupied with an associated probability amplitude of v_a. The probabilities must be normalized as by $u_a^2 + v_a^2 = 1$, which is possible when $u_a^2 = |u_a|^2$ and $v_a^2 = |v_a|^2$, i.e. u_a and v_a are chosen to be real.

We will now derive the BCS equations by using the EoM method. The Hamiltonian operator H expressed in second quantized form follows from equations 150 and 155:

$$H = T + V = \sum_{\alpha\beta} t_{\alpha\beta} c_\alpha^\dagger c_\beta + \frac{1}{4} \sum_{\alpha\beta\gamma\delta} \overline{v}_{\alpha\beta\gamma\delta} c_\alpha^\dagger c_\beta^\dagger c_\delta c_\gamma. \tag{168}$$

The Baranger notation, that was adopted earlier, for the quantum numbers is obvious for the labels α, β and δ. For γ and ω we write $\gamma = (c,m_\gamma)$ and $\omega = (z,m_\omega)$. We will consider the variation $\delta Q = c_\omega$ first. Before computing the commutators $[\delta Q, T]$, $[\delta Q, V]$, $[T,Q_\omega^\dagger]$ and $[V,Q_\omega^\dagger]$, we will consider a number of commutators of creation and annihilation operators. By using equation 148 we get

$$[c_\omega, c_\alpha^\dagger c_\beta] = c_\omega c_\alpha^\dagger c_\beta - c_\alpha^\dagger c_\beta c_\omega = \delta_{\omega\alpha} c_\beta - c_\alpha^\dagger c_\omega c_\beta - c_\alpha^\dagger c_\beta c_\omega = \delta_{\omega\alpha} c_\beta, \tag{169}$$

$$[c_\alpha^\dagger c_\beta, c_\omega^\dagger] = c_\alpha^\dagger c_\beta c_\omega^\dagger - c_\omega^\dagger c_\alpha^\dagger c_\beta = \delta_{\beta\omega} c_\alpha^\dagger - c_\alpha^\dagger c_\omega^\dagger c_\beta - c_\omega^\dagger c_\alpha^\dagger c_\beta = \delta_{\beta\omega} c_\alpha^\dagger, \tag{170}$$

$$[c_\omega,c^\dagger_\alpha c^\dagger_\beta c_\delta c_\gamma] = c_\omega c^\dagger_\alpha c^\dagger_\beta c_\delta c_\gamma - c^\dagger_\alpha c^\dagger_\beta c_\delta c_\gamma c_\omega = \delta_{\omega\alpha} c^\dagger_\beta c_\delta c_\gamma - c^\dagger_\alpha c_\omega c^\dagger_\beta c_\delta c_\gamma - c^\dagger_\alpha c^\dagger_\beta c_\omega c_\delta c_\gamma = \delta_{\omega\alpha} c^\dagger_\beta c_\delta c_\gamma - \delta_{\omega\beta} c^\dagger_\alpha c_\delta c_\gamma, \tag{171}$$

$$[c^\dagger_\alpha c_\beta,\tilde{c}_\omega] = c^\dagger_\alpha c_\beta \tilde{c}_\omega - \tilde{c}_\omega c^\dagger_\alpha c_\beta = (-1)^{j_z+m_\omega} c^\dagger_\alpha c_\beta c_{-\omega} - (-1)^{j_z+m_\omega} c_{-\omega} c^\dagger_\alpha c_\beta = (-1)^{j_z+m_\omega} c^\dagger_\alpha c_\beta c_{-\omega} - (-1)^{j_z+m_\omega} \delta_{-\omega\alpha} c_\beta + (-1)^{j_z+m_\omega} c^\dagger_\alpha c_{-\omega} c_\beta = -(-1)^{j_z+m_\omega} \delta_{-\omega\alpha} c_\beta, \tag{172}$$

$$[c^\dagger_\alpha c^\dagger_\beta c_\delta c_\gamma,c^\dagger_\omega] = c^\dagger_\alpha c^\dagger_\beta c_\delta c_\gamma c^\dagger_\omega - c^\dagger_\omega c^\dagger_\alpha c^\dagger_\beta c_\delta c_\gamma = \delta_{\gamma\omega} c^\dagger_\alpha c^\dagger_\beta c_\delta - c^\dagger_\alpha c^\dagger_\beta c_\delta c^\dagger_\omega c_\gamma - c^\dagger_\alpha c^\dagger_\beta c^\dagger_\omega c_\delta c_\gamma = \delta_{\gamma\omega} c^\dagger_\alpha c^\dagger_\beta c_\delta - \delta_{\delta\omega} c^\dagger_\alpha c^\dagger_\beta c_\gamma \tag{173}$$

and

$$\begin{aligned}[c^\dagger_\alpha c^\dagger_\beta c_\delta c_\gamma,\tilde{c}_\omega] &= c^\dagger_\alpha c^\dagger_\beta c_\delta c_\gamma \tilde{c}_\omega - \tilde{c}_\omega c^\dagger_\alpha c^\dagger_\beta c_\delta c_\gamma = (-1)^{j_z+m_\omega} c^\dagger_\alpha c^\dagger_\beta c_\delta c_\gamma c_{-\omega} - \\ (-1)^{j_z+m_\omega} c_{-\omega} c^\dagger_\alpha c^\dagger_\beta c_\delta c_\gamma &= (-1)^{j_z+m_\omega} c^\dagger_\alpha c^\dagger_\beta c_{-\omega} c_\delta c_\gamma - (-1)^{j_z+m_\omega} \delta_{-\omega\alpha} c^\dagger_\beta c_\delta c_\gamma + \\ (-1)^{j_z+m_\omega} c^\dagger_\alpha c_{-\omega} c^\dagger_\beta c_\delta c_\gamma &= (-1)^{j_z+m_\omega} \delta_{-\omega\beta} c^\dagger_\alpha c_\delta c_\gamma - (-1)^{j_z+m_\omega} \delta_{-\omega\alpha} c^\dagger_\beta c_\delta c_\gamma.\end{aligned} \tag{174}$$

Using the above identities and the symmetry properties of the antisymmetrized two-nucleon interaction matrix element, we get for the aforementioned commutators

$$[\delta Q,T] = \left[c_\omega, \sum_{\alpha\beta} t_{\alpha\beta} c^\dagger_\alpha c_\beta\right] = \sum_{\alpha\beta} t_{\alpha\beta} [c_\omega,c^\dagger_\alpha c_\beta] = \sum_{\alpha\beta} t_{\alpha\beta} \delta_{\omega\alpha} c_\beta = \sum_\beta t_{\omega\beta} c_\beta, \tag{175}$$

$$\begin{aligned}[\delta Q,V] &= \left[c_\omega, \frac{1}{4} \sum_{\alpha\beta\gamma\delta} \overline{v}_{\alpha\beta\gamma\delta} c^\dagger_\alpha c^\dagger_\beta c_\delta c_\gamma\right] = \frac{1}{4} \sum_{\alpha\beta\gamma\delta} \overline{v}_{\alpha\beta\gamma\delta} [c_\omega,c^\dagger_\alpha c^\dagger_\beta c_\delta c_\gamma] = \\ &\frac{1}{4} \sum_{\alpha\beta\gamma\delta} \overline{v}_{\alpha\beta\gamma\delta} (\delta_{\omega\alpha} c^\dagger_\beta c_\delta c_\gamma - \delta_{\omega\beta} c^\dagger_\alpha c_\delta c_\gamma) = \frac{1}{4} \sum_{\beta\gamma\delta} \overline{v}_{\omega\beta\gamma\delta} c^\dagger_\beta c_\delta c_\gamma - \frac{1}{4} \sum_{\alpha\gamma\delta} \overline{v}_{\alpha\omega\gamma\delta} c^\dagger_\alpha c_\delta c_\gamma = \\ &\frac{1}{4} \sum_{\beta\gamma\delta} \overline{v}_{\omega\beta\gamma\delta} c^\dagger_\beta c_\delta c_\gamma + \frac{1}{4} \sum_{\alpha\gamma\delta} \overline{v}_{\omega\alpha\gamma\delta} c^\dagger_\alpha c_\delta c_\gamma = \frac{1}{2} \sum_{\beta\gamma\delta} \overline{v}_{\omega\beta\gamma\delta} c^\dagger_\beta c_\delta c_\gamma,\end{aligned} \tag{176}$$

$$[T,Q_\omega^\dagger] = \left[\sum_{\alpha\beta} t_{\alpha\beta}c_\alpha^\dagger c_\beta, u_z c_\omega^\dagger + v_z\tilde{c}_\omega\right] = \sum_{\alpha\beta} t_{\alpha\beta}u_z[c_\alpha^\dagger c_\beta, c_\omega^\dagger] + \sum_{\alpha\beta} t_{\alpha\beta}v_z[c_\alpha^\dagger c_\beta,\tilde{c}_\omega] =$$
$$\sum_{\alpha\beta} t_{\alpha\beta}u_z\delta_{\beta\omega}c_\alpha^\dagger - \sum_{\alpha\beta} t_{\alpha\beta}v_z(-1)^{j_z+m_\omega}\delta_{-\omega\alpha}c_\beta = u_z\sum_{\alpha\omega} t_{\alpha\omega}c_\alpha^\dagger - (-1)^{j_z+m_\omega}v_z\sum_\beta t_{-\omega\beta}c_\beta, \tag{177}$$

and

$$[V,Q_\omega^\dagger] = \left[\frac{1}{4}\sum_{\alpha\beta\gamma\delta}\overline{v}_{\alpha\beta\gamma\delta}c_\alpha^\dagger c_\beta^\dagger c_\delta c_\gamma, u_z c_\omega^\dagger + v_z\tilde{c}_\omega\right] = \frac{1}{4}\sum_{\alpha\beta\gamma\delta}\overline{v}_{\alpha\beta\gamma\delta}u_z[c_\alpha^\dagger c_\beta^\dagger c_\delta c_\gamma, c_\omega^\dagger] +$$
$$\frac{1}{4}\sum_{\alpha\beta\gamma\delta}\overline{v}_{\alpha\beta\gamma\delta}v_z[c_\alpha^\dagger c_\beta^\dagger c_\delta c_\gamma,\tilde{c}_\omega] = \frac{1}{4}\sum_{\alpha\beta\gamma\delta}\overline{v}_{\alpha\beta\gamma\delta}u_z(\delta_{\gamma\omega}c_\alpha^\dagger c_\beta^\dagger c_\delta - \delta_{\delta\omega}c_\alpha^\dagger c_\beta^\dagger c_\gamma) +$$
$$\frac{1}{4}\sum_{\alpha\beta\gamma\delta}\overline{v}_{\alpha\beta\gamma\delta}(-1)^{j_z+m_\omega}v_z(\delta_{-\omega\beta}c_\alpha^\dagger c_\delta c_\gamma - \delta_{-\omega\alpha}c_\beta^\dagger c_\delta c_\gamma) = \frac{u_z}{4}\sum_{\alpha\beta\delta}\overline{v}_{\alpha\beta\omega\delta}c_\alpha^\dagger c_\beta^\dagger c_\delta -$$
$$\frac{u_z}{4}\sum_{\alpha\beta\gamma}\overline{v}_{\alpha\beta\gamma\omega}c_\alpha^\dagger c_\beta^\dagger c_\gamma + (-1)^{j_z+m_\omega}\frac{v_z}{4}\sum_{\alpha\gamma\delta}\overline{v}_{\alpha-\omega\gamma\delta}c_\alpha^\dagger c_\delta c_\gamma - (-1)^{j_z+m_\omega}\frac{v_z}{4}\sum_{\beta\gamma\delta}\overline{v}_{-\omega\beta\gamma\delta}c_\beta^\dagger c_\delta c_\gamma$$
$$= \frac{u_z}{2}\sum_{\alpha\beta\delta}\overline{v}_{\alpha\beta\omega\delta}c_\alpha^\dagger c_\beta^\dagger c_\delta + (-1)^{j_z+m_\omega}\frac{v_z}{2}\sum_{\alpha\gamma\delta}\overline{v}_{\alpha-\omega\gamma\delta}c_\alpha^\dagger c_\delta c_\gamma. \tag{178}$$

For the anticommutators of equation 164, we again consider a number of anticommutators, namely

$$\{c_\beta^\dagger c_\delta c_\gamma, c_\omega^\dagger\} = c_\beta^\dagger c_\delta c_\gamma c_\omega^\dagger + c_\omega^\dagger c_\beta^\dagger c_\delta c_\gamma = \delta_{\gamma\omega}c_\beta^\dagger c_\delta - c_\beta^\dagger c_\delta c_\omega^\dagger c_\gamma - c_\beta^\dagger c_\omega^\dagger c_\delta c_\gamma =$$
$$\delta_{\gamma\omega}c_\beta^\dagger c_\delta - \delta_{\delta\omega}c_\beta^\dagger c_\gamma, \tag{179}$$

$$\{c_\beta^\dagger c_\delta c_\gamma,\tilde{c}_\omega\} = c_\beta^\dagger c_\delta c_\gamma\tilde{c}_\omega + \tilde{c}_\omega c_\beta^\dagger c_\delta c_\gamma = (-1)^{j_z+m_\omega}c_\beta^\dagger c_\delta c_\gamma c_{-\omega} + (-1)^{j_z+m_\omega}c_{-\omega}c_\beta^\dagger c_\delta c_\gamma =$$
$$(-1)^{j_z+m_\omega}c_\beta^\dagger c_\delta c_\gamma c_{-\omega} + (-1)^{j_z+m_\omega}\delta_{-\omega\beta}c_\delta c_\gamma - (-1)^{j_z+m_\omega}c_\beta^\dagger c_{-\omega}c_\delta c_\gamma =$$
$$(-1)^{j_z+m_\omega}\delta_{-\omega\beta}c_\delta c_\gamma, \tag{180}$$

$$\{c_\omega, c_\alpha^\dagger c_\beta^\dagger c_\delta\} = c_\omega c_\alpha^\dagger c_\beta^\dagger c_\delta + c_\alpha^\dagger c_\beta^\dagger c_\delta c_\omega = \delta_{\omega\alpha}c_\beta^\dagger c_\delta - c_\alpha^\dagger c_\omega c_\beta^\dagger c_\delta + c_\alpha^\dagger c_\beta^\dagger c_\omega c_\delta =$$
$$\delta_{\omega\alpha}c_\beta^\dagger c_\delta - \delta_{\omega\beta}c_\alpha^\dagger c_\delta, \tag{181}$$

and

$$\{c_\omega,c_\alpha^\dagger c_\delta c_\gamma\} = c_\omega c_\alpha^\dagger c_\delta c_\gamma + c_\alpha^\dagger c_\delta c_\gamma c_\omega = \delta_{\omega\alpha} c_\delta c_\gamma - c_\alpha^\dagger c_\omega c_\delta c_\gamma + c_\alpha^\dagger c_\delta c_\gamma c_\omega = \delta_{\omega\alpha} c_\delta c_\gamma. \tag{182}$$

Similarly as before, using the above identities and the basic anticommutation relations of equation 148, we get for the anticommutators

$$\begin{aligned}
&\{[\delta Q, H], Q_\omega^\dagger\} = \left\{\sum_\beta t_{\omega\beta} c_\beta, u_z c_\omega^\dagger + v_z \tilde{c}_\omega\right\} + \left\{\frac{1}{2}\sum_{\beta\gamma\delta} \overline{v}_{\omega\beta\gamma\delta} c_\beta^\dagger c_\delta c_\gamma, u_z c_\omega^\dagger + v_z \tilde{c}_\omega\right\} = \\
&u_z \sum_\beta t_{\omega\beta} \left\{c_\beta, c_\omega^\dagger\right\} + v_z \sum_\beta t_{\omega\beta} \left\{c_\beta, \tilde{c}_\omega\right\} + \frac{u_z}{2}\sum_{\beta\gamma\delta} \overline{v}_{\omega\beta\gamma\delta} \left\{c_\beta^\dagger c_\delta c_\gamma, c_\omega^\dagger\right\} + \\
&\frac{v_z}{2}\sum_{\beta\gamma\delta} \overline{v}_{\omega\beta\gamma\delta} \left\{c_\beta^\dagger c_\delta c_\gamma, \tilde{c}_\omega\right\} = u_z \sum_\beta t_{\omega\beta}\delta_{\beta\omega} + \frac{u_z}{2}\sum_{\beta\gamma\delta} \overline{v}_{\omega\beta\gamma\delta} \left(\delta_{\gamma\omega} c_\beta^\dagger c_\delta - \delta_{\delta\omega} c_\beta^\dagger c_\gamma\right) + \\
&\frac{v_z}{2}\sum_{\beta\gamma\delta} \overline{v}_{\omega\beta\gamma\delta} (-1)^{j_z+m_\omega} \delta_{-\omega\beta} c_\delta c_\gamma = u_z t_{\omega\omega} + \frac{u_z}{2}\sum_{\beta\delta} \overline{v}_{\omega\beta\omega\delta} c_\beta^\dagger c_\delta - \frac{u_z}{2}\sum_{\beta\gamma} \overline{v}_{\omega\beta\gamma\omega} c_\beta^\dagger c_\gamma + \\
&\frac{v_z}{2}\sum_{\gamma\delta} \overline{v}_{\omega-\omega\gamma\delta} (-1)^{j_z+m_\omega} c_\delta c_\gamma = u_z t_{\omega\omega} + u_z \sum_{\beta\delta} \overline{v}_{\omega\beta\omega\delta} c_\beta^\dagger c_\delta + (-1)^{j_z+m_\omega} \frac{v_z}{2}\sum_{\gamma\delta} \overline{v}_{\omega-\omega\gamma\delta} c_\delta c_\gamma
\end{aligned} \tag{183}$$

and

$$\begin{aligned}
&\{\delta Q, [H, Q_\omega^\dagger]\} = \left\{c_\omega, u_z \sum_\alpha t_{\alpha\omega} c_\alpha^\dagger - (-1)^{j_z+m_\omega} v_z \sum_\beta t_{-\omega\beta} c_\beta\right\} + \\
&\left\{c_\omega, \frac{u_z}{2}\sum_{\alpha\beta\delta} \overline{v}_{\alpha\beta\omega\delta} c_\alpha^\dagger c_\beta^\dagger c_\delta + (-1)^{j_z+m_\omega} \frac{v_z}{2}\sum_{\alpha\gamma\delta} \overline{v}_{\alpha-\omega\gamma\delta} c_\alpha^\dagger c_\delta c_\gamma\right\} = u_z \sum_\alpha t_{\alpha\omega} \left\{c_\omega, c_\alpha^\dagger\right\} - \\
&(-1)^{j_z+m_\omega} v_z \sum_\beta t_{-\omega\beta} \left\{c_\omega, c_\beta\right\} + \frac{u_z}{2}\sum_{\alpha\beta\delta} \overline{v}_{\alpha\beta\omega\delta} \left\{c_\omega, c_\alpha^\dagger c_\beta^\dagger c_\delta\right\} + \\
&(-1)^{j_z+m_\omega} \frac{v_z}{2}\sum_{\alpha\gamma\delta} \overline{v}_{\alpha-\omega\gamma\delta} \left\{c_\omega, c_\alpha^\dagger c_\delta c_\gamma\right\} = u_z \sum_\alpha t_{\alpha\omega}\delta_{\omega\alpha} + \frac{u_z}{2}\sum_{\alpha\beta\delta} \overline{v}_{\alpha\beta\omega\delta}\delta_{\omega\alpha} c_\beta^\dagger c_\delta - \\
&\frac{u_z}{2}\sum_{\alpha\beta\delta} \overline{v}_{\alpha\beta\omega\delta}\delta_{\omega\beta} c_\alpha^\dagger c_\delta + (-1)^{j_z+m_\omega} \frac{v_z}{2}\sum_{\alpha\gamma\delta} \overline{v}_{\alpha-\omega\gamma\delta}\delta_{\omega\alpha} c_\delta c_\gamma = u_z t_{\omega\omega} + \frac{u_z}{2}\sum_{\beta\delta} \overline{v}_{\omega\beta\omega\delta} c_\beta^\dagger c_\delta - \\
&\frac{u_z}{2}\sum_{\alpha\delta} \overline{v}_{\alpha\omega\omega\delta} c_\alpha^\dagger c_\delta + (-1)^{j_z+m_\omega} \frac{v_z}{2}\sum_{\alpha\gamma\delta} \overline{v}_{\omega-\omega\gamma\delta} c_\delta c_\gamma = u_z t_{\omega\omega} + u_z \sum_{\beta\delta} \overline{v}_{\omega\beta\omega\delta} c_\beta^\dagger c_\delta + \\
&(-1)^{j_z+m_\omega} \frac{v_z}{2}\sum_{\alpha\gamma\delta} \overline{v}_{\omega-\omega\gamma\delta} c_\delta c_\gamma.
\end{aligned} \tag{184}$$

From these we get

$$[\delta Q,H,Q^\dagger_\omega]_+ = u_z\epsilon_z + u_z\sum_{\beta\delta}\overline{v}_{\omega\beta\omega\delta}c^\dagger_\beta c_\delta + (-1)^{j_z+m_\omega}\frac{v_z}{2}\sum_{\gamma\delta}\overline{v}_{\omega-\omega\gamma\delta}c_\delta c_\gamma, \tag{185}$$

where we have adopted the notation $\epsilon_z = t_{\omega\omega}$ for the energies of the single-particle states. The anticommutator on the right side of equation 163 follows from the basic anticommutation relations of equation 148:

$$\{\delta Q,Q^\dagger_\omega\} = \{c_\omega,u_z c^\dagger_\omega + v_z\tilde{c}_\omega\} = u_z\{c_\omega,c^\dagger_\omega\} + v_z\{c_\omega,\tilde{c}_\omega\} = u_z. \tag{186}$$

For the expectation values of the symmetrized double commutator of equation 185 with respect to the BCS vacuum, we need the to determine $\langle \mathrm{BCS}|\, c^\dagger_\beta c_\delta\, |\mathrm{BCS}\rangle$ and $\langle \mathrm{BCS}|\, c_\delta c_\gamma\, |\mathrm{BCS}\rangle$. For these, we invert equations 165 and 166, along with

$$\tilde{a}^\dagger_\alpha = u_a\tilde{c}^\dagger_\alpha - v_a c_\alpha, \tag{187}$$

which results in

$$c^\dagger_\alpha = u_a a^\dagger_\alpha - v_a\tilde{a}_\alpha \text{ and } c_\alpha = u_a a_\alpha - v_a\tilde{a}^\dagger_\alpha. \tag{188}$$

The vacuum expectation values are then given by

$$\begin{aligned}
&\langle \mathrm{BCS}|\, c^\dagger_\beta c_\delta\, |\mathrm{BCS}\rangle = \langle \mathrm{BCS}|\, (u_b a^\dagger_\beta - v_b\tilde{a}_\beta)(u_d a_\delta - v_d\tilde{a}^\dagger_\delta)\, |\mathrm{BCS}\rangle = \\
&-\langle \mathrm{BCS}|\, (u_b a^\dagger_\beta - v_b\tilde{a}_\beta)v_d\tilde{a}^\dagger_\delta\, |\mathrm{BCS}\rangle = \langle \mathrm{BCS}|\, v_b\tilde{a}_\beta v_d\tilde{a}^\dagger_\delta\, |\mathrm{BCS}\rangle = v_b v_d\,\langle \mathrm{BCS}|\, \tilde{a}_\beta\tilde{a}^\dagger_\delta\, |\mathrm{BCS}\rangle \\
&= v_b v_d(-1)^{j_b+j_d+m_\beta+m_\delta}\,\langle \mathrm{BCS}|\, a_{-\beta}a^\dagger_{-\delta}\, |\mathrm{BCS}\rangle = v_b v_d(-1)^{j_b+j_d+m_\beta+m_\delta}\delta_{-\beta-\delta} = v_b^2\delta_{\beta\delta}
\end{aligned} \tag{189}$$

and

$$\begin{aligned}
&\langle \mathrm{BCS}|\, c_\delta c_\gamma\, |\mathrm{BCS}\rangle = \langle \mathrm{BCS}|\, (u_d a_\delta - v_d\tilde{a}^\dagger_\delta)(u_c a_\gamma - v_c\tilde{a}^\dagger_\gamma)\, |\mathrm{BCS}\rangle = \\
&-\langle \mathrm{BCS}|\, (u_d a_\delta - v_d\tilde{a}^\dagger_\delta)v_c\tilde{a}^\dagger_\gamma\, |\mathrm{BCS}\rangle = -\langle \mathrm{BCS}|\, u_d a_\delta v_c\tilde{a}^\dagger_\gamma\, |\mathrm{BCS}\rangle = \\
&-u_d v_c(-1)^{j_c+m_\gamma}\,\langle \mathrm{BCS}|\, a_\delta a^\dagger_{-\gamma}\, |\mathrm{BCS}\rangle = -u_d v_c(-1)^{j_c+m_\gamma}\delta_{\delta-\gamma} = -u_c v_c(-1)^{j_c+m_\gamma}\delta_{\delta-\gamma}.
\end{aligned} \tag{190}$$

In the above derivations, we used the fact that

$$a_\alpha\, |\mathrm{BCS}\rangle = \tilde{a}_\alpha\, |\mathrm{BCS}\rangle = \langle \mathrm{BCS}|\, a^\dagger_\alpha = \langle \mathrm{BCS}|\, \tilde{a}^\dagger_\alpha = 0. \tag{191}$$

Taking the vacuum expectation value of equation 185 we now get

$$\begin{aligned}
&\langle \mathrm{BCS}| \left[\delta Q,H,Q^\dagger_\omega\right]_\pm |\mathrm{BCS}\rangle = \langle \mathrm{BCS}| u_z\epsilon_z |\mathrm{BCS}\rangle + \langle \mathrm{BCS}| u_z \sum_{\beta\delta} \overline{v}_{\omega\beta\omega\delta} c^\dagger_\beta c_\delta |\mathrm{BCS}\rangle + \\
&\langle \mathrm{BCS}| (-1)^{j_z+m_\omega}\frac{v_z}{2}\sum_{\gamma\delta}\overline{v}_{\omega-\omega\gamma\delta} c_\delta c_\gamma |\mathrm{BCS}\rangle = u_z\epsilon_z + u_z\sum_{\beta\delta}\overline{v}_{\omega\beta\omega\delta}\langle \mathrm{BCS}| c^\dagger_\beta c_\delta |\mathrm{BCS}\rangle + \\
&(-1)^{j_z+m_\omega}\frac{v_z}{2}\sum_{\gamma\delta}\overline{v}_{\omega-\omega\gamma\delta}\langle \mathrm{BCS}| c_\delta c_\gamma |\mathrm{BCS}\rangle = u_z\epsilon_z + u_z\sum_{\beta\delta}\overline{v}_{\omega\beta\omega\delta}v_b^2\delta_{\beta\delta} - \\
&(-1)^{j_z+m_\omega}\frac{v_z}{2}\sum_{\gamma\delta}\overline{v}_{\omega-\omega\gamma\delta}u_c v_c(-1)^{j_c+m_\gamma}\delta_{\delta-\gamma} = u_z\epsilon_z + u_z\sum_{\beta}\overline{v}_{\omega\beta\omega\beta}v_b^2 - \\
&(-1)^{j_z+m_\omega}\frac{v_z}{2}\sum_{\gamma}(-1)^{j_c+m_\gamma}\overline{v}_{\omega-\omega\gamma-\gamma}u_c v_c.
\end{aligned} \tag{192}$$

We will consider the terms on the right side of the above equation separately.

The first term of equation 192 is fine as it is, but for the second and third terms we will express $\overline{v}_{\alpha\beta\gamma\delta}$ in terms of the coupled two-nucleon interaction matrix elements $\langle ab;J,M|\,V\,|cd;J',M'\rangle$ with

$$|ab;J,M\rangle = \mathcal{N}_{ab}(J)[c^\dagger_a c^\dagger_b]_{JM}|0\rangle\,, \quad \mathcal{N}_{ab}(J) = \frac{\sqrt{1+\delta_{ab}(-1)^J}}{1+\delta_{ab}}. \tag{193}$$

It can be shown that[10, Chapter 8.1.1]

$$\overline{v}_{\alpha\beta\gamma\delta} = \sum_{JM}[\mathcal{N}_{ab}(J)\mathcal{N}_{cd}(J)]^{-1}(j_a m_\alpha j_b m_\beta|JM)(j_c m_\gamma j_d m_\delta|JM)\langle ab;J|\,V\,|cd;J\rangle\,, \tag{194}$$

where we have used the fact that[10, Page 207]

$$\langle ab;J,M|\,V\,|cd;J',M'\rangle = \delta_{JJ'}\delta_{MM'}\langle ab;J|\,V\,|cd;J\rangle\,. \tag{195}$$

With these, the second term of equation 192 can be written

$$\begin{aligned}
&u_z\sum_\beta \overline{v}_{\omega\beta\omega\beta}v_b^2 = u_z\sum_\beta v_b^2\sum_{JM}[\mathcal{N}_{zb}(J)]^{-2}(j_z m_\omega j_b m_\beta|JM)^2\langle zb;J|\,V\,|zb;J\rangle = \\
&u_z\sum_{Jb}v_b^2[\mathcal{N}_{zb}(J)]^{-2}\langle zb;J|\,V\,|zb;J\rangle\sum_{Mm_\beta}(j_z m_\omega j_b m_\beta|JM)^2.
\end{aligned} \tag{196}$$

To compute the sum over the magnetic quantum numbers, we change the coupling

order of the angular momenta as by

$$(j_z m_\omega j_b m_\beta | JM) = (-1)^{j_b + m_\beta} \frac{\hat{J}}{\hat{j}_z} (j_b - m_\beta JM | j_z m_\omega). \tag{197}$$

With this change, the sum becomes

$$\sum_{M m_\beta} (j_z m_\omega j_b m_\beta | JM)^2 = \frac{\hat{J}^2}{\hat{j}_z^2} \sum_{M m_\beta} (j_b - m_\beta JM | j_z m_\omega)(j_b - m_\beta JM | j_z m_\omega) = \frac{\hat{J}^2}{\hat{j}_z^2}, \tag{198}$$

where we have used the orthogonality property[10, Page 8]

$$\sum_{m m'} (jmj'm' | JM)(jmj'm' | J'M') = \delta_{JJ'} \delta_{MM'} \tag{199}$$

of the Clebsch-Gordan coefficients. Inserting this into equation 196 above yields

$$\begin{aligned} &u_z \sum_\beta \overline{v}_{\omega\beta\omega\beta} v_b^2 = u_z \sum_{Jb} v_b^2 [\mathcal{N}_{zb}(J)]^{-2} \langle zb; J | V | zb; J \rangle \frac{\hat{J}^2}{\hat{j}_z^2} = \\ &u_z \hat{j}_z^{-2} \sum_{Jb} v_b^2 \hat{J}^2 [\mathcal{N}_{zb}(J)]^{-2} \langle zb; J | V | zb; J \rangle = -u_z \mu_z, \end{aligned} \tag{200}$$

where

$$\mu_z \equiv -\hat{j}_z^{-2} \sum_{Jb} v_b^2 \hat{J}^2 [\mathcal{N}_{zb}(J)]^{-2} \langle zb; J | V | zb; J \rangle . \tag{201}$$

is known as the self-energy[10, Page 404]. We then express the third term of equation 192 in the same way and get

$$\begin{aligned} &- (-1)^{j_z + m_\omega} \frac{v_z}{2} \sum_\gamma (-1)^{j_c + m_\gamma} \overline{v}_{\omega - \omega\gamma - \gamma} u_c v_c = \\ &- (-1)^{j_z + m_\omega} \frac{v_z}{2} \sum_\gamma (-1)^{j_c + m_\gamma} u_c v_c \sum_{JM} [\mathcal{N}_{\omega\omega}(J) \mathcal{N}_{\gamma\gamma}(J)]^{-1} (j_z m_\omega j_z - m_\omega | JM) \cdot \\ &(j_c m_\gamma j_c - m_\gamma | JM) \langle zz; J | V | cc; J \rangle = -(-1)^{j_z + m_\omega} \frac{v_z}{2} \sum_{Jc} u_c v_c \langle zz; J | V | cc; J \rangle \cdot \\ &\mathcal{N}_{\omega\omega}^{-2}(J) \sum_{M m_\gamma} (-1)^{j_c + m_\gamma} (j_z m_\omega j_z - m_\omega | JM)(j_c m_\gamma j_c - m_\gamma | JM). \end{aligned} \tag{202}$$

We first note that in the above equation for the Clebsch-Gordan coefficients not to

vanish, the magnetic quantum numbers must satisfy

$$M = m_\omega - m_\omega = 0. \tag{203}$$

Thus the sum over said quantum numbers reduces to

$$\begin{aligned}&\sum_{Mm_\gamma} (-1)^{j_c+m_\gamma}(j_z m_\omega j_z - m_\omega|JM)(j_c m_\gamma j_c - m_\gamma|JM) = \\ &(j_z m_\omega j_z - m_\omega|J0)\sum_{m_\gamma}(-1)^{j_c+m_\gamma}(j_c m_\gamma j_c - m_\gamma|J0).\end{aligned} \tag{204}$$

This can be simplified further with the identity[2]

$$\begin{aligned}&\sum_m (-1)^{j-m}(jmj-m|J0) = \delta_{J0}\hat{j} \Leftrightarrow \delta_{J0}\hat{j} = (-1)^{j-j}\sum_m (-1)^{j-m}(jmj-m|J0) = \\ &(-1)^{2j}\sum_m (-1)^{-j-m}(jmj-m|J0) = -\sum_m (-1)^{j+m}(jmj-m|J0).\end{aligned} \tag{205}$$

using this we get

$$\begin{aligned}&(j_z m_\omega j_z - m_\omega|J0)\sum_{m_\gamma}(-1)^{j_c+m_\gamma}(j_c m_\gamma j_c - m_\gamma|J0) = -(j_z m_\omega j_z - m_\omega|J0)\delta_{J0}\hat{j}_c = \\ &-(j_z m_\omega j_z - m_\omega|00)\delta_{J0}\hat{j}_c = -(-1)^{j_z-m_\gamma}\delta_{J0}\hat{j}_z^{-1}\hat{j}_c,\end{aligned} \tag{206}$$

where[10, Page 9]

$$(jmjm'|00) = (-1)^{j-m}\hat{j}^{-1}\delta_{m-m'} \tag{207}$$

was used. With the result of equation 206 we get for the third term

$$\begin{aligned}&-(-1)^{j_z+m_\omega}\frac{v_z}{2}\sum_\gamma (-1)^{j_c+m_\gamma}\overline{v}_{\omega-\omega\gamma-\gamma}u_c v_c = \\ &(-1)^{j_z+m_\omega}\frac{v_z}{2}\sum_{Jc} u_c v_c \left\langle zz;J\right|V\left|cc;J\right\rangle \mathcal{N}_{\omega\omega}^{-2}(J)(-1)^{j_z-m_\gamma}\delta_{J0}\hat{j}_z^{-1}\hat{j}_c = \\ &\frac{v_z}{2}\hat{j}_z^{-1}\sum_{Jc}\hat{j}_c u_c v_c \left\langle zz;0\right|V\left|cc;0\right\rangle \mathcal{N}_{\omega\omega}^{-2}(0) = v_z\hat{j}_z^{-1}\sum_{Jc}\hat{j}_c u_c v_c \left\langle zz;0\right|V\left|cc;0\right\rangle = \\ &-v_z\Delta_z,\end{aligned} \tag{208}$$

[2]For a proof of this, we again consider the special case $(jmjm'|00) = (-1)^{j-m}\hat{j}^{-1}\delta_{m(-m')}$, from which we get $\sum_m (-1)^{j-m}(jmj-m|J0) = \hat{j}\sum_m (jmj-m|00)(jmj-m|J0) = \hat{j}\delta_{J0}$, where we used the orthogonality relation[10, Page 8] $\sum_{m_1,m_2}(j_1m_1j_2m_2|JM)(j_1m_1j_2m_2|J'M') = \delta_{JJ'}\delta_{MM'}$.

where

$$\Delta_z \equiv -\hat{j}_z^{-1} \sum_{Jc} \hat{j}_c u_c v_c \langle zz;0| V |cc;0\rangle . \tag{209}$$

is known as the pairing gap[10, Page 403].

By combining equations 200 and 208 with equation 192 along with equations 163 and 186 we finally get

$$u_z\epsilon_z - u_z\mu_z - v_z\Delta_z = E_\omega u_z \Leftrightarrow u_z\tilde{\eta}_z - v_z\Delta_z = E_\omega u_z, \tag{210}$$

where

$$\epsilon_z - \mu_z = \tilde{\eta}_z. \tag{211}$$

Had we picked instead of $\delta Q = c_\omega$ the other variation $\delta Q = \tilde{c}_\omega^\dagger$ and done the same derivation, we would have arrived at the equation

$$-v_z\tilde{\eta}_z - u_z\Delta_z = E_\omega v_z. \tag{212}$$

By squaring both of these equations and summing them together we get for the excitation energy (or quasiparticle energy, as it is appropriately called)

$$\begin{aligned} &E_\omega^2 u_z^2 = u_z^2\tilde{\eta}_z^2 - 2u_z v_z\tilde{\eta}_z\Delta_z + v_z^2\Delta_z^2,\ E_\omega^2 v_z^2 = v_z^2\tilde{\eta}_z^2 + 2u_z v_z\tilde{\eta}_z\Delta_z + u_z^2\Delta_z^2 \Rightarrow \\ &E_\omega^2(u_z^2+v_z^2) = E_\omega^2 = u_z^2\tilde{\eta}_z^2 - 2u_z v_z\tilde{\eta}_z\Delta_z + v_z^2\Delta_z^2 + v_z^2\tilde{\eta}_z^2 + 2u_z v_z\tilde{\eta}_z\Delta_z + u_z^2\Delta_z^2 = \\ &(u_z^2+v_z^2)\tilde{\eta}_z^2 + (u_z^2+v_z^2)\Delta_z^2 = \tilde{\eta}_z^2 + \Delta_z^2 \Rightarrow E_\omega = \sqrt{\tilde{\eta}_z^2+\Delta_z^2}, \end{aligned} \tag{213}$$

where the normalization condition $u_z^2+v_z^2 = 1$ was used extensively. The normalization and the above result can be used to solve equations 210 and 212 in terms of u_z and v_z. For the former we get

$$\begin{aligned} &u_z\tilde{\eta}_z - v_z\Delta_z = E_\omega u_z \Leftrightarrow v_z\Delta_z = (\tilde{\eta}_z - E_\omega)u_z \Rightarrow v_z^2\Delta_z^2 = (1-u_z^2)\Delta_z^2 = (E_\omega-\tilde{\eta}_z)^2 u_z^2 \\ &\Leftrightarrow \left[(E_\omega-\tilde{\eta}_z)^2 + \Delta_z^2\right] u_z^2 = \Delta_z^2 \Leftrightarrow u_z^2 = \frac{\Delta_z^2}{(E_\omega-\tilde{\eta}_z)^2+\Delta_z^2} = \frac{\Delta_z^2}{E_\omega^2 - 2E_\omega\tilde{\eta}_z + \tilde{\eta}_z^2 + \Delta_z^2} \\ &= \frac{E_\omega^2-\tilde{\eta}_z^2}{E_\omega^2 - 2E_\omega\tilde{\eta}_z + \tilde{\eta}_z^2 + E_\omega^2 - \tilde{\eta}_z^2} = \frac{(E_\omega-\tilde{\eta}_z)(E_\omega+\tilde{\eta}_z)}{2E_\omega(E_\omega-\tilde{\eta}_z)} = \frac{1}{2}\left(1+\frac{\tilde{\eta}_z}{E_\omega}\right) \Rightarrow u_z = \\ &\frac{\theta^{(l_z)}}{\sqrt{2}}\sqrt{1+\frac{\tilde{\eta}_z}{E_\omega}} \end{aligned} \tag{214}$$

and similarly for the latter

$$v_z = \frac{1}{\sqrt{2}}\sqrt{1 - \frac{\tilde{\eta}_z}{E_\omega}}. \tag{215}$$

Here $\theta^{(l_z)}$ is a phase factor which depends on the convention chosen[10, p. 401]. In the Condon-Shortley (CS) convention, which is commonly used in quantum mechanics because of its desirable properties, we have $\theta^{(l_z)} = (-1)^{l_z}$. In an alternative phase convention, the Biedenharn-Rose (BR) convention, we instead have $\theta^{(l_z)} = 1$, making the occupation amplitudes u_z and v_z non-negative. For this reason the BR-convention is usually preferred over the CS-convention when dealing with BCS quasiparticles.

The BCS equations derived above are formally correct and describe a quantum mechanical many-body system and its excitations. There is, however, a considerable conceptual shortcoming in the theory that needs to be addressed. That is, the BCS state doesn't have a good particle number in the general case[10, Chapter 13.3]. The BCS theory was originally developed to explain superconductivity in conventional superconductors[9], where the lack of a good particle number is not a major concern as the system consists of a number of electrons that is of the order of 10^{23}. There is no a priori reason to expect that in an atomic nucleus, where the particle number is of the order of 10^2, the effects of a lack of a good particle number would be negligible, and only comparison with experimental data can verify the validity of such an assumption. Nevertheless, some constraints need to be put on the particle number of the BCS state to have any hope of having a theory fit for describing a nucleus of good particle number.

There are two commonly used methods for dealing with the particle number of the BCS state[10, Page 398]. The first is to project states of good particle number and consider them instead, and the second is to require that the expectation value of the particle number (or average particle number) matches the nucleon number. We will take the latter approach here. The average particle number can be deduced easily by noting that the probability for a single-particle orbital a to be occupied is v_a^2, and that the degeneracy of an orbital is $2j_a + 1 = \hat{j}_a^2$. Thus the average number of particles in a particular single-particle orbital is $\hat{j}_a^2 v_a^2$. The average particle number of the entire system n is given by summing over the average particle numbers of all the orbitals

$$n = \sum_a \hat{j}_a^2 v_a^2. \tag{216}$$

Alternatively, the particle number operator

$$\hat{n} = \sum_{\alpha} c_{\alpha}^{\dagger} c_{\alpha} \tag{217}$$

can be expressed in terms of the operators $a_{\alpha}^{\dagger}$ and $\tilde{a}_{\alpha}$ by the use of equations 188, resulting in[10, Page 399]

$$\hat{n} = \sum_{a} \hat{j}_a^2 v_a^2 + \sum_{a} \hat{j}_a (u_a^2 - v_a^2)[a_a^{\dagger}\tilde{a}_a]_{00} + \sum_{a} \hat{j}_a u_a v_a \left([a_a^{\dagger} a_a^{\dagger}]_{00} - [\tilde{a}_a \tilde{a}_a]_{00} \right). \tag{218}$$

It can be clearly seen that only the first term on the right side of the above equation doesn't annihilate the BCS vacuum from neither the left nor the right, and is thus the only term to contribute to $\langle \mathrm{BCS} | \, \hat{n} \, | \mathrm{BCS} \rangle = n$, leading to the same result as before.

Applying the constraint on the average particle number turns out to be quite simple. The problem of deriving of the BCS equations discussed earlier can be thought of as an unconstrained variational problem of minimizing the energy of the BCS state $E = \langle \mathrm{BCS} | \, H \, | \mathrm{BCS} \rangle$. To convert this into a constrained variational problem, the method of undetermined Lagrange multipliers[28, Chapter 13.3] can be utilized. This amounts to adding a term of $-\lambda \hat{n}$ to the Hamiltonian H and treating the problem as a regular unconstrained variational problem with an extra variational parameter λ, the undetermined multiplier. The simplicity of all this, is that it turns out that after expressing the Hamiltonian in terms of the quasiparticle creation and annihilation operators like the particle number operator above, the Hamiltonian of the constrained system H' with single particle energies ϵ can be expressed as[10, Chapter 13.3.1]

$$\Big|_{\epsilon} H' = \Big|_{\epsilon - \lambda} H, \tag{219}$$

that is, constraining the variational problem amounts to shifting the single-particle energies of the unconstrained Hamiltonian by $-\lambda$. In the following we drop the prime and denote the constrained Hamiltonian by H.

The aforederived unconstrained BCS equations can be easily transformed into the constrained ones by shifting the single-particle energies. For this, we write

$$\eta_z \equiv \tilde{\eta}_z - \lambda \equiv \epsilon_z - \mu_z - \lambda. \tag{220}$$

The constrained BCS equations then consist of

$$
\begin{aligned}
u_z &= \frac{\theta^{(l_z)}}{\sqrt{2}}\sqrt{1+\frac{\eta_z}{E_\omega}},\\
v_z &= \frac{1}{\sqrt{2}}\sqrt{1-\frac{\eta_z}{E_\omega}},\\
\eta_z &= \epsilon_z - \mu_z - \lambda,\\
E_\omega &= \sqrt{\eta_z^2+\Delta_z^2},\\
\mu_z &= -\hat{j}_z^{-2}\sum_{Jb} v_b^2 \hat{J}^2[\mathcal{N}_{zb}(J)]^{-2}\left\langle zb;J\right|V\left|zb;J\right\rangle,\\
\Delta_z &= -\hat{j}_z^{-1}\sum_{Jc}\hat{j}_c u_c v_c \left\langle zz;0\right|V\left|cc;0\right\rangle \text{ and}\\
n &= \sum_a \hat{j}_a^2 v_a^2.
\end{aligned}
\tag{221}
$$

In practice these equations are solved iteratively by, for example, supplying the initial values of Δ_z and λ_z, calculating the other relevant quantities of equations 221, calculating new values for Δ_z and λ_z and repeating the process until self-consistency is reached[10, Chapter 14]. This is usually measured in the absolute difference between the calculated average particle number and the desired particle number, with self-consistency considered achieved when this number is smaller than a limit set before starting the calculations. Different species of nucleons are also considered separately in practical calculations.

2.2.4 QRPA and MQPM

While the BCS model which was presented earlier is a successful nuclear model by itself, it is not the model that is of primary interest in this thesis. Instead, we will use it as a starting point in deriving a more sophisticated model known as the quasiparticle random-phase approximation (QRPA), which in turn will serve as a basis for the actual model used, the microscopic quasiparticle-phonon model (MQPM). The primary advantage of the QRPA over similar models, such as the quasiparticle Tamm-Dancoff approximation (QTDA)[10, Chapter 16], is the inclusion of ground-state correlations which can lead to transitions between states that are highly collective in nature. The most prominent flaw of the model is that the equations do not arise from a variational principle and they are approximations by nature. Similar to the BCS equations, the QRPA equations can be derived with the

EoM method. The derivation is relatively straightforward but somewhat tedious, and an overview of this is presented below.

The basic excitation of QRPA can be written in terms of the variational parameters X^{ω}_{ab} and Y^{ω}_{ab}, and the quasiparticle operators defined previously as[10, Page 558]

$$\begin{aligned} Q^{\dagger}_{\omega} &= \sum_{ab} \left[X^{\omega}_{ab} \mathcal{N}_{ab}(J) \left[a^{\dagger}_{a} a^{\dagger}_{b} \right]_{JM} + Y^{\omega}_{ab} \mathcal{N}_{ab}(J) \left[\tilde{a}_{a} \tilde{a}_{b} \right]_{JM} \right] \\ &\equiv \sum_{ab} \left[X^{\omega}_{ab} A^{\dagger}_{ab}(JM) - Y^{\omega}_{ab} \tilde{A}_{ab}(JM) \right], \end{aligned} \tag{222}$$

where

$$\begin{aligned} &A^{\dagger}_{ab}(JM) \equiv \mathcal{N}_{ab}(J) \left[a^{\dagger}_{a} a^{\dagger}_{b} \right]_{JM}, \quad \tilde{A}_{ab}(JM) = -\mathcal{N}_{ab}(J) \left[\tilde{a}_{a} \tilde{a}_{b} \right]_{JM} \text{ and} \\ &\mathcal{N}_{ab}(J) = \frac{\sqrt{1 + \delta_{ab}(-1)^{J}}}{1 + \delta_{ab}}. \end{aligned} \tag{223}$$

The variations are then $A_{ab}(JM)$ and $\tilde{A}^{\dagger}_{ab}(JM)$. The basic excitation is bosonic so we have for the former variation

$$\begin{aligned} &\langle \text{QRPA} | \left[\delta Q, H, Q^{\dagger}_{\omega} \right]_{-} | \text{QRPA} \rangle = E_{\omega} \langle \text{QRPA} | \left[\delta Q, Q^{\dagger}_{\omega} \right] | \text{QRPA} \rangle \Leftrightarrow \\ &\langle \text{QRPA} | \left[A_{ab}(JM), H, \sum_{cd} \left[X^{\omega}_{cd} A^{\dagger}_{cd}(JM) - Y^{\omega}_{cd} \tilde{A}_{cd}(JM) \right] \right] | \text{QRPA} \rangle = \\ &E_{\omega} \langle \text{QRPA} | \left[A_{ab}(JM), \sum_{cd} \left[X^{\omega}_{cd} A^{\dagger}_{cd}(JM) - Y^{\omega}_{cd} \tilde{A}_{cd}(JM) \right] \right] | \text{QRPA} \rangle \end{aligned} \tag{224}$$

and for the latter

$$\begin{aligned} &\langle \text{QRPA} | \left[\tilde{A}^{\dagger}_{ab}(JM), H, \sum_{cd} \left[X^{\omega}_{cd} A^{\dagger}_{cd}(JM) - Y^{\omega}_{cd} \tilde{A}_{cd}(JM) \right] \right] | \text{QRPA} \rangle = \\ &E_{\omega} \langle \text{QRPA} | \left[\tilde{A}^{\dagger}_{ab}(JM), \sum_{cd} \left[X^{\omega}_{cd} A^{\dagger}_{cd}(JM) - Y^{\omega}_{cd} \tilde{A}_{cd}(JM) \right] \right] | \text{QRPA} \rangle . \end{aligned} \tag{225}$$

The derivation essentially consists of determining the expectation values of

$$\begin{aligned} &\left[A_{ab}(JM), H, A^{\dagger}_{cd}(JM) \right], \ \left[A_{ab}(JM), H, \tilde{A}_{cd}(JM) \right], \ \left[A_{ab}(JM), A^{\dagger}_{cd}(JM) \right] \text{ and} \\ &\left[A_{ab}(JM), \tilde{A}_{cd}(JM) \right] \end{aligned} \tag{226}$$

along with their hermitian conjugates with respect to the the QRPA vacuum $|\text{QRPA}\rangle$.

The exact form of the correlated QRPA ground state $|\text{QRPA}\rangle$ is not known prior to solving the QRPA equations, so the BCS ground state $|\text{BCS}\rangle$ will be used as an approximate vacuum to derive the equations[10, Page 558]. The approximation of replacing the QRPA vacuum expectation value of the commutator of operators Q_ω and $Q_\omega^\dagger$ with the corresponding expectation value with respect to the BCS vacuum is known as the quasiboson approximation (QBA). The replacement of the QRPA ground state with the BCS ground state as an effective vacuum is the reason that the QRPA does not satisfy a variational principle.

With the BCS ground state as the approximate vacuum, it can then be shown that[10, Page 558]

$$\langle\text{BCS}|\left[A_{ab}(JM),A^\dagger_{cd}(J'M')\right]|\text{BCS}\rangle = \langle\text{BCS}|\left[A_{ab}(JM),\tilde{A}_{cd}(J'M')\right]|\text{BCS}\rangle = \delta_{ac}\delta_{bd}\delta_{JJ'}\delta_{MM'}. \tag{227}$$

This reduces the right sides of equations 224 and 225 to $E_\omega X^\omega_{ab}$ and $E_\omega Y^\omega_{ab}$ respectively. For the left sides, we can define matrices A and B with elements[10, Page 559]

$$A_{ab,cd} = \langle\text{BCS}|\left[A_{ab}(JM),H,A^\dagger_{cd}(JM)\right] \text{ and } B_{ab,cd} = -\langle\text{BCS}|\left[A_{ab}(JM),H,\tilde{A}_{cd}(JM)\right] \tag{228}$$

when the Hamiltonian H is expressed in terms of the BCS quasiparticle operators as[10, Chapter 13.3.2]

$$H = \frac{1}{2}\sum_b \frac{\hat{j}_b^2}{E_b}\left[(E_b-\eta_b)\left(\eta_b+\frac{1}{2}\mu_b\right)-\frac{1}{2}\Delta_b^2\right] + \sum_b \hat{j}_b E_b[a_b^\dagger\tilde{a}_b]_{00} + V_{\text{RES}}, \tag{229}$$

where

$$V_{\text{RES}} = \frac{1}{4}\sum_{\alpha\beta\gamma\delta}\overline{v}_{\alpha\beta\gamma\delta}\mathcal{N}[c^\dagger_\alpha c^\dagger_\beta c_\delta c_\gamma], \tag{230}$$

with the normal ordering $\mathcal{N}[\cdots]$ taken with respect to the BCS vacuum. By substituting the particle-hole operators by their expressions in terms of the quasiparticle operators (equations 188) in the above expression, the residual interaction V_{RES} can be shown to consist of a sum of parts[10, Chapter 16.1]

$$H_{40} = \frac{1}{2}\sum_{abcdJ}(-1)^J V^{(40)}_{abcd}(J)\left(\left[a^\dagger_a a^\dagger_b\right]_J\cdot\left[a^\dagger_c a^\dagger_d\right]_J + \text{h.c.}\right), \tag{231}$$

$$H_{31} = \sum_{abcdJ} (-1)^J V^{(31)}_{abcd}(J) \left(\left[a^\dagger_a a^\dagger_b \right]_J \cdot \left[a^\dagger_c \tilde{a}_d \right]_J + \text{h.c.} \right), \tag{232}$$

and

$$H_{22} = \frac{1}{2} \sum_{abcdJ} (-1)^J V^{(22)}_{abcd}(J) \left[a^\dagger_a a^\dagger_b \right]_J \cdot \left[\tilde{a}_c \tilde{a}_d \right]_J, \tag{233}$$

where

$$V^{(40)}_{abcd}(J) = -\frac{1}{2} \left[\mathcal{N}_{ab}(J) \mathcal{N}_{cd}(J) \right]^{-1} u_a u_b v_c v_d \left\langle ab; J \right| V \left| cd; J \right\rangle, \tag{234}$$

$$V^{(31)}_{abcd}(J) = -\frac{1}{2} \left[\mathcal{N}_{ab}(J) \mathcal{N}_{cd}(J) \right]^{-1} \left(u_a u_b v_c u_d - v_a v_b u_c v_d \right) \left\langle ab; J \right| V \left| cd; J \right\rangle \tag{235}$$

and

$$\begin{aligned} V^{(22)}_{abcd}(J) = & -\frac{1}{2} \left[\mathcal{N}_{ab}(J) \mathcal{N}_{cd}(J) \right]^{-1} \left(u_a u_b u_c u_d - v_a v_b v_c v_d \right) \left\langle ab; J \right| V \left| cd; J \right\rangle + \\ & 2 u_a v_b u_c v_d \sum_{J'} \left[\mathcal{N}_{ad}(J') \mathcal{N}_{cb}(J') \right]^{-1} \hat{J'}^2 \begin{Bmatrix} j_a & j_b & J \\ j_c & j_d & J' \end{Bmatrix} \left\langle ad; J' \right| V \left| cb; J' \right\rangle. \end{aligned} \tag{236}$$

The above equations can be used to determine the explicit forms of the matrix elements of A and B. After a long, but a rather straightforward derivation these can be shown to be[10, Chapters 16.2 and 18.1.2]

$$\begin{aligned} A_{ab,cd} = & (E_a + E_b) \delta_{ac} \delta_{bd} + \left(u_a u_b u_c u_d + v_a v_b v_c v_d \right) \left\langle ab; J \right| V \left| cd; J \right\rangle + \\ & \mathcal{N}_{ab}(J) \mathcal{N}_{cd}(J) \Big[\left(u_a v_b u_c v_d + v_a u_b v_c u_d \right) \left\langle ab^{-1}; J \right| V_{\text{RES}} \left| cd^{-1}; J \right\rangle - \\ & (-1)^{j_c + j_d + J} \left(u_a v_b v_c u_d + v_a u_b u_c v_d \right) \left\langle ab^{-1}; J \right| V_{\text{RES}} \left| dc^{-1}; J \right\rangle \Big] \end{aligned} \tag{237}$$

and

$$\begin{aligned} B_{ab,cd} = & -\left(u_a u_b v_c v_d + v_a v_b u_c u_d \right) \left\langle ab; J \right| V \left| cd; J \right\rangle + \\ & \mathcal{N}_{ab}(J) \mathcal{N}_{cd}(J) \Big[\left(u_a v_b v_c u_d + v_a u_b u_c v_d \right) \left\langle ab^{-1}; J \right| V_{\text{RES}} \left| cd^{-1}; J \right\rangle - \\ & (-1)^{j_c + j_d + J} \left(u_a v_b u_c v_d + v_a u_b v_c u_d \right) \left\langle ab^{-1}; J \right| V_{\text{RES}} \left| dc^{-1}; J \right\rangle \Big]. \end{aligned} \tag{238}$$

The matrices can be shown to have the properties

$$\mathsf{A}^\dagger = \mathsf{A} \text{ and } \mathsf{B}^{\text{T}} = \mathsf{B}, \tag{239}$$

and they can be used to write equations 224 and 225 as[10, Chapters 11.2.1 and 18.1.1]

$$\sum_{c\leq d} A_{ab,cd}X^{\omega}_{cd} + \sum_{c\leq d} B_{ab,cd}Y^{\omega}_{cd} = E_{\omega}X^{\omega}_{ab} \tag{240}$$

and

$$-\sum_{c\leq d}(\mathsf{B}^{\dagger})_{ab,cd}X^{\omega}_{cd} - \sum_{c\leq d}(\mathsf{A}^{\mathrm{T}})_{ab,cd}Y^{\omega}_{cd} = E_{\omega}Y^{\omega}_{ab}, \tag{241}$$

which together constitute the QRPA equations. They can be combined into a single matrix equation

$$\begin{pmatrix} \mathsf{A} & \mathsf{B} \\ -\mathsf{B}^{*} & -\mathsf{A}^{*} \end{pmatrix} \begin{pmatrix} X^{\omega} \\ Y^{\omega} \end{pmatrix} = E_{\omega} \begin{pmatrix} X^{\omega} \\ Y^{\omega} \end{pmatrix}. \tag{242}$$

This is a non-Hermitian matrix eigenvalue problem for the excited states and excitation energies.

The QRPA is a realistic many-body theory that is widely in use in the present day nuclear physics research, but for the nuclei considered in this thesis it is not applicable by itself. The reason for this is that the QRPA is capable of describing even-even nuclei only (or odd-odd nuclei in the case of pnQRPA[10, Chapter 19]). To model odd-even nuclei, we will first consider even-even nuclei adjacent to the odd-even nuclei of interest and solve the BCS and QRPA equations for the occupation amplitudes u_a and v_a, and the QRPA parameters X^{ω} and Y^{ω}. These will then be used to define the basic excitation $\Gamma^{\dagger}_{k}(jm)$ of the microscopic quasiparticle-phonon model by[8]

$$\Gamma^{\dagger}_{i}(jm) = \sum_{n_b} C^{i}_{n_b} a^{\dagger}_{b=n_b jm} + \sum_{a\omega} D^{i}_{a\omega} \left[a^{\dagger}_{a} Q^{\dagger}_{\omega}\right]_{jm}. \tag{243}$$

The MQPM states thus consist of single-quasiparticle components and quasiparticles coupled together with QRPA phonons that are essentially three-quasiparticle components with good angular momentum quantum numbers j and m.

The derivation of the MQPM equations is again similar to the derivation of the equations of the previous two models, and we will only present the key features of it below. A detailed derivation can be found in e.g. [8]. In the EoM method we have the variations a_b and $\left[a^{\dagger}_{a}Q^{\dagger}_{\omega}\right]^{\dagger}_{jm}$. Running these through the EoM method equations 163 while using the BCS state as the vacuum results in the matrix equation

$$\begin{pmatrix} A & B \\ B^{\mathrm{T}} & A' \end{pmatrix} \begin{pmatrix} C^{i} \\ D^{i} \end{pmatrix} = E_{\omega} \begin{pmatrix} 1 & 0 \\ 0 & N \end{pmatrix} \begin{pmatrix} C^{i} \\ D^{i} \end{pmatrix}. \tag{244}$$

The explicit forms of the submatrices A, B, A' and N are presented in appendix C.

After solving the above equation for C^i and D^i, the MQPM states can be constructed by operating with $\Gamma^\dagger_k(jm)$ on the BCS state. In the case of this thesis, the most relevant quantities associated with these states are the reduced neutral-current one-body transition densities between them. To see why, we return to the definitions of the multipole operators of equations 78. These operators $\mathcal{O}_{\lambda\mu}$ are spherical tensors, so they can be expressed in the second quantized form of equation 152 as[24]

$$\mathcal{O}_{\lambda\mu} = \lambda^{-1}\left(\sum_{\text{proton orbitals } ab}(a||O^p_\lambda||b)\left[c^\dagger_a\tilde{c}_b\right]_{\lambda\mu} + \sum_{\text{neutron orbitals } ab}(a||O^n_\lambda||b)\left[c^\dagger_a\tilde{c}_b\right]_{\lambda\mu}\right), \tag{245}$$

where we have decomposed the operator $\mathcal{O}_{\lambda\mu}$ into parts $O^p_{\lambda\mu}$ and $O^n_{\lambda\mu}$ that operate on only the protons and neutrons respectively ($\mathcal{O}_{\lambda\mu}$, $O^p_{\lambda\mu}$ and $O^n_{\lambda\mu}$ are functions of q in the case of the multipole operators of equations 78). The reduced matrix elements of the multipole operators appearing in equation 104 then consist of sums of terms proportional to (again suppressing the quantum numbers of the nuclear states other than the angular momenta J_i and J_f) $(a||O^r_\lambda||b)(J_f||\left[c^\dagger_a\tilde{c}_b\right]_\lambda||J_i)$, where $r = p$ or n. The factor $(a||O^r_\lambda||b)$ will be considered in the next section while $(J_f||\left[c^\dagger_a\tilde{c}_b\right]_\lambda||J_i)$, the reduced one-body neutral-current transition density, is precisely where the nuclear physics enters into the scattering cross section calculation. It is independent of the scattering process and is determined solely from the nuclear model employed. The explicit forms of these reduced transition densities are somewhat complicated and will not be derived here. They can be found in appendix C.

2.3 The nuclear current and nucleon form factors

In this section we will present the final two pieces of the theoretical machinery needed to model the scattering between nuclei and astrophysical neutrinos. The first of these is to find expressions for the multipole operators, that were used to decompose the nuclear current operator in the effective Hamiltonian in terms of spherical tensors, in terms of quantities that we can input into our cross section calculations. The second is to properly take into account the composite particle nature of the nucleons, which up until now have been treated as point-like elementary particles. Their internal structure will be considered in terms of form factors, which will be the topic of the

second part of this section.

2.3.1 The nuclear current

To conclude the review on the theory behind neutrino-nucleus scattering, we need to find expressions for the reduced matrix elements of the multipole operators defined in equations 78. These operators are given in terms of the nuclear current operator $\mathcal{J}^\mu(\mathbf{x})$, and we will thus need to consider it first. In this section we will first construct the first quantized form of the nuclear current operator and use it to acquire the second quantized forms of the multipole operators. Our starting point is to consider the decomposition of the nuclear current $\mathcal{J}^\mu(\mathbf{x})$ into vector and axial vector parts $J^{V,\mu}$ and $J^{A,\mu}$, so that

$$\mathcal{J}^\mu(\mathbf{x}) = J^{V,\mu}(\mathbf{x}) - J^{A,\mu}(\mathbf{x}). \tag{246}$$

The different parts can be decomposed further by considering the currents of different species of nucleons separately, leading to

$$J^{V/A,\mu}(\mathbf{x}) = J_{\mathrm{p}}^{V/A,\mu}(\mathbf{x}) + J_{\mathrm{n}}^{V/A,\mu}(\mathbf{x}). \tag{247}$$

where $J_{\mathrm{p(n)}}^{V/A,\mu}(\mathbf{x})$ is the current due to protons (neutrons).

The first quantized forms of $J_{\mathrm{p(n)}}^{V/A,\mu}(\mathbf{x})$ can be written as[11, Chapter 45.2]

$$J_{\mathrm{p(n)}}^{V/A,\mu}(\mathbf{x}) = \sum_{k=1}^{Z(N)} J_{\mathrm{p(n)}}^{V/A,\mu}(k)\delta^{(3)}(\mathbf{x}-\mathbf{x}_k). \tag{248}$$

The corresponding second quantized form can then be shown to be[11, Page 472]

$$\sum_{\mathbf{p}'\mathbf{p}\sigma'\sigma} \langle \mathbf{p}'\sigma'|J_{\mathrm{p(n)}}^{V/A,\mu}(\mathbf{x})|\mathbf{p}\sigma\rangle\, c^\dagger_{\mathbf{p}'\sigma'}c_{\mathbf{p}\sigma}, \tag{249}$$

where the single-nucleon states $|\mathbf{p}\sigma\rangle$ are free particles with wave functions

$$\langle \mathbf{x}|\mathbf{p}\sigma\rangle = \frac{1}{\sqrt{V}}e^{i\mathbf{p}\cdot\mathbf{x}}\chi_\sigma \equiv \phi_{\mathbf{p}\sigma}, \tag{250}$$

i.e. box-normalized plane waves. We can write the explicit form of the matrix elements $\langle \mathbf{p}'\sigma'|J_{\mathrm{p(n)}}^{V/A,\mu}(\mathbf{x})|\mathbf{p}\sigma\rangle$ as

$$\langle \mathbf{p}'\sigma'|J_{\mathrm{p(n)}}^{V/A,\mu}(\mathbf{x})|\mathbf{p}\sigma\rangle = \int \phi^\dagger_{\mathbf{p}'\sigma'}(\mathbf{y})J_{\mathrm{p(n)},1}^{V/A,\mu}(\mathbf{y})\delta^{(3)}(\mathbf{x}-\mathbf{y})\phi_{\mathbf{p}\sigma}(\mathbf{y})\mathrm{d}^3\mathbf{y}. \tag{251}$$

To make use of the above equation, we first note that the most general forms of the matrix elements at the origin are[29, Chapter 10.9]

$$\langle \mathbf{p}'\sigma'|J^{V,\mu}_{\mathrm{p(n)}}(0)|\mathbf{p}\sigma\rangle = \frac{1}{V}\overline{u}(\mathbf{p}'\sigma')\left[F_1^{\mathrm{NC};p(n)}(Q^2)\gamma^\mu - F_2^{\mathrm{NC};p(n)}(Q^2)\frac{i}{m_{\mathrm{N}}}\sigma^{\mu\nu}q_\nu\right]u(\mathbf{p}\sigma) \tag{252}$$

and

$$\langle \mathbf{p}'\sigma'|J^{A,\mu}_{\mathrm{p(n)}}(0)|\mathbf{p}\sigma\rangle = \frac{1}{V}\overline{u}(\mathbf{p}'\sigma')F_A^{\mathrm{NC};p(n)}(Q^2)\gamma_5\gamma^\mu u(\mathbf{p}\sigma), \tag{253}$$

when we impose the requirements of Lorentz covariance and parity conservation[3]. In the above equations $F_1^{\mathrm{NC};p(n)}(Q^2)$, $F_2^{\mathrm{NC};p(n)}(Q^2)$ and $F_A^{\mathrm{NC};p(n)}(Q^2)$ are the nucleon weak neutral current Dirac, Pauli and axial form factors respectively, and $Q^2 = -q_\mu q^\mu$. These result from the requirements that the matrix elements be invariant under time-reversal and isospin. The assumption that the second quantized nuclear current operator at the origin can be written as[24]

$$\begin{aligned} J^{V/A,\mu}(0) = &\sum_{\mathbf{p}'\mathbf{p}\sigma'\sigma} {}_p\langle \mathbf{p}'\sigma'|J^{V/A,\mu}(0)|\mathbf{p}\sigma\rangle_p \, c^\dagger_{\mathbf{p}'\sigma'}c_{\mathbf{p}\sigma} + \\ &\sum_{\mathbf{p}'\mathbf{p}\sigma'\sigma} {}_n\langle \mathbf{p}'\sigma'|J^{V/A,\mu}(0)|\mathbf{p}\sigma\rangle_n \, c^\dagger_{\mathbf{p}'\sigma'}c_{\mathbf{p}\sigma} \end{aligned} \tag{254}$$

(with $p(n)$ denoting a single-particle proton (neutron) state) can then be used to compare the above expression with equation 251 at $\mathbf{x} = 0$.

To do the comparison, we expand the matrix elements of equations 252 and 253 in powers of $1/m_{\mathrm{N}}$ by using the explicit expression of equation 106 for the Dirac spinors for the free nucleons (with $m = m_{\mathrm{N}}$), resulting in[11, Chapter 45.2]

$${}_{p(n)}\langle \mathbf{p}'\sigma'|J^{V/A,\mu}(0)|\mathbf{p}\sigma\rangle_{p(n)} = \frac{1}{V}\chi^\dagger_{\sigma'}M^{V/A,\mu}_{p(n)}(Q^2)\chi_\sigma + O(1/m_{\mathrm{N}}^2), \tag{255}$$

where the components of the four-vectors $M^{V/A,\mu}_{p(n)}(Q^2)$ are defined by[24]

$$\begin{aligned} &M^{V,0}_{p(n)}(Q^2) = F_1^{\mathrm{NC};p(n)}(Q^2), \quad M^{A,0}_{p(n)}(Q^2) = -\frac{F_A^{\mathrm{NC};p(n)}(Q^2)}{2m_{\mathrm{N}}}\boldsymbol{\sigma}\cdot(\mathbf{p}+\mathbf{p}'), \\ &\mathbf{M}^{V}_{p(n)}(Q^2) = \frac{F_1^{\mathrm{NC};p(n)}(Q^2)}{2m_{\mathrm{N}}}(\mathbf{p}+\mathbf{p}') + \frac{F_1^{\mathrm{NC};p(n)}(Q^2)+F_2^{\mathrm{NC};p(n)}(Q^2)}{2m_{\mathrm{N}}}i\mathbf{q}\times\boldsymbol{\sigma}, \\ &\mathbf{M}^{A}_{p(n)}(Q^2) = -F_A^{\mathrm{NC};p(n)}(Q^2)\boldsymbol{\sigma}. \end{aligned} \tag{256}$$

[3]We utilize the Conserved vector current hypothesis (CVC)[11, Chapter 42.7] here, and also assume that there are no second class currents.

We can make the substitution $\mathbf{q} \to -i\nabla$ in the above equations on the basis that the nuclei involved in the scattering are highly localized in space. This guarantees vanishing surface terms when partial integration is applied to equation 7 that defines the kinematics of the system, which then leads to the substitution being justified[24]. Comparing the matrix elements of equations 251 and 255 now yields for the nuclear current operator four-vector time components[24]

$$\begin{aligned} J^{V,0}_{p(n)}(\mathbf{x}) &= F_1^{\mathrm{NC};p(n)}(Q^2) \sum_{k=1}^{Z(N)} \delta^{(3)}(\mathbf{x}-\mathbf{x}_k) = \rho^V_{p(n)} \text{ and} \\ J^{A,0}_{p(n)}(\mathbf{x}) &= F_A^{\mathrm{NC};p(n)}(Q^2) \sum_{k=1}^{Z(N)} \boldsymbol{\sigma}(k) \cdot \left\{ \frac{\mathbf{p}_k}{2m_{\mathrm{N}}}, \delta^{(3)}(\mathbf{x}-\mathbf{x}_k) \right\} = \rho^A_{p(n)}, \end{aligned} \tag{257}$$

and similarly for the spatial components

$$\mathbf{J}^V_{p(n)}(\mathbf{x}) = \mathbf{J}^V_{C,p(n)}(\mathbf{x}) + \nabla \times \boldsymbol{\mu}_{p(n)}(\mathbf{x}), \quad \mathbf{J}^A_{p(n)}(\mathbf{x}) = -\mathbf{A}_{p(n)}(\mathbf{x}), \tag{258}$$

where

$$\begin{aligned} \mathbf{J}^V_{C,p(n)}(\mathbf{x}) &= F_1^{\mathrm{NC};p(n)}(Q^2) \sum_{k=1}^{Z(N)} \left\{ \frac{\mathbf{p}_k}{2m_{\mathrm{N}}}, \delta^{(3)}(\mathbf{x}-\mathbf{x}_k) \right\}, \\ \boldsymbol{\mu}_{p(n)}(\mathbf{x}) &= \frac{F_1^{\mathrm{NC};p(n)}(Q^2) + F_2^{\mathrm{NC};p(n)}(Q^2)}{2m_{\mathrm{N}}} \sum_{k=1}^{Z(N)} \boldsymbol{\sigma}(k) \delta^{(3)}(\mathbf{x}-\mathbf{x}_k) \text{ and} \\ \mathbf{A}_{p(n)}(\mathbf{x}) &= F_A^{\mathrm{NC};p(n)}(Q^2) \sum_{k=1}^{Z(N)} \boldsymbol{\sigma}(k) \delta^{(3)}(\mathbf{x}-\mathbf{x}_k). \end{aligned} \tag{259}$$

In the defining equation of $\boldsymbol{\mu}_{p(n)}(\mathbf{x})$ above, we can abbreviate $\mu^{\mathrm{NC};p(n)} \equiv F_1^{\mathrm{NC};p(n)}(Q^2) + F_2^{\mathrm{NC};p(n)}(Q^2)$.

The expressions above and equations 78 can then be used to derive single-particle vector and axial vector operators for each of the multipole operators. For $\mathcal{M}_{JM}$ we get

$$M^{V;p(n)}_{JM}(q) = \int M_{JM}(q') F_1^{\mathrm{NC};p(n)}(Q'^2) \delta^{(3)}(\mathbf{y}-\mathbf{x}) \mathrm{d}^3\mathbf{y} = M_{JM}(q) F_1^{\mathrm{NC};p(n)}(Q^2) \tag{260}$$

and

$$M_{JM}^{A;p(n)}(q) = -\int M_{JM}(q')F_A^{\mathrm{NC};p(n)}(Q'^2)\boldsymbol{\sigma}\cdot\left\{\frac{\mathbf{p}_y}{2m_\mathrm{N}},\delta^{(3)}(\mathbf{y}-\mathbf{x})\right\}\mathrm{d}^3\mathbf{y} = \\ -\int M_{JM}(q')F_A^{\mathrm{NC};p(n)}(Q'^2)\boldsymbol{\sigma}\cdot\left(\frac{\mathbf{p}_y}{2m_\mathrm{N}}\delta^{(3)}(\mathbf{y}-\mathbf{x})+\delta^{(3)}(\mathbf{y}-\mathbf{x})\frac{\mathbf{p}_y}{2m_\mathrm{N}}\right)\mathrm{d}^3\mathbf{y}. \tag{261}$$

To evaluate the above integral, we utilize the identity[4]

$$[F(\mathbf{x}),\mathbf{p}] = i\nabla F(\mathbf{x}), \tag{262}$$

from which it follows that

$$[F(\mathbf{x}),\mathbf{p}] = F(\mathbf{x})\mathbf{p}-\mathbf{p}F(\mathbf{x}) = i\nabla F(\mathbf{x}) \Leftrightarrow \mathbf{p}F(\mathbf{x}) = F(\mathbf{x})\mathbf{p}-i\nabla F(\mathbf{x}). \tag{263}$$

By choosing $F(\mathbf{y}) = \delta^{(3)}(\mathbf{y}-\mathbf{x})$ we get for the integrand

$$M_{JM}(q')F_A^{\mathrm{NC};p(n)}(Q'^2)\boldsymbol{\sigma}\cdot\left(\frac{\mathbf{p}_y}{2m_\mathrm{N}}\delta^{(3)}(\mathbf{y}-\mathbf{x})+\delta^{(3)}(\mathbf{y}-\mathbf{x})\frac{\mathbf{p}_y}{2m_\mathrm{N}}\right) = \\ M_{JM}(q')F_A^{\mathrm{NC};p(n)}(Q'^2)\boldsymbol{\sigma}\cdot\left(-\frac{i}{2m_\mathrm{N}}\nabla\delta^{(3)}(\mathbf{y}-\mathbf{x})+\delta^{(3)}(\mathbf{y}-\mathbf{x})\frac{\mathbf{p}_y}{m_\mathrm{N}}\right). \tag{264}$$

We will consider the terms inside the parentheses separately. For the latter, we have

$$-\int M_{JM}(q')F_A^{\mathrm{NC};p(n)}(Q'^2)\boldsymbol{\sigma}\cdot\left(\delta^{(3)}(\mathbf{y}-\mathbf{x})\frac{\mathbf{p}_y}{m_\mathrm{N}}\right)\mathrm{d}^3\mathbf{y} = M_{JM}(q)F_A^{\mathrm{NC};p(n)}(Q^2)\boldsymbol{\sigma}\cdot\frac{\mathbf{p}}{m_\mathrm{N}} \\ = iM_{JM}(q)F_A^{\mathrm{NC};p(n)}(Q^2)\boldsymbol{\sigma}\cdot\frac{\nabla}{m_\mathrm{N}} = i\frac{q}{m_\mathrm{N}}F_A^{\mathrm{NC};p(n)}(Q^2)M_{JM}(q)\boldsymbol{\sigma}\cdot\frac{\nabla}{q} = \\ i\frac{q}{m_\mathrm{N}}F_A^{\mathrm{NC};p(n)}(Q^2)\Omega_{JM}(q), \tag{265}$$

where we have defined[24]

$$\Omega_{JM}(q) \equiv M_{JM}(q)\boldsymbol{\sigma}\cdot\frac{\nabla}{q} \tag{266}$$

and made the substitution $\mathbf{p} = -i\nabla$. For the former term we can first apply the

[4]Proof: For functions $F(\mathbf{x}),G(\mathbf{x}) : \mathbb{R}^3 \to \mathbb{R}$ we have $[F(\mathbf{x}),\mathbf{p}]\,G(\mathbf{x}) = -iF(\mathbf{x})\nabla G(\mathbf{x}) + i\nabla(F(\mathbf{x})G(\mathbf{x})) = -iF(\mathbf{x})\nabla G(\mathbf{x}) + iF(\mathbf{x})\nabla G(\mathbf{x}) + iG(\mathbf{x})\nabla F(\mathbf{x}) = (i\nabla F(\mathbf{x}))G(\mathbf{x}) \Rightarrow [F(\mathbf{x}),\mathbf{p}] = i\nabla F(\mathbf{x})$, where we have used the substitution $\mathbf{p} = -i\nabla$ and the identity $\nabla(F(\mathbf{x})G(\mathbf{x})) = F(\mathbf{x})\nabla G(\mathbf{x}) + G(\mathbf{x})\nabla F(\mathbf{x})$[28, Page 915].

identity

$$\nabla' f(\mathbf{x}-\mathbf{x}') = -\nabla f(\mathbf{x}-\mathbf{x}'), \tag{267}$$

from which we get

$$\begin{aligned} &\int M_{JM}(q') F_A^{\mathrm{NC};p(n)}(Q'^2)\boldsymbol{\sigma}\cdot\frac{i}{2m_{\mathrm{N}}}\nabla\delta^{(3)}(\mathbf{y}-\mathbf{x})\mathrm{d}^3\mathbf{y} = \\ &-\int M_{JM}(q') F_A^{\mathrm{NC};p(n)}(Q'^2)\boldsymbol{\sigma}\cdot\frac{i}{2m_{\mathrm{N}}}\nabla_y\delta^{(3)}(\mathbf{y}-\mathbf{x})\mathrm{d}^3\mathbf{y}. \end{aligned} \tag{268}$$

We can then use partial integration, noting again that the surface term disappears, to obtain

$$\begin{aligned} &-\int M_{JM}(q') F_A^{\mathrm{NC};p(n)}(Q'^2)\boldsymbol{\sigma}\cdot\frac{i}{2m_{\mathrm{N}}}\nabla_y\delta^{(3)}(\mathbf{y}-\mathbf{x})\mathrm{d}^3\mathbf{y} = \\ &\int F_A^{\mathrm{NC};p(n)}(Q'^2)\nabla\cdot(M_{JM}(q')\boldsymbol{\sigma})\frac{i}{2m_{\mathrm{N}}}\delta^{(3)}(\mathbf{y}-\mathbf{x})\mathrm{d}^3\mathbf{y} = \\ &\frac{i}{2m_{\mathrm{N}}}\int F_A^{\mathrm{NC};p(n)}(Q'^2)\boldsymbol{\sigma}\cdot(\nabla M_{JM}(q'))\delta^{(3)}(\mathbf{y}-\mathbf{x})\mathrm{d}^3\mathbf{y}. \end{aligned} \tag{269}$$

By defining the operator[24]

$$\Sigma''_{JM}(q) \equiv \left[\frac{\nabla M_{JM}(q)}{q}\right]\cdot\boldsymbol{\sigma} \tag{270}$$

we can finally get

$$\begin{aligned} &\frac{i}{2m_{\mathrm{N}}}\int F_A^{\mathrm{NC};p(n)}(Q'^2)\boldsymbol{\sigma}\cdot(\nabla M_{JM}(q'))\delta^{(3)}(\mathbf{y}-\mathbf{x})\mathrm{d}^3\mathbf{y} = \\ &\frac{i}{2m_{\mathrm{N}}}F_A^{\mathrm{NC};p(n)}(Q^2)\boldsymbol{\sigma}\cdot(\nabla M_{JM}(q)) = i\frac{q}{m_{\mathrm{N}}}F_A^{\mathrm{NC};p(n)}(Q^2)\frac{1}{2}\left(\frac{\nabla M_{JM}(q)}{q}\right)\cdot\boldsymbol{\sigma} = \\ &i\frac{q}{m_{\mathrm{N}}}F_A^{\mathrm{NC};p(n)}(Q^2)\frac{1}{2}\Sigma''_{JM}(q). \end{aligned} \tag{271}$$

Combining the results we get

$$M_{JM}^{A;p(n)}(q) = i\frac{q}{m_{\mathrm{N}}}F_A^{\mathrm{NC};p(n)}(Q^2)\left[\Omega_{JM}(q)+\frac{1}{2}\Sigma''_{JM}(q)\right]. \tag{272}$$

The corresponding operators for the other multipole operators of equation 78 are found in a similar manner.

For $\mathcal{L}_{JM}$, we can relate its vector component to that of $\mathcal{M}_{JM}$ and the excitation

energy E_ω of the nuclear state by

$$L^V_{JM}(q) = -\frac{E_\omega}{q} M^V_{JM}(q), \tag{273}$$

which follows from the CVC[21]. The axial vector part can be shown to be[24]

$$L^{A;p(n)}_{JM} = -iF_A^{\mathrm{NC};p(n)}(Q^2)\Sigma''_{JM}(q). \tag{274}$$

By defining operators

$$\begin{aligned}
&\Delta_{JM}(q) \equiv \mathbf{M}^M_{JJ}(q)\cdot\frac{1}{q}\nabla, \quad \Delta'_{JM}(q) \equiv -\left[\frac{1}{q}\nabla\times\mathbf{M}^M_{JJ}(q)\right]\cdot\frac{1}{q}\nabla = \\
&\hat{J}^{-1}\left[-\sqrt{J}\mathbf{M}^M_{JJ+1}(q) + \sqrt{J+1}\mathbf{M}^M_{JJ-1}(q)\right]\cdot\frac{1}{q}\nabla, \quad \Sigma_{JM}(q) \equiv \mathbf{M}^M_{JJ}(q)\cdot\boldsymbol{\sigma} \text{ and} \\
&\Sigma'_{JM}(q) \equiv -\left[\frac{1}{q}\nabla\times\mathbf{M}^M_{JJ}(q)\right]\cdot\boldsymbol{\sigma} = \hat{J}^{-1}\left[-\sqrt{J}\mathbf{M}^M_{JJ+1}(q) + \sqrt{J+1}\mathbf{M}^M_{JJ-1}(q)\right]\cdot\boldsymbol{\sigma},
\end{aligned} \tag{275}$$

the single-particle operators for $\mathcal{T}^{\mathrm{el}}_{JM}$ and $\mathcal{T}^{\mathrm{mag}}_{JM}$ can expressed as[24]

$$\begin{aligned}
T^{\mathrm{el},V}_{JM} &= \frac{q}{m_{\mathrm{N}}}\left[F_1^{\mathrm{NC};p(n)}(Q^2)\Delta'_{JM}(q) + \frac{1}{2}\mu^{\mathrm{NC};p(n)}(Q^2)\Sigma_{JM}(q)\right], \\
T^{\mathrm{mag},V}_{JM} &= -i\frac{q}{m_{\mathrm{N}}}\left[F_1^{\mathrm{NC};p(n)}(Q^2)\Delta_{JM}(q) - \frac{1}{2}\mu^{\mathrm{NC};p(n)}(Q^2)\Sigma'_{JM}(q)\right] \\
T^{\mathrm{el},A}_{JM} &= -iF_A^{\mathrm{NC};p(n)}(Q^2)\Sigma'_{JM}(q) \text{ and } T^{\mathrm{mag},A}_{JM} = -F_A^{\mathrm{NC};p(n)}(Q^2)\Sigma_{JM}(q).
\end{aligned} \tag{276}$$

The second quantized forms of the multipole operators $\mathcal{O}_{JM}$ of equation 78 can then be written in terms of these first quantized single-particle operators $O^{V/A;p(n)}_{JM}$. From equation 245 we get

$$\begin{aligned}
\mathcal{O}_{JM} = \lambda^{-1}\Bigg[&\sum_{\text{proton orbitals } ab}\Big((a||O^{V,p}_\lambda||b) - (a||O^{A,p}_\lambda||b)\Big)\left[c^\dagger_a\tilde{c}_b\right]_{\lambda\mu} + \\
&\sum_{\text{neutron orbitals } ab}\Big((a||O^{V,n}_\lambda||b) - (a||O^{A,n}_\lambda||b)\Big)\left[c^\dagger_a\tilde{c}_b\right]_{\lambda\mu}\Bigg].
\end{aligned} \tag{277}$$

It can be then seen that the reduced matrix elements of the multipole operators can be expressed in terms of the reduced matrix elements of the operators $M_{JM}(q)$, $\mathbf{M}^M_{JL}(q)\cdot(1/q)\nabla$, $\mathbf{M}^M_{JL}(q)\cdot(1/q)\boldsymbol{\sigma}$ and $M_{JM}(q)\boldsymbol{\sigma}\cdot(1/q)\nabla$, where $L \in \{J-1, J, J+1\}$.

For these we have[24]

$$(a||M_J(q)||b) = \frac{(-1)^{J+j_b+\frac{1}{2}}}{\sqrt{4\pi}}\hat{l}_a\hat{l}_b\hat{j}_a\hat{j}_b\hat{J}\begin{Bmatrix} l_a & j_a & \frac{1}{2} \\ j_b & l_b & J \end{Bmatrix}\begin{pmatrix} l_a & J & l_b \\ 0 & 0 & 0 \end{pmatrix}\mathcal{R}^{(0)}_{abJ}, \tag{278}$$

$$\begin{aligned}(a||\mathbf{M}^M_{JL}(q)\cdot\frac{1}{q}\nabla||b) = \frac{(-1)^{L+j_b+\frac{1}{2}}}{\sqrt{4\pi}}\hat{l}_a\hat{j}_a\hat{j}_b\hat{J}\hat{L}\begin{Bmatrix} l_a & j_a & \frac{1}{2} \\ j_b & l_b & J \end{Bmatrix}\cdot \\ \left[-\sqrt{(l_b+1)(2l_b+3)}\begin{Bmatrix} L & 1 & J \\ l_b & l_a & l_b+1 \end{Bmatrix}\begin{pmatrix} l_a & L & l_b+1 \\ 0 & 0 & 0 \end{pmatrix}\mathcal{R}^{(-)}_{abJ}+\right. \\ \left.\sqrt{l_b(2l_b-1)}\begin{Bmatrix} L & 1 & J \\ l_b & l_a & l_b-1 \end{Bmatrix}\begin{pmatrix} l_a & L & l_b-1 \\ 0 & 0 & 0 \end{pmatrix}\mathcal{R}^{(+)}_{abJ}\right],\end{aligned} \tag{279}$$

$$(a||\mathbf{M}^M_{JL}(q)\cdot\boldsymbol{\sigma}||b) = \frac{(-1)^{l_a}}{\sqrt{4\pi}}\sqrt{6}\hat{l}_a\hat{l}_b\hat{j}_a\hat{j}_b\hat{J}\hat{L}\begin{Bmatrix} l_a & l_b & L \\ \frac{1}{2} & \frac{1}{2} & 1 \\ j_a & j_b & J \end{Bmatrix}\begin{pmatrix} l_a & L & l_b \\ 0 & 0 & 0 \end{pmatrix}\mathcal{R}^{(0)}_{abJ} \tag{280}$$

and

$$\begin{aligned}(a||M_{JM}(q)\boldsymbol{\sigma}\cdot\frac{1}{q}\nabla||b) = \frac{(-1)^{l_b}}{\sqrt{4\pi}}\hat{l}_a\hat{j}_a\hat{j}_b\sqrt{2(2j_b-l_b)+1}\begin{Bmatrix} l_a & j_a & \frac{1}{2} \\ j_b & 2j_b-l_b & J \end{Bmatrix}\cdot \\ \begin{pmatrix} l_a & J & 2j_b-l_b \\ 0 & 0 & 0 \end{pmatrix}\left[-\delta_{j_b,l_b+\frac{1}{2}}\mathcal{R}^{(-)}_{abJ}+\delta_{j_b,l_b-\frac{1}{2}}\mathcal{R}^{(+)}_{abJ}\right],\end{aligned} \tag{281}$$

where

$$\begin{aligned}&\mathcal{R}^{(-)}_{abJ} \equiv \langle n_a l_a|\, j_L(\rho)\left(\frac{\mathrm{d}}{\mathrm{d}\rho}-\frac{l_b}{\rho}\right)|n_b l_b\rangle\,, \quad \mathcal{R}^{(+)}_{abJ} \equiv \langle n_a l_a|\, j_L(\rho)\left(\frac{\mathrm{d}}{\mathrm{d}\rho}-\frac{l_b+1}{\rho}\right)|n_b l_b\rangle \\ &\text{and } \mathcal{R}^{(0)}_{abJ} \equiv \langle n_a l_a|j_L(\rho)|n_b l_b\rangle\,.\end{aligned} \tag{282}$$

2.3.2 Form factors

In this section we will finish the theoretical review of this thesis with a brief discussion on the form factors introduced in the previous section. We will first express the previously mentioned neutral current form factors in terms of the electromagnetic form factors, following closely the discussion presented in [30]. Starting off, we consider the weak neutral current $\mathcal{J}_\mu^{(0)}$ of equation 2. The structure of this current in the Standard Model is

$$\mathcal{J}_\mu = 2j_\mu^3 - 2\sin^2\theta_W j_\mu^{\mathrm{EM}}, \tag{283}$$

which follows from the electroweak unification condition. In the above equation θ_W is the Weinberg angle, and the j_μ^3 part consists of the sum of V-A couplings of the forms

$$\overline{x}\gamma_\mu(1-\gamma_5)\frac{1}{2}x \text{ and } -\overline{y}\gamma_\mu(1-\gamma_5)\frac{1}{2}y, \tag{284}$$

where x denotes all neutrinos and the quarks u, c and t, while y denotes the leptons e, μ and τ and the quarks d, s and b. The j_μ^{EM} term is just the electromagnetic current. For low energy neutrino scattering the most relevant part of j_μ^3 is that of the u and d quarks. We therefore define

$$V_\mu^3 = \overline{u}\gamma_\mu\frac{1}{2}u - \overline{d}\gamma_\mu\frac{1}{2}d, \quad A_\mu^3 = \overline{u}\gamma_\mu\gamma_5\frac{1}{2}u - \overline{d}\gamma_\mu\gamma_5\frac{1}{2}d, \quad V_\mu^s = \overline{s}\gamma_\mu s, \text{ and } A_\mu^s = \overline{s}\gamma_\mu\gamma_5 s, \tag{285}$$

and consider only the current

$$j_\mu^{\mathrm{NC}} = V_\mu^3 - A_\mu^3 - \frac{1}{2}\left(V_\mu^s - A_\mu^s\right) - 2\sin^2\theta_W j_\mu^{\mathrm{EM}}. \tag{286}$$

We will also separate the electromagnetic part of the current by considering only the electromagnetic currents of u, d and s quarks. If we denote

$$V_\mu^0 = \frac{1}{6}\overline{u}\gamma_\mu u + \frac{1}{6}\overline{d}\gamma_\mu d - \frac{1}{3}\overline{s}\gamma_\mu s, \tag{287}$$

we can write the relevant quark electromagnetic current J_μ^{EM} as

$$J_\mu^{\mathrm{EM}} = V_\mu^3 + V_\mu^0. \tag{288}$$

We will next consider the matrix elements of the current j_μ^{NC}.

The single-nucleon matrix element of the weak neutral current in the case of neutrino-nucleon scattering can be written in terms of the currents discussed (in Heisenberg picture) as

$$\langle p'|j_\mu^{\rm NC}(0)|p\rangle = \langle p'|V_\mu^3|p\rangle - \langle p'|A_\mu^3|p\rangle - \frac{1}{2}\Big(\langle p'|V_\mu^s|p\rangle - \langle p'|A_\mu^s|p\rangle\Big) - 2\sin^2\theta_W\,\langle p'|j_\mu^{\rm EM}|p\rangle\,, \tag{289}$$

where

$$\langle p'|j_\mu^{\rm EM}|p\rangle = \langle p'|V_\mu^3|p\rangle + \langle p'|V_\mu^0|p\rangle\,. \tag{290}$$

We have suppressed quantum numbers other than the nucleon 4-momenta p and p' before and after the scattering event. If we again denote proton and neutron single-particle states with subscripts, it then follows from isospin invariance of strong interactions that

$${}_p\langle p'|V_\mu^3|p\rangle_p = -\,{}_n\langle p'|V_\mu^3|p\rangle_n \;\text{ and }\; {}_p\langle p'|V_\mu^0|p\rangle_p = {}_n\langle p'|V_\mu^0|p\rangle_n\,. \tag{291}$$

From these and equation 290 we then get

$${}_p\langle p'|V_\mu^3|p\rangle_p = \frac{1}{2}\Big({}_p\langle p'|j_\mu^{\rm EM}|p\rangle_p - {}_n\langle p'|j_\mu^{\rm EM}|p\rangle_n\Big) \tag{292}$$

and

$${}_p\langle p'|V_\mu^0|p\rangle_p = \frac{1}{2}\Big({}_p\langle p'|j_\mu^{\rm EM}|p\rangle_p + {}_n\langle p'|j_\mu^{\rm EM}|p\rangle_n\Big)\,. \tag{293}$$

Now, using the equations presented so far, the fact that the matrix element of the electromagnetic current can be expressed in terms of the electromagnetic Dirac and Pauli form factors $F_1^{{\rm EM};p(n)}(Q^2)$ and $F_2^{{\rm EM};p(n)}(Q^2)$ as

$${}_{p(n)}\langle p'|j_\mu^{\rm EM}|p\rangle_{p(n)} = \overline{u}(\mathbf{p}')\left[\gamma_\mu F_1^{{\rm EM};p(n)}(Q^2) + \frac{i}{2m_{\rm N}}\sigma_{\mu\nu}\gamma^\nu F_2^{{\rm EM};p(n)}(Q^2)\right]u(\mathbf{p}), \tag{294}$$

and a similar expression for the matrix element

$$\begin{aligned}{}_{p(n)}\langle p'|V_\mu^s|p\rangle_{p(n)} = \overline{u}(\mathbf{p}')\Big[&\gamma_\mu F_1^{s;p(n)}(Q^2) + \frac{i}{2m_{\rm N}}\sigma_{\mu\nu}\gamma^\nu F_2^{s;p(n)}(Q^2) + \\ &\frac{1}{2m_{\rm N}}q_\mu F_3^{s;p(n)}(Q^2)\Big]u(\mathbf{p}),\end{aligned} \tag{295}$$

in terms of the strange form factors $F_1^{s;p(n)}(Q^2)$, $F_2^{s;p(n)}(Q^2)$ and $F_3^{s;p(n)}(Q^2)$, we arrive at the following expression for the weak neutral current vector form factors

$F_{1,2}^{\mathrm{NC};p(n)}(Q^2)$ and the strange form factors $F_{1,2}^{s;p(n)}(Q^2)$:

$$F_{1,2}^{\mathrm{NC};p(n)}(Q^2) = \frac{1}{2}\left(F_{1,2}^{\mathrm{EM};p(n)}(Q^2) - F_{1,2}^{\mathrm{EM};n(p)}(Q^2)\right) - 2\sin^2\theta_W F_{1,2}^{\mathrm{EM};p(n)}(Q^2) - \frac{1}{2}F_{1,2}^{s;p(n)}(Q^2), \tag{296}$$

where we have used the value $F_3^{s;p(n)}(Q^2) = 0$. For this and the other details in the derivation of the above equation, we again refer to [30]. A similar expression can be found for the weak neutral current axial form factor $F_A^{\mathrm{NC};p(n)}(Q^2)$ in terms of the charged current axial form factors $G_A(Q^2)$ and $G_A^s(Q^2)$:

$$F_A^{\mathrm{NC};p(n)}(Q^2) = \frac{1}{2}\left(+(-)G_A(Q^2) - G_A^s(Q^2)\right). \tag{297}$$

The values of the form factors presented so far will be discussed next.

The electromagnetic Dirac and Pauli form factors are conveniently expressed in terms of the Sachs electric and magnetic form factors $G_{\mathrm{E}}^{p(n)}(Q^2)$ and $G_{\mathrm{M}}^{p(n)}(Q^2)$ as[24]

$$F_1^{\mathrm{EM};p(n)}(Q^2) = \frac{G_{\mathrm{E}}^{p(n)}(Q^2) + \tau G_{\mathrm{M}}^{p(n)}(Q^2)}{1+\tau} \text{ and } F_2^{\mathrm{EM};p(n)}(Q^2) = \frac{G_{\mathrm{M}}^{p(n)}(Q^2) - G_{\mathrm{E}}^{p(n)}(Q^2)}{1+\tau} \tag{298}$$

with the abbreviation $\tau = Q^2/m_{\mathrm{N}}$. In this thesis we will adopt the parametrizations (parameters denoted by a, b, A and B)

$$G_{\mathrm{E}}^{p}(Q^2) = \frac{1 + a_{p,1}^{\mathrm{E}}\tau}{1 + b_{p,1}^{\mathrm{E}}\tau + b_{p,2}^{\mathrm{E}}\tau^2 + b_{p,3}^{\mathrm{E}}\tau^3} \text{ and } G_{\mathrm{E}}^{n}(Q^2) = \frac{A\tau}{1+B\tau}G_D(Q^2) \tag{299}$$

for the electric Sachs form factor and

$$\frac{G_{\mathrm{M}}^{p(n)}(Q^2)}{\mu_{p(n)}} = \frac{1 + a_{p(n),1}^{\mathrm{M}}\tau}{1 + b_{p(n),1}^{\mathrm{M}}\tau + b_{p(n),2}^{\mathrm{M}}\tau^2 + b_{p(n),3}^{\mathrm{M}}\tau^3} \tag{300}$$

for the magnetic Sachs form factor[24]. The function $G_D(Q^2)$ in the above equation is known as the dipole form factor, and in the case of $G_{\mathrm{M}}^{n}(Q^2)$, it is of the form

$$G_D(Q^2) = \frac{1}{\left(1 + \frac{Q^2}{M_V^2}\right)^2}, \tag{301}$$

while $\mu_{p(n)}$ is the magnetic moment of the corresponding nucleon. For the strange

form factors $F_{1,2}^{s;p(n)}(Q^2)$ we use[24]

$$F_1^{s;p(n)}(Q^2) = \frac{F_1^s Q^2}{1+\tau} G_D(Q^2) \text{ and } F_2^{s;p(n)}(Q^2) = \frac{\mu_s}{1+\tau} G_D(Q^2), \tag{302}$$

where F_1^s and μ_s are parameters. Finally, for the axial form factors we have[24]

$$G_A(Q^2) = G_A(0) G'_D(Q^2) \text{ and } G_A^s(Q^2) = G_A^s(0) G''_D(Q^2), \tag{303}$$

where the functions $G'_D(Q^2)$ and $G''_D(Q^2)$ are identical to $G_D(Q^2)$ with the exception that in place of the parameter M_V, they have M_A and M_A^s respectively. All the values for the parameters that were used in this thesis are presented in Appendix A. For the theory behind these parametrizations and how the values were determined, we refer to [31] for the electromagnetic Sachs form factors, [30] for the strange form factors, and [32] for the axial form factors.

3 Calculations and results

In this section we will discuss the numerical calculations of this thesis and present their results. The calculations consisted of three distinct parts: numerically solving the eigenstates and -energies of the nuclei of interest using the models discussed in section 2.2, calculating the reduced single-particle neutral current transition densities and nuclear matrix elements, and then using these to compute the neutrino scattering cross sections. We will discuss the first and the last of these steps and their corresponding results in detail. The second step of calculating the transition densities was computationally rather straightforward and the results not particularly illuminating when presented, so we have omitted most of the details on the discussion on this step. For the explicit expressions for these quantities we refer to Appendix C.

3.1 The Nuclear physics part

The process of modeling the nuclei of interest consisted of multiple parts as the model used, MQPM, is built upon other nuclear models, namely the BCS model and the QRPA, as was discussed in section 2.2. Thus, to model ^{127}I and ^{133}Cs, the two proton-odd neutron-even nuclei considered in this thesis, using MQPM, the states of the adjacent even-even nuclei ^{126}Te, ^{128}Xe, ^{132}Xe and ^{134}Ba needed to be first constructed using QRPA. The first step in the nuclear physics part of the calculations was then to construct the BCS states of these even-even nuclei. There were, however, a number of preliminary steps that preceded the primary nuclear model calculations outlined above. These steps were essential for the later ones, and we will discuss them first.

The zeroth step in the calculations before BCS or any other nuclear physics related calculations could be undertaken was to specify the valence space of the calculations, choose the residual interaction to be used and construct the single-particle basis states. The valence space was bounded from below by choosing an inert core consisting of 8 of both nucleons, i.e. an ^{16}O nucleus, making 0d the lowest single-particle orbital of the valence space. The proton and neutron numbers of

^{127}I and ^{133}Cs all lie between the shell model magic numbers 50 and 82, and all orbitals between them were included, of which 2s was the highest. The valence space 0d-2s contains for all the orbitals contained in it their respective spin-orbit parters[5], with the exception of $0i_{11/2}$, partner to $0i_{13/2}$. The missing $0i_{11/2}$ orbital was included despite it lying above the shell closure gap to form a valence space complete in terms of spin-orbit partners. The single-particle states and their energies for both species of nucleons have been illustrated for all even-even reference nuclei in figures 6, 7, 8 and 9. For the other preliminaries, the residual interaction we used was the Bonn-A one-boson exchange potential[33], and for the single-particle basis, the wave functions associated with the single-particle Hamiltonian of equation 141 were solved in harmonic oscillator basis[10, Chapter 3.2.1]. The values used for the various parameters present in equation 141 have been discussed in Appendix A.

After the preliminary preparations explained above were completed, the first step in the nuclear physics part of the calculations was next to follow. The procedure adopted for solving equations 221, i.e. the BCS equations, for the even-even nuclei mentioned above was that of using phenomenological pairing parameters with values chosen so that the theoretical pairing gaps were as close as possible to the corresponding experimental values. To elaborate, we note that the pairing gaps Δ_z that appear in equations 221 are a result of an odd-even effect that is seen when comparing the binding energies of adjacent even-A and odd-A nuclei; individual nucleons have a tendency to form pairs with zero total angular momentum, reducing the energy of the nucleon pair which leads to even-A nuclei typically having a higher binding energy than an adjacent odd-A nuclei[10, Chapter 12]. The pairing gap Δ can then be defined through the mass difference of odd and even nuclei by equation[10, Page 371]

$$M_A = \frac{1}{2}(M_{A+1} + M_{A-1}) + \Delta, \tag{304}$$

where M_A is the mass of the odd-A nucleus.

The experimental pairing gaps can then be solved from equation 304. When considering the nucleons separately, the pairing gaps are more conveniently expressed in terms of the proton and neutron separation energies S_p and S_n, instead of the

[5]Two single-particle orbitals are said to be spin-orbit parters if they have the same n and l quantum numbers, but differ in j as a result of the spin-orbit interaction splitting the states of different j in energy.

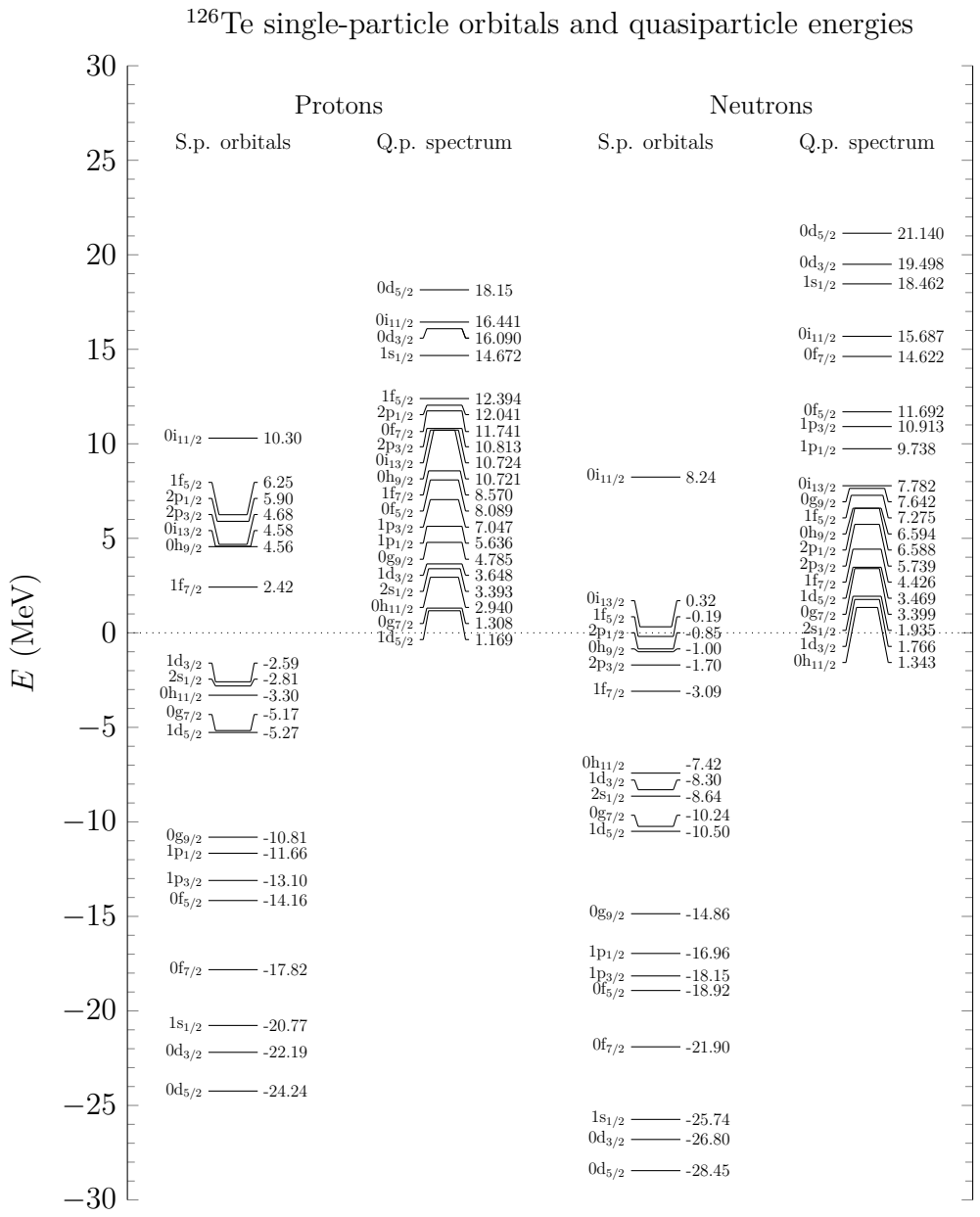

Figure 6. The used single-particle orbitals and their energies for ^{126}Te, along with the quasiparticle spectrum. The shell model structure and shell gaps for the orbitals are clearly visible. Results for both species of nucleons are illustrated.

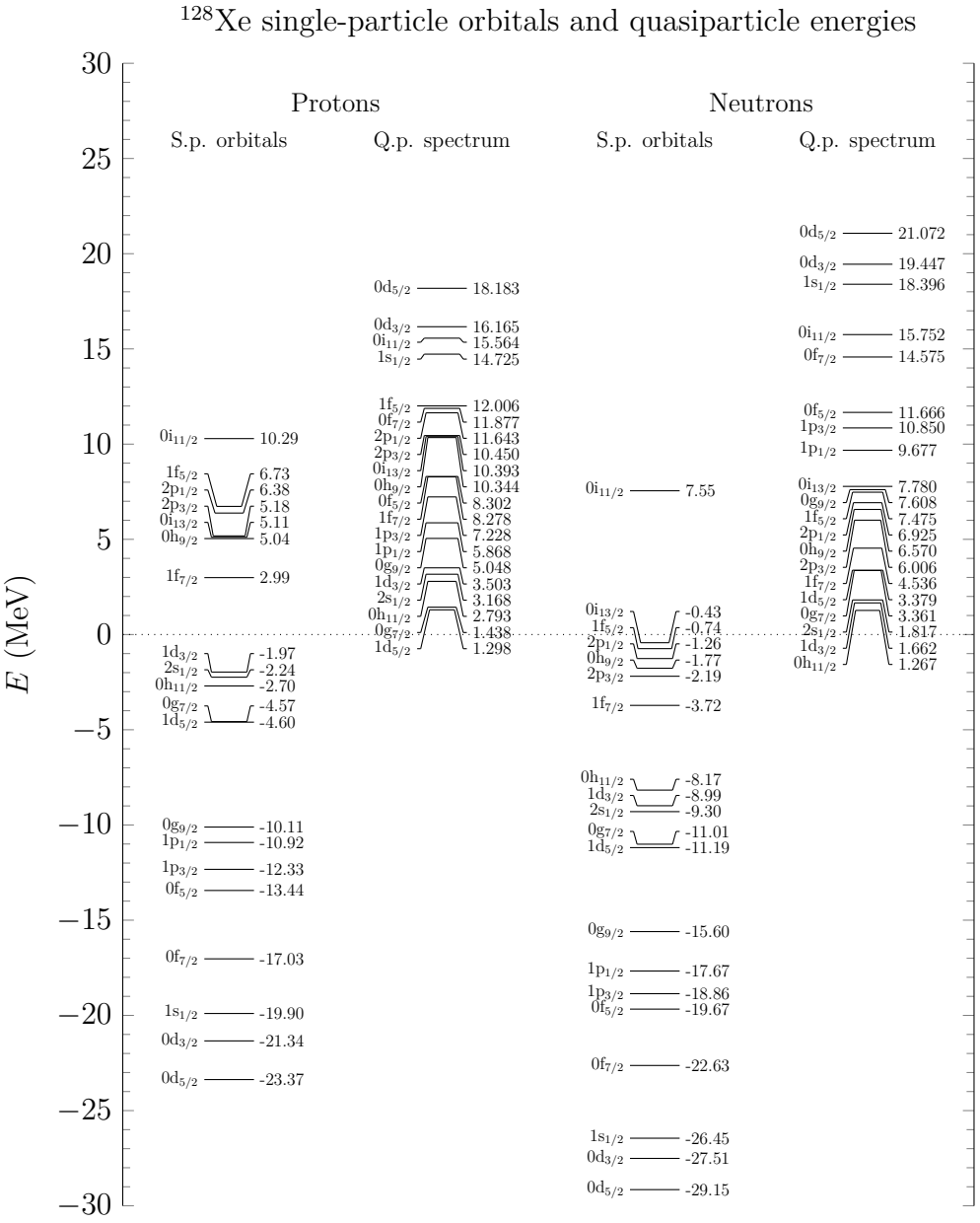

Figure 7. The used single-particle orbitals and their energies for ^{128}Xe, along with the quasiparticle spectrum. The shell model structure and shell gaps for the orbitals are clearly visible. Results for both species of nucleons are illustrated.

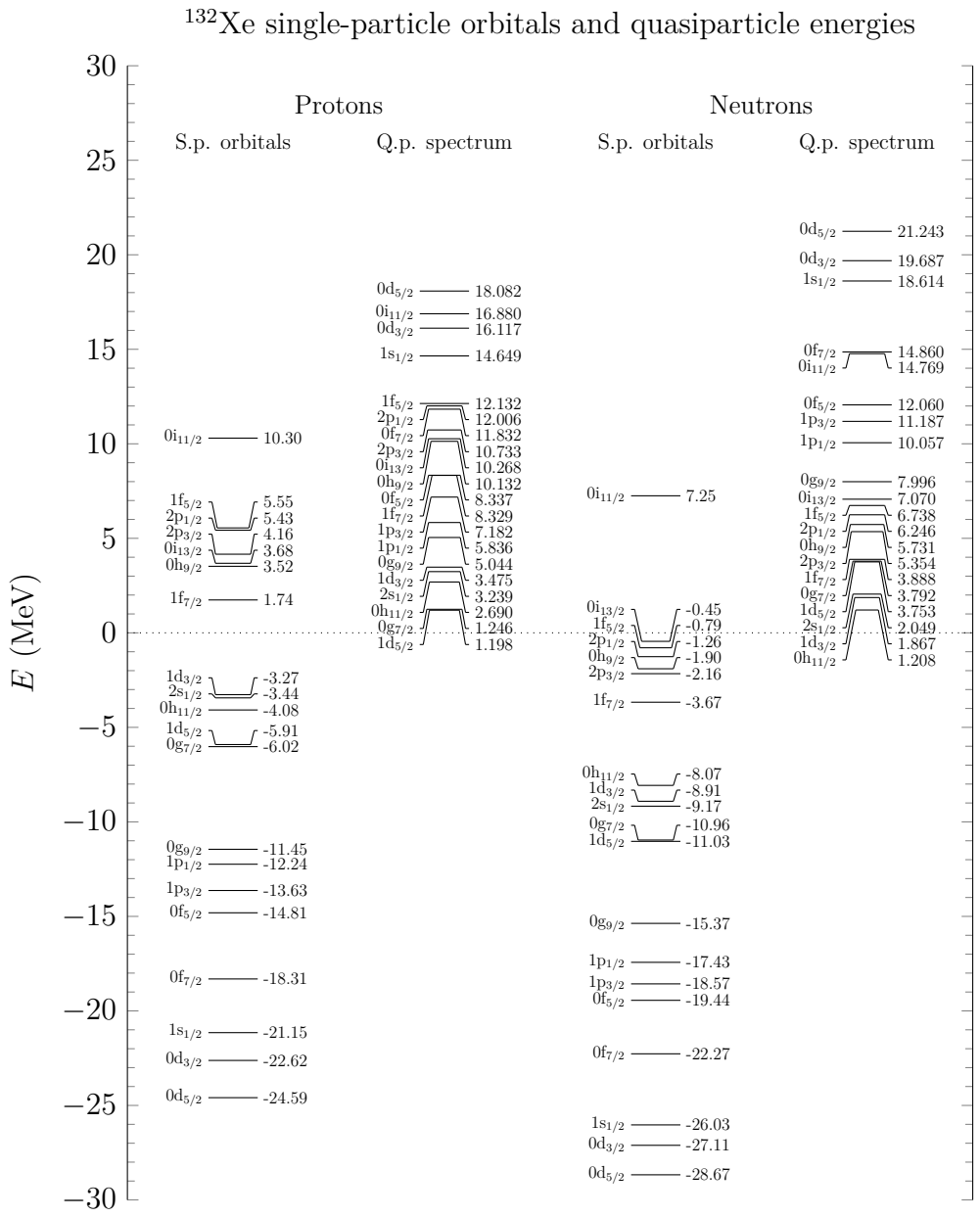

Figure 8. The used single-particle orbitals and their energies for ^{132}Xe, along with the quasiparticle spectrum. The shell model structure and shell gaps for the orbitals are clearly visible. Results for both species of nucleons are illustrated.

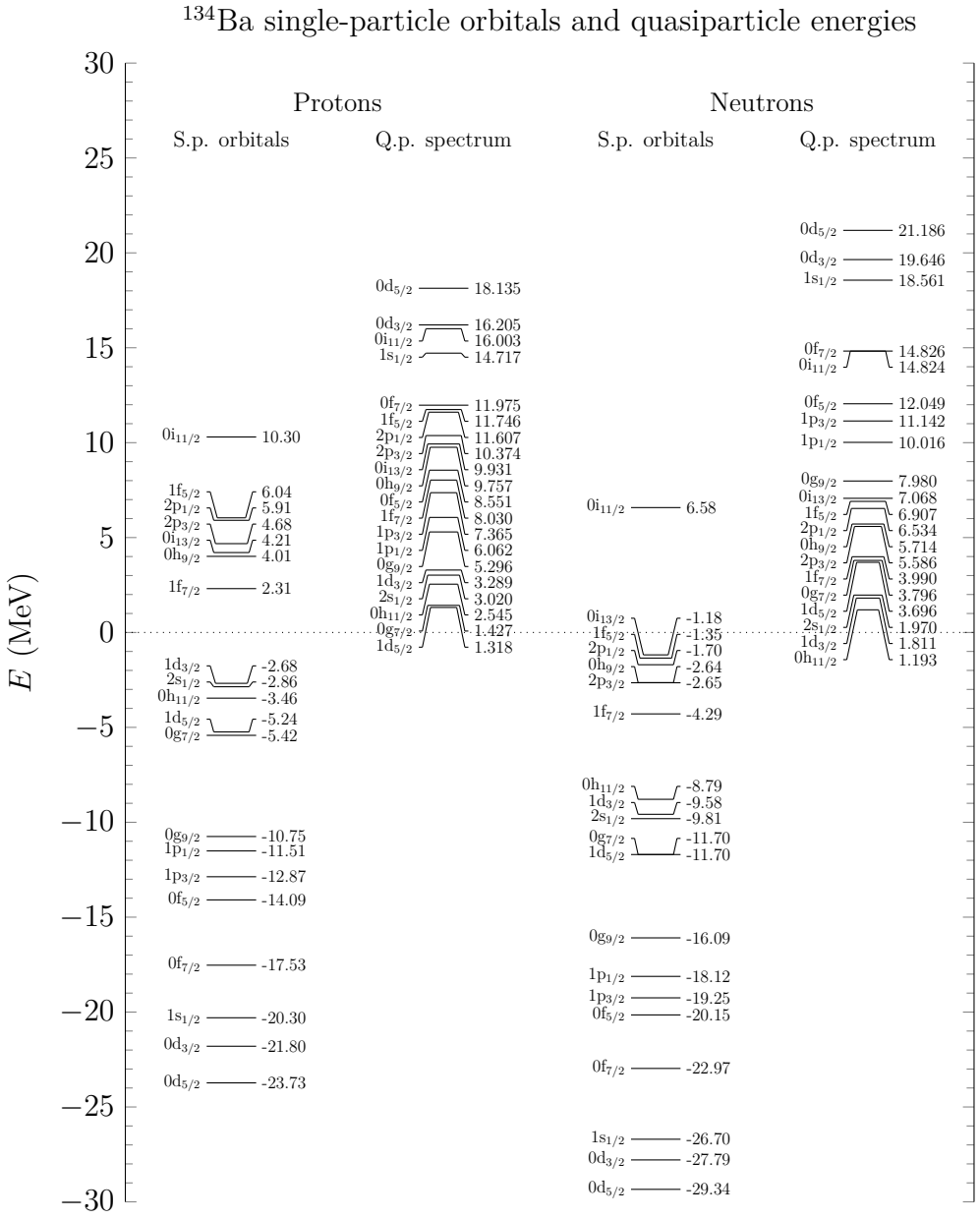

Figure 9. The used single-particle orbitals and their energies for ^{134}Ba, along with the quasiparticle spectrum. The shell model structure and shell gaps for the orbitals are clearly visible. Results for both species of nucleons are illustrated.

nuclear masses. We have the simple equations[10, Page 500]

$$\Delta_p(A,Z) = \frac{1}{2}\left[S_p(A+1,Z+1) - S_p(A,Z)\right] \tag{305}$$

and

$$\Delta_n(A,Z) = \frac{1}{2}\left[S_n(A+1,Z) - S_n(A,Z)\right] \tag{306}$$

for proton and neutron pairing gaps, which follow directly from equation 304 and the definitions of the separation energies. These simple two-point formulae were, however, not used to determine the experimental pairing gaps. Instead, the more accurate three-point formulae[10, Page 500]

$$\Delta_p(A,Z) = \frac{1}{4}(-1)^{Z+1}\left[S_p(A+1,Z+1) - 2S_p(A,Z) + S_p(A-1,Z-1)\right] \tag{307}$$

and

$$\Delta_n(A,Z) = \frac{1}{4}(-1)^{A-Z+1}\left[S_n(A+1,Z) - 2S_n(A,Z) + S_n(A-1,Z)\right], \tag{308}$$

that better account for the surrounding nuclear landscape around the nucleus of interest were used.

For the theoretical pairing gaps, we have from the BCS equations

$$E_\omega = \sqrt{\eta_z^2 + \Delta_z^2} \geq \Delta_z. \tag{309}$$

Based on this, the results of the BCS calculations were fit to experimental data so that

$$\Delta_p = E_{\omega,p,\text{lowest}} \text{ and } \Delta_n = E_{\omega,n,\text{lowest}}, \tag{310}$$

i.e. so that the lowest excitation energies E_ω, or quasiparticle energies, for both species of nucleons were as close to the corresponding experimental pairing gaps as possible. To perform these fits for the even-even nuclei adjacent to ^{127}I and ^{133}Cs, the nucleon separation energies for a number of nuclei surrounding these were used. They have been presented in tables 1 and 2 along with the calculated experimental pairing gaps. the full BCS quasiparticle spectra for all reference nuclei and both species of nucleons are illustrated in the same figures (6, 7, 8 and 9,) above as the single-particle orbitals.

After solving the BCS equations and obtaining the occupation amplitudes and

Table 1. The proton and neutron separation energies of the nuclei surrounding the even-even nuclei ^{126}Te and ^{128}Xe adjacent to ^{127}I[34][35][36][37][38]. The separation energies were used to calculate the pairing gaps defined in equations 307 and 308, and they are grouped based on which one of the even-even nuclei they were used for. The calculated proton and neutron pairing gaps are also listed.

^{127}I					
^{126}Te			^{128}Xe		
Nucleus	S_p (MeV)	S_n (MeV)	Nucleus	S_p (MeV)	S_n (MeV)
^{127}I	6.208	-	^{129}Cs	4.928	-
^{126}Te	9.0980	9.11369	^{128}Xe	8.165	9.610
^{125}Sb	7.311	-	^{127}I	6.208	-
^{127}Te	-	6.28765	^{129}Xe	-	6.9071
^{125}Te	-	6.56897	^{127}Xe	-	7.246
$\Delta_p = 1.1693$, $\Delta_n = 1.3427$			$\Delta_p = 1.2985$, $\Delta_n = 1.2667$		

Table 2. The proton and neutron separation energies of the nuclei surrounding the even-even nuclei ^{132}Xe and ^{134}Ba adjacent to ^{133}Cs[39][40][41][42][43]. The separation energies were used to calculate the pairing gaps defined in equations 307 and 308, and they are grouped based on which one of the even-even nuclei they were used for. The calculated proton and neutron pairing gaps are also listed.

^{133}Cs					
^{132}Xe			^{134}Ba		
Nucleus	S_p (MeV)	S_n (MeV)	Nucleus	S_p (MeV)	S_n (MeV)
^{133}Cs	6.080940	-	^{135}La	4.982	-
^{132}Xe	9.1252	8.936720	^{134}Ba	8.1679	9.4676
^{131}I	7.3787	-	^{133}Cs	6.080940	-
^{133}Xe	-	6.4359	^{135}Ba	-	6.97196
^{131}Xe	-	6.604410	^{133}Ba	-	7.1899
$\Delta_p = 1.1977$, $\Delta_n = 1.2083$			$\Delta_p = 1.3182$, $\Delta_n = 1.1933$		

other quantities of interest for the even-even nuclei, the second step in the nuclear physics part of the calculations could be undertaken. This consisted of using the results of the BCS calculations to construct the QRPA matrices A and B of equations 237 and 238, and numerically solving the QRPA equation (equation 242). Similar to the BCS calculations, phenomenological parameters were again used to fit the calculated theoretical values of observables as close to the corresponding experimental values as possible. For the QRPA calculations, the chosen observables were the energies of some of the lowest states of the even-even nuclei. Before presenting the results, we first briefly discuss the properties of the QRPA solutions and how they affected the choice of the states used in the fits.

As was discussed in section 2.2, solving the QRPA equation yields the parameters X^ω and Y^ω, which define the QRPA phonons $Q^\dagger_\omega$ as by equation 222. The excited states can then be constructed by operating on the QRPA vacuum with the phonon operator, i.e.

$$|\omega\rangle = Q^\dagger_\omega \, |\mathrm{QRPA}\rangle \, . \tag{311}$$

This is not the only way to generate excited states with the phonon operators. Instead of using only a single phonon operator to create an excited state, multiple phonon operators can be coupled together to form operators with a definite angular momentum[10, Chapter 18.5]. For the purposes of this thesis, the most interesting of such multiphonon states is the most simple of them, that is the case when two identical phonons are coupled to form a collective vibrational state

$$|\omega\omega; J,M\rangle = \frac{1}{\sqrt{2}} \left[Q^\dagger_\omega Q^\dagger_\omega \right]_{J,M} |\mathrm{QRPA}\rangle \, . \tag{312}$$

There is ample experimental evidence for the existence of such states in the case of quadrupole (2^+) and octupole (3^-) phonons[10, Chapter 18.5], of which the former was relevant for the calculations in this thesis.

Coupling together two quadrupole phonons gives possible total angular momenta 0^+, 2^+ and 4^+. Theoretically, this type of triplet of states is degenerate in energy that is twice that of the single-phonon quadrupole state. In practice, however, in the nuclei where collective vibrational two phonon states are found, the states of the triplet are not exactly equal in energy, but typically close to each other and found around the energy of twice that of the first 2^+ state. Of all the even-even nuclei considered in this thesis, all four of them had a lowest 4^+ state that fit the description

of a collective two-phonon vibrational state. The program used to solve the QRPA equation and generate the states was only concerned with single-phonon states of the form of equation 311, so the 4_1^+ states could not be used for fitting. Another notable feature of the QRPA solutions is a spuriosity affecting the lowest 1^- state. The cause of this is due to the constancy of the origin of the nuclear coordinates, which, as the nucleons move, results in unphysical movement of the nuclear centre of mass around the origin. This effect is discussed in more detail in [10, chapter 18.3.4], and we merely note here that the energies of the 1_1^- states for all the even-even nuclei considered were not suitable to be used as fitting parameters due to contamination of the states by this spurious effect.

Based on the factors discussed above, we chose the states 2_1^+, 3_1^-, 4_2^+, 5_1^- and 6_1^+ of the even-even nuclei to use in the fits. In addition to this, there is another spuriosity regarding the 0_2^+ states discussed in [25, 44]. As a result, its energy was fit as close to zero as possible. The rest of the states were fit according to the corresponding experimental values. The maximum value of angular momentum of a QRPA phonon in the calculations was chosen to be 6[6]. Part of the results of these calculations are presented in figures 10 and 11, where we have illustrated some of the lowest theoretical and experimental states of the even-even nuclei.

The agreement between theoretical and experimental spectra for all even-even nuclei can be seen to be decent overall. The typical QRPA trend of agreement between theoretical and experimental states being good at low energies and degrading as the energies of the states increase is clearly seen, with a few, but not surprising exceptions. In particular, the 2_2^+ and 4_1^+ states belonging to the two-phonon triplet are not reproduced with single-phonon states considered in this thesis, and thus their absence from the theoretical spectra was expected for all nuclei. One notable feature regarding this supposed quadrupole phonon triplet is that it does not appear to be a triplet. The energies of the lowest excited 0^+ states are all around the range of three times of that of the 2_1^+ state for all nuclei, which is considerably too high to be considered a two-phonon state composed of two quadrupole phonons. This was of course already taken into account when the states that were used for fitting were chosen. The discrepancy involving the missing 0^+ of the triplet and its causes have

[6]The MQPM results are said to converge for a particular maximum value of QPRA phonon angular momentum if the addition of higher multipoles into the QRPA calculations does not significantly alter the energies of the lowest MQPM states. This was the case in this thesis with the chosen maximum value of 6.

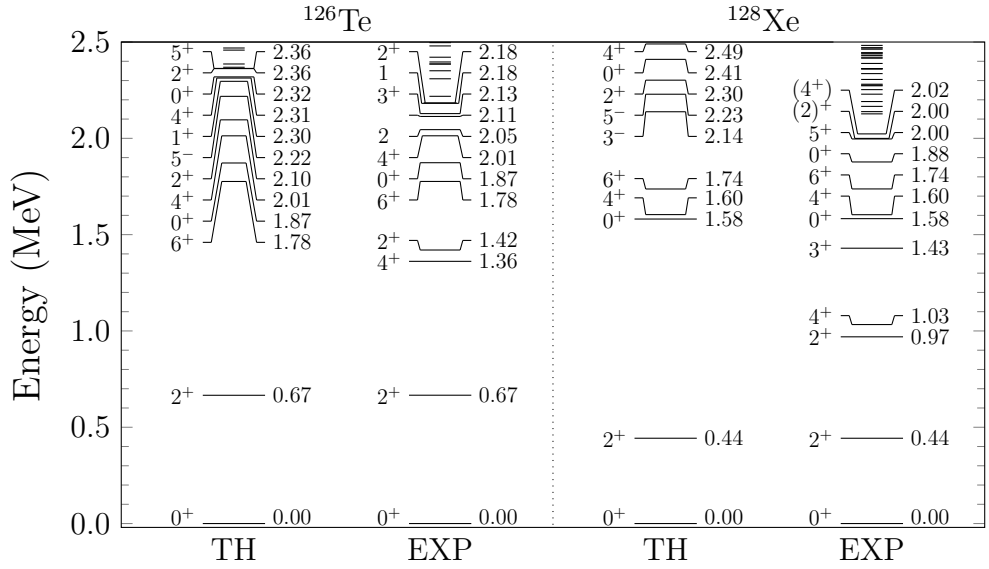

Figure 10. The low-lying (< 2.5 MeV) theoretical QRPA energy spectra of the even-even nuclei ^{126}Te and ^{128}Xe, and the corresponding experimental spectra[35][37]. Only the ten lowest states above the first 2^+ are labeled.

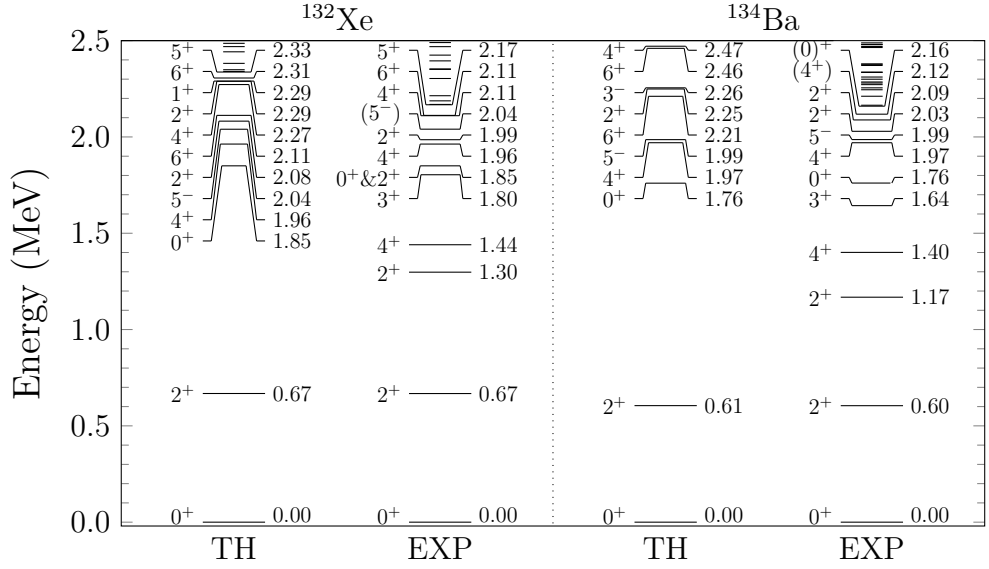

Figure 11. The low-lying (< 2.5 MeV) theoretical QRPA energy spectra of the even-even nuclei ^{132}Xe and ^{134}Ba, and the corresponding experimental spectra[40][42]. Only the ten lowest states above the first 2^+ are labeled.

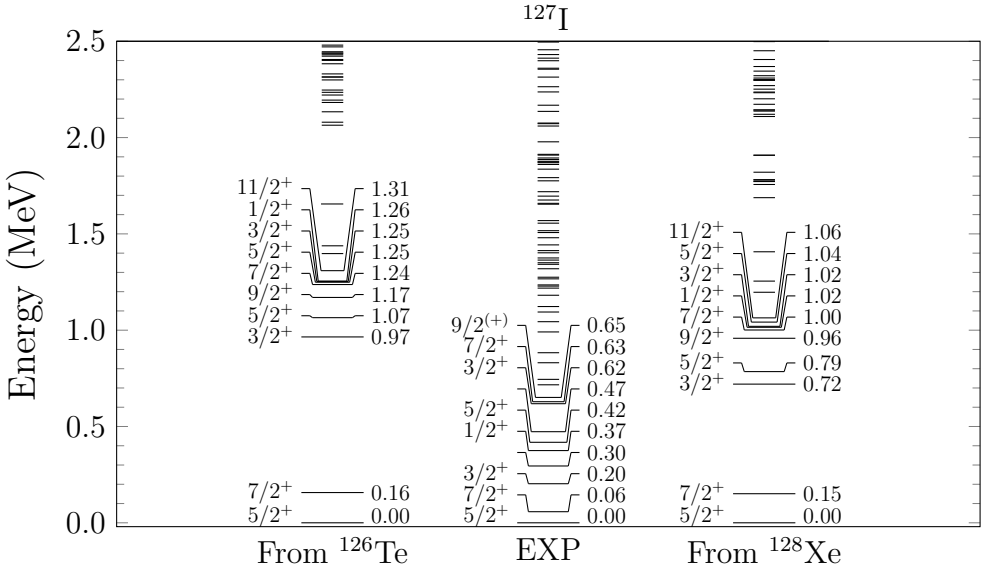

Figure 12. The low-lying (< 2.5 MeV) theoretical MQPM energy spectra of ^{127}I when the reference nuclei were ^{126}Te (left) and ^{128}Xe (right), along with the corresponding experimental spectrum[36] (middle). Only the ten lowest states are labeled.

also already been discussed in an earlier work[45] at mass numbers $A \leq 126$ in the context of QRPA calculations involving Xe isotopes.

The third and the final part of the nuclear state generation in the nuclear physics calculations was utilizing the results of the QRPA calculations, specifically the QRPA phonon operators $Q^{\dagger}_{\omega}$, along with the earlier BCS results to construct the MQPM equations (equation 244) for the nuclei ^{127}I and ^{133}Cs. Both of the adjacent even-even nuclei were used as the reference nucleus for each of the odd nuclei for a total of 4 different MQPM calculations. The aforementioned spurious QRPA states 0^+_2 and 1^-_1 were entirely excluded from the MQPM calculations. Solving the MQPM equations then yielded the states and energies of the nuclei of interest. The resulting low-lying MQPM spectra have been presented in figures 12 and 13.

The agreement between theoretical ^{127}I spectra and the corresponding experimental spectrum is less than fair at the lower end of the spectra. While the ground state is correctly reproduced for both reference nuclei, the experimental spectrum has a number of states below 1 MeV of which nearly all are missing in both theoretical spectra, excluding the first $7/2^+$ state which is predicted to be very close to its measured energy. The effect of the absence of these low-lying states to the neutrino scattering cross sections is unlikely to be very significant, as supernova neutrinos

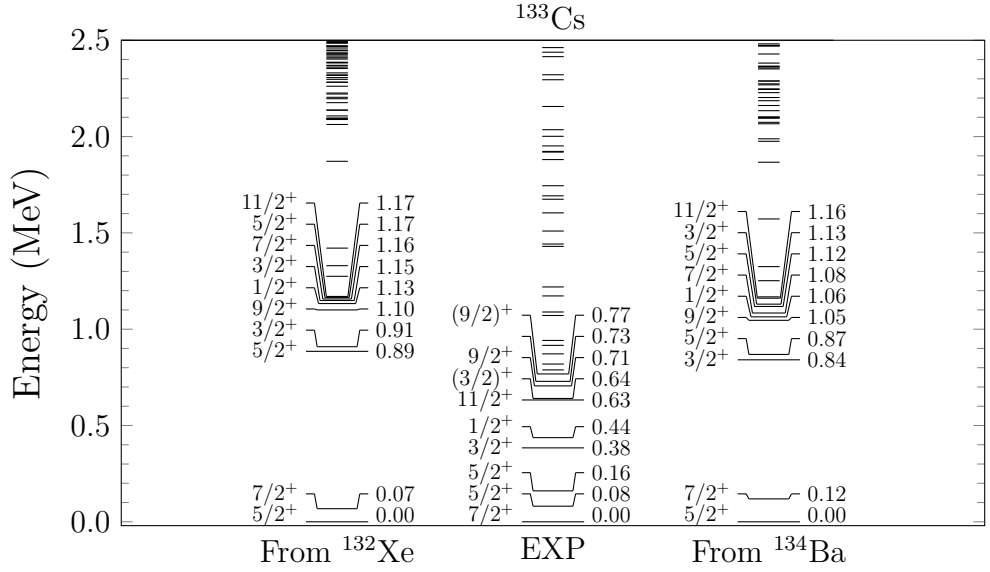

Figure 13. The low-lying (< 2.5 MeV) theoretical MQPM energy spectra of ^{133}Cs when the reference nuclei were ^{132}Xe (left) and ^{134}Ba (right), along with the corresponding experimental spectrum[41] (middle). Only the ten lowest states are labeled.

and antineutrinos are emitted at relatively high (≥ 10 MeV) average energies[46][47], so it is reasonable to expect that the most likely final nuclear states would also be high in energy. Similar calculations[48][49][50] involving other nuclei have indeed shown that the bulk of the contributions to the cross section do in fact come from high-energy states, thus lessening the concerns over inaccuracies at the lower end of the theoretical spectra. There are also noticeable gaps between certain states in the theoretical spectra, and states seem to form bands separated by these gaps. This is likely due to similar band-gap structure of the BCS quasiparticle states which, while not as pronounced as for the single-particle orbitals, is seen in the quasiparticle spectra in figures 6 and 7.

For the case of ^{133}Cs, the same conclusions mostly apply as the ones drawn for ^{127}I. The most prominent difference between the two is that for ^{133}Cs the ground state is not correctly reproduced in either of the theoretical calculations. There is, however, a state matching the parity and angular momentum ($7/2^+$) of the experimental ground state that is very close to the theoretical ground state ($5/2^+$), which in turn matches the first experimental excited state. In other words, had the two lowest theoretical states in the cases of both reference nuclei been predicted the other way around (the lower being the higher, and vice versa), the situation would have been the same as

with ^{127}I. Because of the incorrectly predicted ^{133}Cs ground state, the first excited state was used as the initial state in neutrino scattering calculations discussed in the next section. As a final note regarding the MQPM results, the question of which of the even-even nuclei performed better as an reference nucleus for the MQPM calculations should be addressed. For this, there was no clear winner for either of the odd nuclei considered here. While one could make the argument that one even-even nucleus provides marginally better predictions than its counterpart, the differences are minor and no definite conclusions regarding this comparison can be drawn based solely on the energy spectra.

After the MQPM states had been solved, the only thing left was to connect the numerical nuclear physics results to the scattering reaction formalism. As discussed in section 2, the nuclear physics entered into the calculations of the reaction cross sections in the form of the reduced one-body transition densities, which were entirely determined by the nuclear model used. These were computed after the previously discussed nuclear calculations using the BCS, QRPA and MQPM results. The final step linking the nuclear physics to the double-differential cross section is equation 122. To utilize this, we calculated the nuclear matrix elements, finishing the nuclear physics portion of the numerical part of this thesis.

3.2 Reaction cross sections

In this section we will present the results for the reaction cross sections. The calculations presented in the previous section culminated in obtaining all of the necessary quantities required for computing the double-differential cross section. Summing over the contributions of all the final nuclear states then produced the differential cross section, which was (numerically) integrated to get the reaction cross section with a given neutrino energy E_ν. The neutrinos considered in this thesis originate from supernova core collapses and are not emitted with one particular value of energy. Instead, they lie on a spectrum determined by the details of the physics of supernovae. To account for this, we averaged the cross section over an appropriately chosen energy distribution. These averaged cross sections are also experimentally significant as they are the quantities that are actually measured, further highlighting the importance of the choice of energy spectrum. While a detailed description of the mechanics of a supernova core collapse is beyond the scope of this thesis, we will nevertheless present some general features that provide insight into our choice

of neutrino energy spectrum next. For a more detailed look at this topic, we refer to [1, Chapter 5.4], which we have also used as the primary source in the following discussion.

The interior of a massive star at the onset of a supernova event is an environment of immense pressure and temperature. The electron degeneracy pressure prevents the core of the star from undergoing gravitational collapse when the mass of the core is below the Chandrasekhar limit. Thermonuclear reactions inside the star, which at that point in its lifespan consist primarily of silicon burning, eventually increase the mass of the core beyond the limit, which causes the core to collapse inwards. This considerably increases the electron density and thus the electron capture rates by nuclei in the inner core. These electron capture reactions in the inner core are, along with electron captures in the outer core after the rebound of the collapsing core and a number of other reactions that occur in the core, the primary source of electron neutrinos in supernova explosions, and the focus of this thesis. Secondary neutrino sources include, for example, β-decay of the material ejected into space during the explosion, and they were not considered in this work.

Neutrinos created inside the core travel through the interior of the star, interacting with matter on the way, eventually arriving at the surface and escaping into space. Matter density inside the core during a collapse eventually increases to a point where the neutrino diffusion time exceeds the collapse time, forming a sphere-shaped region of trapped neutrinos. The neutrinos inside this so called neutrino sphere interact with the surrounding matter and reach thermal equilibrium, which played a key part in our choice of the neutrino energy spectrum. As a system in thermal equilibrium, the neutrino sphere has a well defined surface temperature inversely proportional its radius. Based on these considerations, we assumed that the supernova neutrinos could be reasonably accurately treated as being emitted as black-body radiation with a thermal spectrum[24].

The energy of a gas of weakly interacting (with the term ”weak” in this context pertaining to the strength of the interaction, being independent of its type) fermions such as neutrinos in thermal equilibrium follows a Fermi-Dirac distribution[14, Chapter 3.6]. The average number of fermions n_i occupying the single-particle state i with an energy E_i in a Fermi-Dirac distribution with a negligible chemical potential is given by

$$n_i = \frac{1}{e^{E_i/T} + 1}. \tag{313}$$

To account for degeneracy, we note that for massless particles, the density of states in three dimensions is proportional to the square of the energy E_i^2, which follows from equation 10 and the well known dispersion relation

$$E^2 = p^2 = k^2. \tag{314}$$

for massless particles. The average number of particles having energy E_i is then $An_iE_i^2$, with A being a proportionality factor. This can be expressed as a probability distribution by integrating the expression over energy and using the result as a normalization factor, leading to

$$\int_0^\infty A\frac{E_i^2}{e^{E_i/T}+1}\mathrm{d}E_i = AN, \tag{315}$$

and

$$p_{\mathrm{FD}}(E_\nu) = \frac{1}{AN}A\frac{E_\nu^2}{e^{E_\nu/T}+1} = \frac{1}{N}\frac{E_\nu^2}{e^{E_\nu/T}+1}, \tag{316}$$

where

$$N = \int_0^\infty \frac{E_i^2}{e^{E_i/T}+1}\mathrm{d}E_i. \tag{317}$$

It is more convenient for our purposes to express the normalization factor N as a Fermi-Dirac integral[51, Chapter 25.12][7]

$$F_j(x) = \int_0^\infty \frac{y^j}{e^{y-x}+1}\mathrm{d}y, \quad j > -1, \tag{318}$$

by a change of variables $x = E_i/T$, $\mathrm{d}x = \mathrm{d}E_i/T$, from which we get

$$N = \int_0^\infty \frac{E_i^2}{e^{E_i/T}+1}\mathrm{d}E_i = T^3\int_0^\infty \frac{(E_i/T)^2}{e^{E_i/T}+1}\frac{\mathrm{d}E_i}{T} = T^3\int_0^\infty \frac{x^2}{e^{x-0}+1}\mathrm{d}x = T^3F_2(0). \tag{319}$$

The distribution can thus be written as

$$p_{\mathrm{FD}}(E_\nu) = \frac{1}{T^3F_2(0)}\frac{E_\nu^2}{e^{E_\nu/T}+1}, \tag{320}$$

which can then be used to calculate the averaged cross section.

Equation 320 represents the energy distribution of a highly simplified model of supernova neutrinos. While it is based on the general features that characterize the

[7]Some authors include a factor of $1/\Gamma(j+1)$ on the right side of the definition, while others omit it. In this work we choose to omit it.

circumstances under which neutrinos are emitted and provides a good first approximation, there is considerable room for improvement. In particular, there exists evidence based on Monte Carlo simulations of neutrino transport inside supernovae that the actual energy spectrum is damped in its high-energy tail portion in comparison to the Fermi-Dirac spectrum[46][47]. We consequently adopted a modified version of the above distribution known as the pinched Fermi-Dirac spectrum[24] to better model the tail part. This spectrum is obtained by introducing a term $-\alpha$ into the exponent function in the Fermi-Dirac distribution, giving

$$p_{\mathrm{FD}p}(E_\nu) = \frac{1}{T^3 F_2(\alpha)} \frac{E_\nu^2}{e^{E_\nu/T-\alpha}+1}. \tag{321}$$

The quantity α in the above equation is known as the degeneracy parameter, and it is mathematically equivalent to the chemical potential multiplied by the temperature T in a grand canonical ensemble treatment of non-interacting fermion gas[14, Chapter 3.6]. The convenience of expressing the Fermi-Dirac distribution in terms of the Fermi-Dirac integral is also clearly seen, as pinching the distribution affects the normalization by simply changing $F_2(x)$ in the denominator to be evaluated at α instead of 0.

The distribution of equation 321 can then be used to calculate the energy averaged cross sections $\langle\sigma\rangle$ of the scattering reactions considered by

$$\langle\sigma\rangle = \int_0^\infty p_{\mathrm{FD}p}(E_\nu)\sigma(E_\nu)\mathrm{d}E_\nu = \frac{1}{T^3 F_2(\alpha)} \int_0^\infty \frac{\sigma(E_\nu)E_\nu^2}{e^{E_\nu/T-\alpha}+1}\mathrm{d}E_\nu, \tag{322}$$

i.e. by folding the cross section $\sigma(E_\nu)$ with the distribution $p_{\mathrm{FD}p}(E_\nu)$, after specifying both the surface temperature of the neutrino sphere T and the degeneracy parameter α. As mentioned earlier, the surface temperature of the neutrino sphere depends on its radius. The radii at which neutrinos and antineutrinos are trapped are, however, not identical. Up until now, we have considered mainly electron neutrinos when discussing the creation of supernova neutrinos. While the processes that produce electron antineutrinos are mostly different (reactions involving pair formation produce both types of particles) from those that produce neutrinos, the same considerations for the mechanics of the core collapse and explosion apply.

The formation of the neutrino sphere is intimately tied to the reactions responsible for the coupling of the neutrinos inside the sphere. The most notable difference

Table 3. The calculated energy averaged total scattering cross sections defined in equation 322 for neutrino (ν_e) and antineutrino ($\overline{\nu}_e$) reactions with ^{127}I, along with the associated neutrino temperatures T and chosen degeneracy parameters α. Results from using both even-even nuclei (^{126}Te and ^{128}Xe) adjacent to ^{127}I as the base nucleus for MQPM calculations are presented. The neutrino temperatures were obtained by applying equation 324 and the values for average energies of neutrinos used were $\langle E_\nu \rangle_{\nu_e} = 11$ MeV and $\langle E_\nu \rangle_{\overline{\nu}_e} = 16$ MeV. The cross sections of inelastic reactions are in units of 10^{-42}cm^2 and the cross sections of elastic reactions in units of 10^{-40}cm^2.

^{127}I						
Parameters			From ^{126}Te		From ^{128}Xe	
Type	α	T	$\langle\sigma\rangle_{\text{inel}}$	$\langle\sigma\rangle_{\text{el}}$	$\langle\sigma\rangle_{\text{inel}}$	$\langle\sigma\rangle_{\text{el}}$
ν_e	0.0	3.49	5.15	29.9	3.79	29.7
ν_e	3.0	2.76	3.69	28.3	2.61	28.1
$\overline{\nu}_e$	0.0	5.08	16.9	57.5	13.1	57.2
$\overline{\nu}_e$	3.0	4.01	13.5	55.5	10.2	55.2

Table 4. The calculated energy averaged total scattering cross sections defined in equation 322 for neutrino (ν_e) and antineutrino ($\overline{\nu}_e$) reactions with ^{133}Cs, along with the associated neutrino temperatures T and chosen degeneracy parameters α. Results from using both even-even nuclei (^{132}Xe and ^{134}Ba) adjacent to ^{133}Cs as the base nucleus for MQPM calculations are presented. The neutrino temperatures were obtained by applying equation 324 and the values for average energies of neutrinos used were $\langle E_\nu \rangle_{\nu_e} = 11$ MeV and $\langle E_\nu \rangle_{\overline{\nu}_e} = 16$ MeV. The cross sections of inelastic reactions are in units of 10^{-42}cm^2 and the cross sections of elastic reactions in units of 10^{-40}cm^2.

^{133}Cs						
Parameters			From ^{132}Xe		From ^{134}Ba	
Type	α	T	$\langle\sigma\rangle_{\text{inel}}$	$\langle\sigma\rangle_{\text{el}}$	$\langle\sigma\rangle_{\text{inel}}$	$\langle\sigma\rangle_{\text{el}}$
ν_e	0.0	3.49	5.16	33.1	4.03	33.0
ν_e	3.0	2.76	3.68	31.4	2.74	31.2
$\overline{\nu}_e$	0.0	5.08	16.8	63.6	13.8	63.3
$\overline{\nu}_e$	3.0	4.01	13.6	61.4	10.9	61.1

between electron neutrinos and antineutrinos is that the charged current reactions

$$n + \nu_e \longleftrightarrow p + e^- \text{ and } p + \overline{\nu}_e \longleftrightarrow n + e^+ \tag{323}$$

do not occur at the same rate inside the core. The larger number of neutrons relative to the protons in the core leads to the former of these reactions to occur more frequently than the latter. Thus a higher mass density is needed to trap antineutrinos, leading to a smaller sphere radius and higher average energy. This was taken into account in the calculations of this thesis, and we adopted the commonly used values of $\langle E_\nu \rangle_{\nu_e} = 11$ MeV and $\langle E_\nu \rangle_{\overline{\nu}_e} = 16$ MeV for the average neutrino energies[24]. As the temperature is related to the average energy by[52, Chapter 4.1]

$$T = \frac{F_2(\alpha)}{F_3(\alpha)} \langle E_\nu \rangle , \tag{324}$$

specifying the average energies also uniquely determines the temperatures.

For our choice of the value for the degeneracy parameter α, we followed the approach of [24], and performed the calculations of the total energy averaged cross sections using the values $\alpha = 0$ and $\alpha = 3.0$ for both nuclei. We calculated these cross sections for both nuclei, using all four adjacent even-even nuclei as the reference nucleus, for both neutrinos and antineutrinos and elastic and inelastic scatterings. The results are presented in tables 3 and 4 along with the neutrino temperatures used.

It can be seen from the results that for both nuclei, neutrino types and choices of degeneracy parameter, the elastic cross sections are considerably higher than the corresponding inelastic cross sections. The elastic cross sections are experimentally less significant, as they cannot be directly measured. Their primary use is mainly as input parameters in computer simulations involving supernovae. The effect of the neutrino temperature to the cross section is also apparent in the results. The cross sections are quite sensitive to the temperature, with higher temperatures leading to higher cross sections. This effect is clearly seen in the cross sections of the inelastic scatterings, where the dependence between the cross section and the neutrino temperature is strong, and to a lesser but still remarkable extent in the elastic scatterings. This temperature sensitivity highlights the importance of the contributions of the high-energy tail part of the neutrino spectrum on the cross sections, and thus the value of the degeneracy parameter that controls the ”pinching”

of the spectrum. Overall, the results, as far as their magnitude is concerned, are in agreement with similar calculations from earlier works, performed in compareable nuclear mass ranges[52][53].

4 Conclusions

In this thesis we have explored the possibility of using the nuclei ^{127}I and ^{133}Cs in the detection of electron neutrinos and antineutrinos of astrophysical origin from a theoretical point of view. We have reviewed the theory underlying neutrino-nucleus scattering in considerable detail and derived expressions for several key quantities involved in the scattering reactions. We have discussed the standard formalism of many-body quantum mechanics applied to nuclear systems, reviewed the features of the equations-of-motion method and applied it to present a detailed derivation of the BCS equations, the general features of the derivation leading to the QRPA equations and a brief overview of how the MQPM equations arise from the said method. We have also presented the necessary details on nucleon form factors needed to account for the effects of their internal structure, which was otherwise neglected.

In the numerical part of this thesis, we have performed the BCS calculations for the even-even nuclei adjacent to ^{127}I and ^{133}Cs, namely ^{126}Te, ^{128}Xe, ^{132}Xe and ^{134}Ba, then used these results to do the QRPA calculations for the same nuclei, and finally used the results of both of these calculations to generate the MQPM states for the two odd nuclei. In these calculations we have used a single-particle basis based on a Coulomb-corrected Woods-Saxon potential and Bonn-A one-boson exchange potential for the residual interaction with a valence space spanning the orbitals 0d-2s in addition to $0i_{11/2}$. We have also computed the required neutral current transition densities and nuclear matrix elements needed for the cross section calculations.

We have computed the energy averaged cross sections for neutrino and antineutrino scatterings for both nuclei of interest using all the obtained MQPM results, for both elastic and inelastic scattering reactions. In these computations, we have used a neutrino energy distribution based on a thermal Fermi-Dirac spectrum with a modification in the form of a degeneracy parameter to account for the behaviour of the tail of the distribution. All cross sections were calculated with both the degeneracy parameter set to zero for a pure Fermi-Dirac neutrino spectrum, and with a value commonly used in literature for comparison. We have also briefly discussed the mechanics behind supernova explosions and the conditions that causes

the neutrinos to be emitted with a different average energy to that of antineutrinos, which was taken into account in the calculations of the cross sections.

For the results that were obtained, the QRPA spectra of the even-even nuclei were in fair agreement with the corresponding experimental spectra. One so far unaddressed issue regarding these results is that equations 307 and 308 are valid only at a sufficient distance away from shell closures where the separation energies can behave irregularly[10, Page 500]. In the case of the proton gap of ^{126}Te, ^{125}Sb has one proton above a closed shell making the application of equation 307 somewhat questionable. For this, we consulted the chart of nuclides and noted that the separation energies of the nuclei around ^{126}Te behave in a suitably regular manner for equation 307 to be used in determining the pairing gap. The later MQPM calculations resulted in two very similar theoretical spectra for ^{127}I without radical differences for both of the reference nuclei ^{126}Te and ^{128}Xe, further supporting the notion that the use of equation 307 for determining the proton pairing gap of ^{126}Te was justified.

Another decision that could be contested regarding the QRPA fits is the identification of the experimental 2_2^+ and 4_1^+ states as being part of a two-phonon triplet when no experimental candidates for the 0^+ state belonging to this triplet were found for any of the even-even nuclei. The choice to adopt this interpretation for the two aforementioned states was touched upon in the previous section, and also indirectly justified later on in the same section. Similarly to the entirely spurious 0^+ state which was fit as close to zero energy as possible, the exact energy of the 4_1^+ state was less important in the grand scheme of things. Modeling supernova neutrino-nucleus scattering requires a reasonably accurate description of high-lying excited nuclear states to properly account for all the possible final states, so whether the fit of the lowest theoretical 4^+ state was done to the lowest or second lowest experimental state which differ by around 0.5 MeV makes very little difference in the end. As a final note on this, the theoretical 4^+ state used for fitting could not have actually even been fit to the lowest experimental 4^+ state in the case of ^{126}Te and ^{128}Xe, as the parameter used to adjust the energy of this state could not be set to a value inside its range of applicability that would have lowered the energy of the theoretical state to the first experimental state.

The MQPM results for both odd nuclei had discrepancies with respect to the experimental results, particularly at the low-energy end of the spectra. These were

discussed in the previous section where we noted that most of the contributions to the supernova neutrino scattering cross section come from nuclear states that are relatively high in energy, meaning that disagreements between theoretical and experimental low-energy spectra are not a serious concern. While no singular reason that would explain these discrepancies could be named, there are ways to improve the accuracy of the low-lying theoretical spectrum. One of these ways has to do with the chosen Woods-Saxon single-particle parametrization. In this work, we chose the standard Bohr-Mottelson parametrization[54, Chapter 2] discussed in Appendix A. This parametrization is a result of fitting the parameter values in a simple way to produce a single-particle potential that can be used to describe a large number of nuclei with at least decent agreement with experiment. This has the disadvantage that agreement for any particular nucleus may be poor, deviating from the general trend captured in the parametrization. One way to improve the theoretical results is then to change the single-particle potential parametrization in a suitable way.

A simple way to adjust the parametrization without abandoning the Bohr-Mottelson parametrization entirely is to scale it phenomenologically until it reproduces the desired single-particle energies. Studying the low-lying spectrum of an odd-A nucleus can then be used determine how the single-particle energies should be set. With the quasiparticle based models used in this work, it is natural to interpret the lowest-lying states as simple one-quasiparticle states. Constructing these states in this way can be achieved by adjusting the single-particle energies of the adjacent even-even nucleus, so that its BCS quasiparticle spectrum contains quasiparticles with energies matching the lowest states of the odd nucleus. With our choice of parametrization in this thesis, the quasiparticle spectra do not match any of the adjacent odd-A nuclei for any of the used reference nuclei particularly well. Aside from the lowest few of the quasiparticle states, they are considerably higher in energy when compared to the lowest experimental states. This has been illustrated in figures 14 through 21.

The procedure outlined above can be expected to produce nearly perfect agreement with theoretical and experimental spectra at low levels, and it has been applied to a number nuclei in the vicinity of the ones studied in this work with good results[8]. The question of whether this is worth the effort for the nuclei considered here in possible future studies is another matter. While the states that contribute the most to the total scattering cross section are mostly high in energy, having an energy

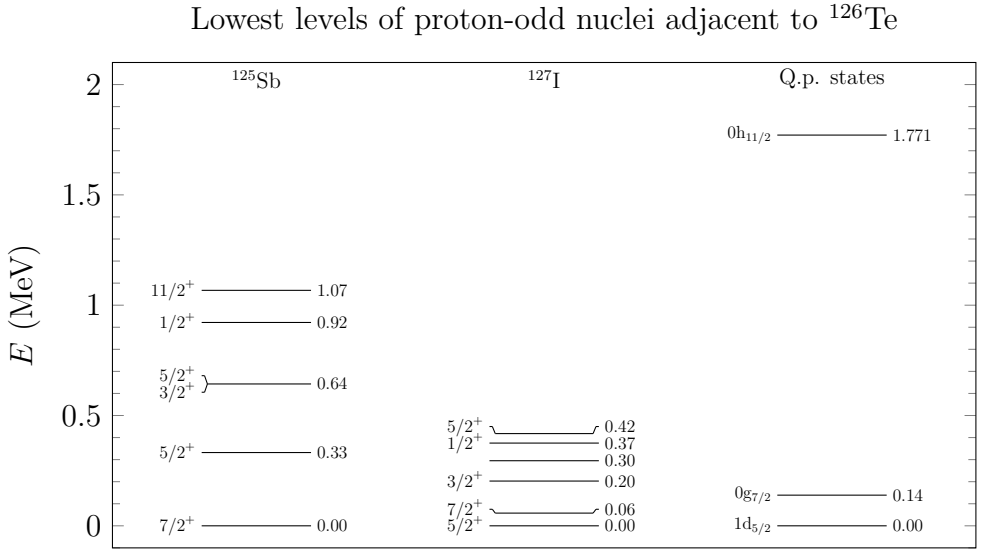

Figure 14. The five lowest states above ground state for both proton-odd nuclei adjacent to ^{126}Te, along with the lowest (< 2 MeV) proton quasiparticle states of ^{126}Te for comparison.

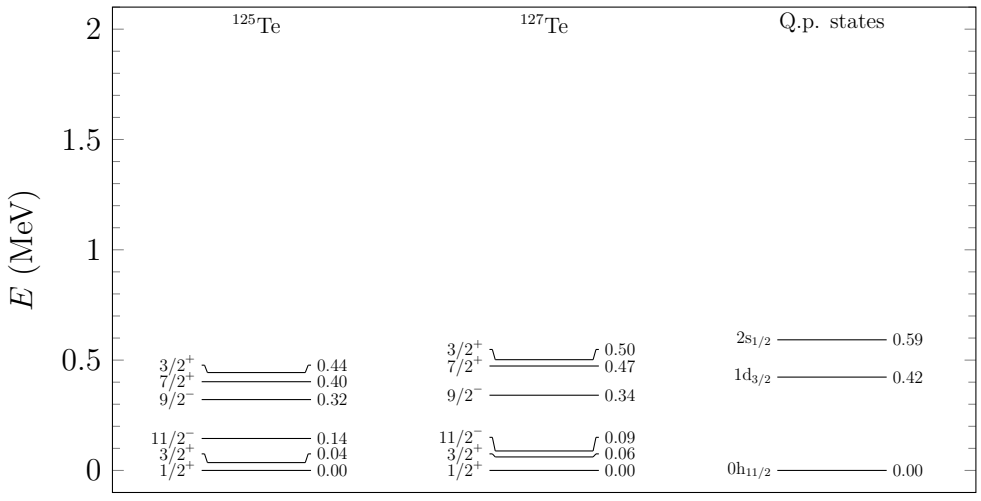

Figure 15. The five lowest states above ground state for both neutron-odd nuclei adjacent to ^{126}Te, along with the lowest (< 2 MeV) neutron quasiparticle states of ^{126}Te for comparison.

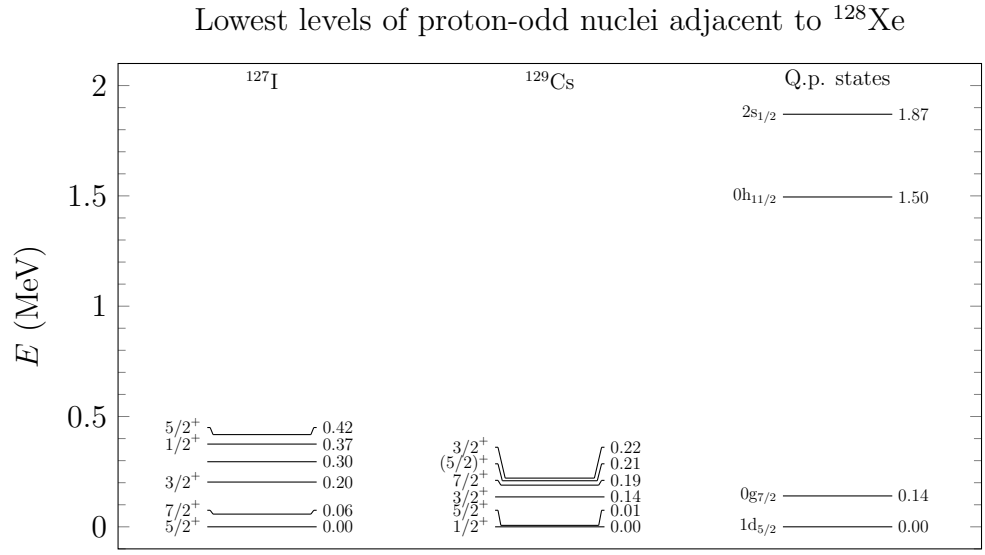

Figure 16. The five lowest states above ground state for both proton-odd nuclei adjacent to ^{128}Xe, along with the lowest (< 2 MeV) proton quasiparticle states of ^{128}Xe for comparison.

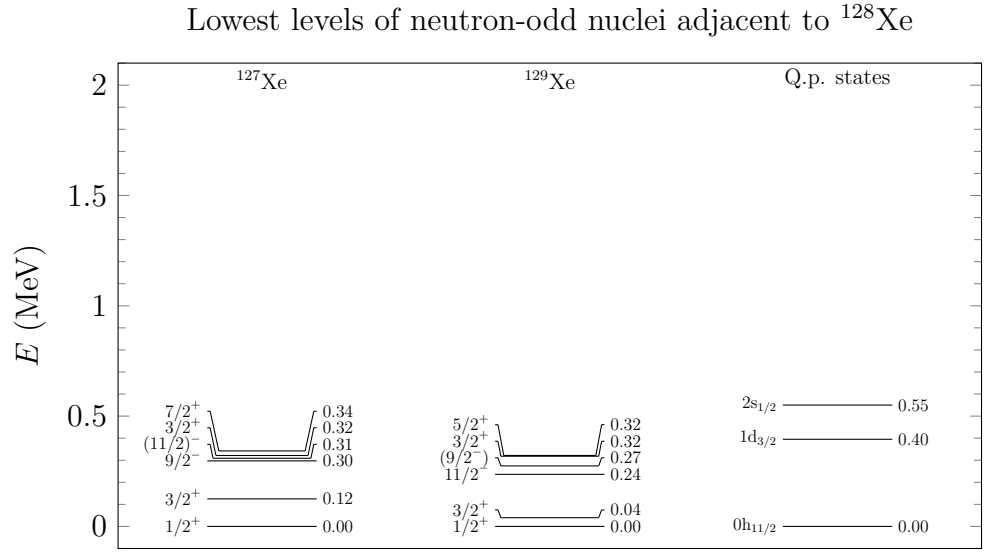

Figure 17. The five lowest states above ground state for both neutron-odd nuclei adjacent to ^{128}Xe, along with the lowest (< 2 MeV) neutron quasiparticle states of ^{128}Xe for comparison.

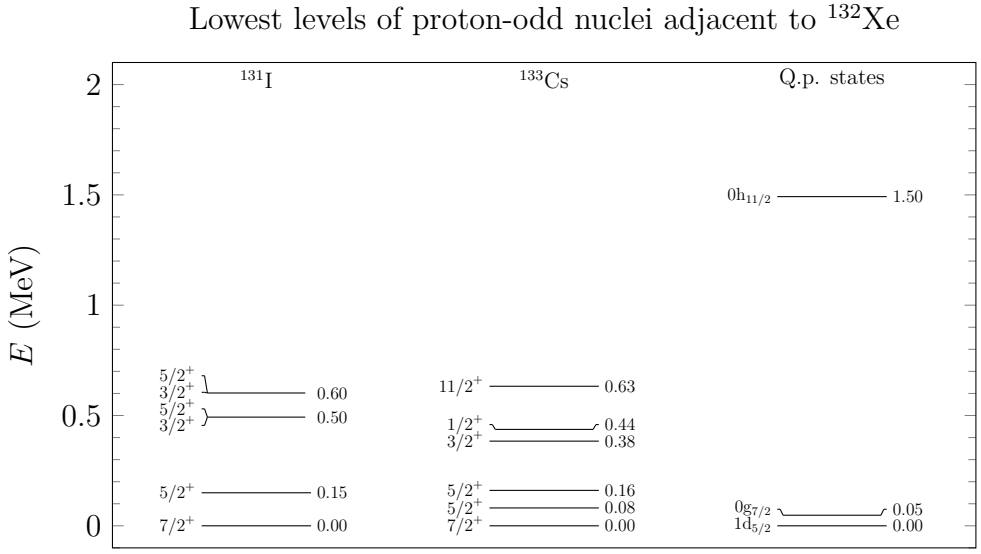

Figure 18. The five lowest states above ground state for both proton-odd nuclei adjacent to ^{132}Xe, along with the lowest (< 2 MeV) proton quasiparticle states of ^{132}Xe for comparison.

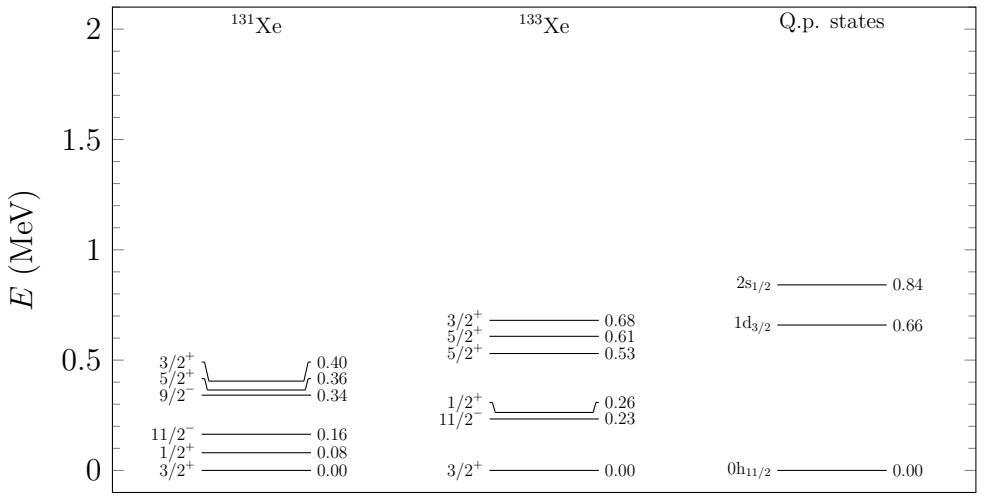

Figure 19. The five lowest states above ground state for both neutron-odd nuclei adjacent to ^{132}Xe, along with the lowest (< 2 MeV) neutron quasiparticle states of ^{132}Xe for comparison.

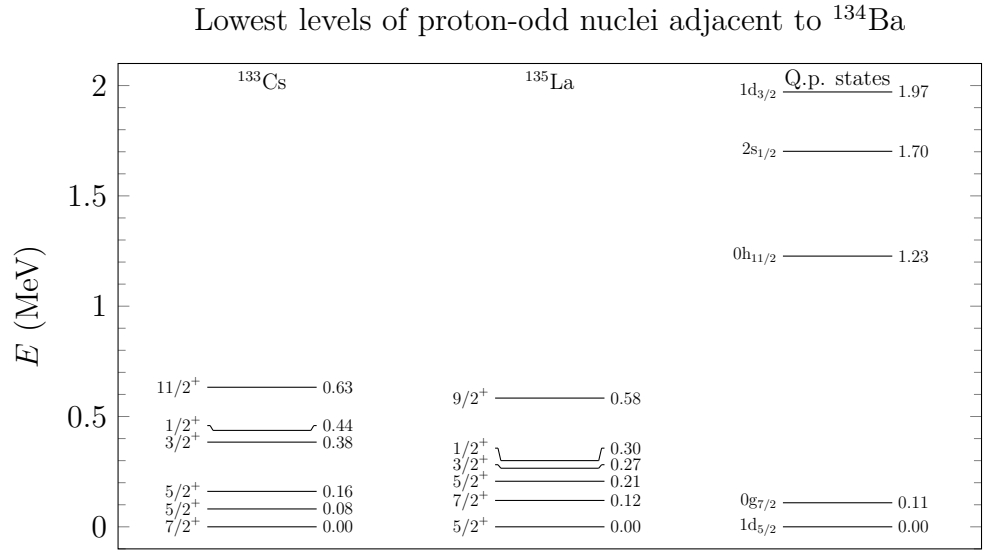

Figure 20. The five lowest states above ground state for both proton-odd nuclei adjacent to ^{134}Ba, along with the lowest (< 2 MeV) proton quasiparticle states of ^{134}Ba for comparison.

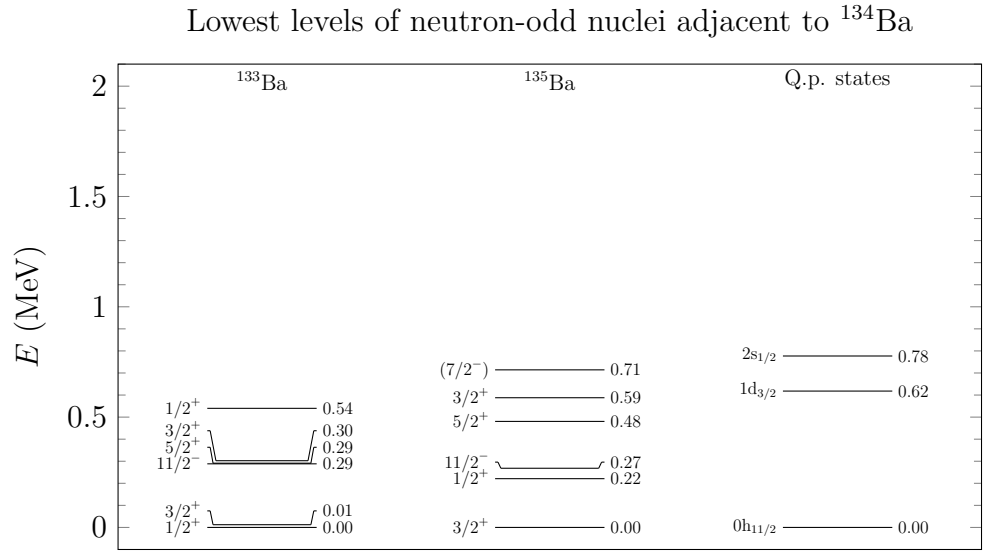

Figure 21. The five lowest states above ground state for both neutron-odd nuclei adjacent to ^{134}Ba, along with the lowest (< 2 MeV) neutron quasiparticle states of ^{134}Ba for comparison.

spectrum with more accurate low-lying states can be beneficial when analyzing the different contributions to the total cross section discussed at the end of this section. At the very least, it would be desirable for the theoretical spectrum of ^{133}Cs to reproduce the correct spin and parity for the ground state.

In general, the question of whether particular computed MQPM wave functions are suitable to use in neutrino scattering calculations is hard to answer based solely on the energy spectrum. In this thesis, the suitability of the MQPM states relied on the success of similar calculations in comparable mass ranges, and the acquired results for the scattering cross sections, which were in line with the results of other similar calculations. One way to actually test how well the wave functions perform, is to use them to compute $\log ft$ values of β-decay and compare these with experimental values[45]. This manner of extensive calculations were, however, not undertaken in this work as their inclusion would have added to the already time consuming numerical contents of this thesis, and done so without contributing to the discussion of its primary topics in a sufficiently meaningful way. They were thus considered an addition beyond the scope of this master's degree thesis that would be more appropriately included in a doctoral dissertation more exhaustive and extensive than this work.

The results for the energy averaged cross sections were found to be in line with results of similar calculations for nuclei comparable in mass to the ones examined in this thesis. The elastic cross sections dominated the corresponding inelastic cross sections as expected, and the results were relatively sensitive to the neutrino temperature. In the context of supernova neutrino detection, the results were promising in the sense that nothing outright indicated that the nuclei considered would be unfit for such use. Nevertheless, determination of the suitability of these nuclei for neutrino detection will require further studies into them. In this thesis we have focused solely on electron neutrinos and antineutrinos while ignoring neutrinos of other flavours. Investigations into the cross sections of μ- and τ-neutrino scatterings are thus one priority in a possible follow-up study on the matter.

Another aspect to consider in the future is the effect of different contributions to the total cross section. Analysis of the individual contributions from different multipole channels together with knowledge of the distribution of the theoretical final nuclear states can be used to interpret the effect of a scattering on the nucleus as a transition in the quasiparticle picture between states with definite

quasiparticle-phonon configurations, which can be illuminating when discussing the nuclear structure in scattering reactions. The contributions to these multipole channels from terms with different tensorial character (vector, axial-vector, interference) are also of interest. The distribution of final nuclear states is also important as it determines the profile of the decay radiation, which can be detected to indirectly detect neutrino-nucleus scattering.

Finally, we have only considered weak neutral current reactions in this work. For a truly exhaustive study of the nuclei considered here, weak charged current processes need to be examined as well. They provide methods of detecting neutrino-nucleus scattering reactions that are unavailable for neutral current processes, such as the possibility of measuring the accumulation of species of nuclei neighbouring the nuclei used in detectors as a result of the transmutation of elements in charged current reactions[8]. When only the number of scattering reactions is of interest, this manner of detecting apparatus has the benefit that instead of actively monitoring for decay products of highly excited nuclear states, the amount of accrued elements can be checked over longer periods of time.

In conclusion, the study of the nuclei ^{127}I and ^{133}Cs presented in this thesis provides a preliminary look into their suitability in detecting supernova neutrinos. The results that were obtained can function as a reference frame for future studies into other nuclei with similar mass numbers and as inputs for supernova simulations, but they do not conclusively settle the question of the viability of using them in neutrino detectors. While there are a number of additional aspects related to the nuclei that need to be covered in the future to accurately gauge whether they would perform adequately in this role, the key results presented in this work seem to suggest that these sort of studies could be worthwhile.

[8]It should be noted that weak neutral current reactions can also lead to transmutation of elements, as high energy neutrinos can excite nuclei into states well above their proton and neutron separation energies, which can then decay by particle emission.

Appendix A: Conventions and parameter values

The following conventions were adopted throughout this thesis unless stated otherwise. The fundamental constants were chosen so that

$$\hbar = c = k_B = 1.$$

For the metric tensor $g^{\mu\nu}$ and four-vectors a^μ we have

$$g^{\mu\nu} = g_{\mu\nu} \equiv \mathrm{diag}(1, -1, -1, -1), \quad a^\mu \equiv \begin{pmatrix} a_0 \\ \boldsymbol{a} \end{pmatrix}, \qquad a_\mu \equiv (a_0, -\boldsymbol{a}) \quad a_\mu = g_{\mu\nu} a^\nu.$$

For arbitrary four-vectors a^μ and b^μ we have

$$a \cdot b = a_\mu b^\mu = g_{\mu\nu} a^\nu b^\mu = g^{\mu\nu} a_\mu b_\nu = a^0 b^0 - \boldsymbol{a} \cdot \boldsymbol{b}. \tag{325}$$

The gamma matrices γ^μ were defined in terms of the Pauli matrices σ^i ($i \in \{1,2,3\}$) by

$$\gamma^0 \equiv \begin{pmatrix} \mathbb{1}_2 & 0 \\ 0 & -\mathbb{1}_2 \end{pmatrix}, \quad \gamma^i \equiv \begin{pmatrix} 0 & \sigma^i \\ -\sigma^i & 0 \end{pmatrix},$$

which were in turn used to define the quantities

$$\gamma_5 = \gamma^5 \equiv i\gamma^0\gamma^1\gamma^2\gamma^3, \quad \sigma^{\mu\nu} \equiv \frac{i}{2}\left[\gamma^\mu, \gamma^\nu\right], \quad \overline{\psi} \equiv \psi^\dagger \gamma^0, \quad \not{a} \equiv \gamma^\mu a_\mu.$$

In section 2.2.1 we introduced the Woods-Saxon potential along with the parameters $V_0^{(WS)}$, R and a which fully characterize it. For a nucleus of nucleon numbers Z and N and mass number A, the values of these parameters that were used in this thesis were determined by equations

$$R = r_0 A^{1/3}, \quad r_0 = 1.27 \text{ fm}, \quad a = 0.67 \text{ fm}, \quad V_0^{(WS)} = \left(51 \pm 33\frac{N-Z}{A}\right) \text{MeV},$$

Table 5. The values of the parameters used in calculating Sachs electric and magnetic form factors.

i	$a^{\mathrm{M}}_{p,i}$	$b^{\mathrm{M}}_{p,i}$	$a^{\mathrm{M}}_{n,i}$	$b^{\mathrm{M}}_{n,i}$	$a^{\mathrm{E}}_{p,i}$	$b^{\mathrm{E}}_{p,i}$
1	1.09	12.31	8.28	21.30	-0.19	11.12
2	-	25.57	-	77	-	15.16
3	-	30.61	-	238	-	21.25

Table 6. The phenomenological scaling parameters used in the BCS calculations in this thesis.

Parameter	^{126}Te	^{128}Xe	^{132}Xe	^{134}Ba
gpairp	0.8793	0.9114	0.8627	0.8990
gpairn	0.9915	0.9648	0.9710	0.9640

where in the last equality the $+(-)$ sign is used for protons (neutrons). For the parameter $V_0^{(SO)}$ of the spin-orbit part of the single-particle potential, we used

$$\frac{V_0^{(SO)}}{V_0^{(WS)}} = 0.44 \Leftrightarrow V_0^{(SO)} = 0.44 V_0^{(WS)}.$$

In the following we list the values of the parameters that were used to determine the values of Sachs electric and magnetic form factors discussed in section 3.1. These have been presented in table 5. The adopted parametrization is that of reference [31]. We also list here the phenomenological parameters of the BCS and QRPA calculations that were used to fit theoretical observables to experimentally determined values. The BCS parameters have been presented in table 6 and the QRPA parameters in table 7 for states of natural parity (even J, positive parity and odd J, negative parity) and table 8 for states of unnatural parity (even J, negative parity and odd J, positive parity). The QRPA parameters are used to scale the two-body matrix elements in the QRPA equations for the particle-particle (gpp) and particle-hole (gph) channels, which can be, and usually is, done separately for different multipoles, which is exactly what was done in the QRPA calculations in this thesis.

Table 7. The phenomenological renormalization parameters used for the states of natural parity in the QRPA calculations in this thesis.

Nucleus	Parameter	0^+	1^-	2^+	3^-	4^+	5^-	6^+
^{126}Te	gpp	0.6916	1.0	1.0	1.0	1.0	1.0	1.0
	gph	0.3476	0.5	0.5578	0.6410	0.4880	0.8753	0.9304
^{128}Xe	gpp	0.7971	1.0	1.0	1.0	1.0	1.0	1.0
	gph	0.2976	0.5	0.5269	0.6303	0.6525	0.7911	0.9343
^{132}Xe	gpp	0.6520	1.0	1.0	1.0	1.0	1.0	1.0
	gph	0.3191	0.5	0.5329	0.6139	0.4328	0.9324	0.3600
^{134}Ba	gpp	0.7333	1.0	1.0	1.0	1.0	1.0	1.0
	gph	0.3051	0.5	0.5229	0.6143	0.4691	0.8948	0.4580

Table 8. The phenomenological renormalization parameters used for the states of unnatural parity in the QRPA calculations in this thesis.

Nucleus	Parameter	0^-	1^+	2^-	3^+	4^-	5^+	6^-
^{126}Te	gpp	1.0	1.0	1.0	1.0	1.0	1.0	1.0
	gph	1.0	1.0	1.0	1.0	1.0	1.0	1.0
^{128}Xe	gpp	1.0	1.0	1.0	1.0	1.0	1.0	1.0
	gph	1.0	1.0	1.0	1.0	1.0	1.0	1.0
^{132}Xe	gpp	1.0	1.0	1.0	1.0	1.0	1.0	1.0
	gph	1.0	1.0	1.0	1.0	1.0	1.0	1.0
^{134}Ba	gpp	1.0	1.0	1.0	1.0	1.0	1.0	1.0
	gph	1.0	1.0	1.0	1.0	1.0	1.0	1.0

Appendix B: Gamma matrix identities and trace theorems

Some of the following trace theorems and properties of the γ-matrices[29] were used in the derivation of certain quantities in section 2.1. They can also be used to derive the quantities that were not explicitly derived in said section.

$$\{\gamma^\mu,\gamma^\nu\} = 2g^{\mu\nu}, \quad \gamma_\mu\gamma^\mu = 4, \quad \overline{\gamma^\mu} = \gamma^\mu, \quad \overline{\sigma^{\mu\nu}} = \sigma^{\mu\nu}, \quad \overline{i\gamma^5} = i\gamma^5, \quad \gamma_\mu \not{a} \gamma^\mu = -2\not{a},$$
$$\gamma_\mu \not{a}\not{b}\gamma^\mu = 4a\cdot b, \quad \gamma_\mu \not{a}\not{b}\not{c}\gamma^\mu = -2\not{c}\not{b}\not{a}, \quad \gamma_\mu \not{a}\not{b}\not{c}\not{d}\gamma^\mu = 2\left(\not{d}\not{a}\not{b}\not{c} + \not{c}\not{b}\not{a}\not{d}\right),$$
$$\not{a}\not{b} = a\cdot b - i\sigma_{\mu\nu}a^\mu b^\nu.$$

For odd $n \in \mathbb{N}$

$$\mathrm{Tr}\not{a}_1\cdots\not{a}_n = 0, \quad \mathrm{Tr}\not{a}_1\cdots\not{a}_{2n} = \mathrm{Tr}\not{a}_{2n}\cdots\not{a}_1, \quad \mathrm{Tr}1 = 4, \quad \mathrm{Tr}\not{a}\not{b} = 4a\cdot b, \quad \mathrm{Tr}\gamma_5 = 0,$$
$$\mathrm{Tr}\gamma_5\not{a}\not{b} = 0, \quad \mathrm{Tr}\not{a}_1\not{a}_2\not{a}_3\not{a}_4 = 4\left(a_1\cdot a_2 a_3\cdot a_4 + a_1\cdot a_4 a_2\cdot a_3 - a_1\cdot a_3 a_2\cdot a_4\right),$$
$$\mathrm{Tr}\gamma_5\not{a}\not{b}\not{c}\not{d} = 4i\epsilon_{\alpha\beta\gamma\delta}a^\alpha b^\beta c^\gamma d^\delta.$$

There were also a number of additional trace theorems that can be found here[15, section 12.4]. It is worth noting that these are not presented in the standard conventions adopted in this thesis. For changing between different conventions, we refer to[11, Appendix D].

Appendix C: MQPM matrices and reduced neutral-current one-body transition densities for proton-odd nuclei

In this appendix we present the MQPM submatrices A, B, A' and N. We rely mostly on references[8, 53] for these explicit expressions. To express the matrices in a convenient manner, we adopt the notation

$$\overline{X}^{\omega}_{aa'} \equiv \begin{cases} X^{\omega}_{aa'} & \text{when } a < a', \\ 2X^{\omega}_{aa'} & \text{when } a = a', \\ (-1)^{j_a + j_{a'} + J_\omega} X^{\omega}_{a'a} & \text{when } a > a'. \end{cases} \tag{326}$$

We define the quantity $\overline{Y}^{\omega}_{aa'}$ in a similar manner. By working backwards in the MQPM derivation, we expand the MQPM equations

$$\langle \text{BCS} | \left\{ a_{njm}, \hat{H}, \Gamma^{\dagger}_{i}(jm) \right\} | \text{BCS} \rangle = \Omega_i \langle \text{BCS} | \left\{ a_{njm}, \Gamma^{\dagger}_{i}(jm) \right\} | \text{BCS} \rangle \tag{327}$$

and

$$\langle \text{BCS} | \left\{ \left[a^{\dagger}_{a} Q^{\dagger}_{\omega} \right]^{\dagger}_{jm}, \hat{H}, \Gamma^{\dagger}_{i}(jm) \right\} | \text{BCS} \rangle = \langle \text{BCS} | \left\{ \left[a^{\dagger}_{a} Q^{\dagger}_{\omega} \right]^{\dagger}_{jm}, \Gamma^{\dagger}_{i}(jm) \right\} | \text{BCS} \rangle , \tag{328}$$

which arise from the EoM treatment of the MQPM basic excitations, using equation 243 (keeping only terms proportional to $|X^{\omega}_{aa'}|^2$ and $|Y^{\omega}_{aa'}|^2$), to get the expressions

$$A(aa'; j) = \langle \text{BCS} | \left\{ a_a, \hat{H}, a^{\dagger}_{a'} \right\} | \text{BCS} \rangle , \tag{329}$$

$$A'(\omega a \omega' a'; j) = \langle \text{BCS} | \left\{ \left[a^{\dagger}_{a} Q^{\dagger}_{\omega} \right]^{\dagger}_{j}, \hat{H}, \left[a^{\dagger}_{a'} Q^{\dagger}_{\omega'} \right]_{j} \right\} | \text{BCS} \rangle \tag{330}$$

$$B(\omega a a'; j) = \langle \text{BCS} | \left\{ \left[a_a Q_{\omega} \right]_{j}, \hat{H}, a^{\dagger}_{a'} \right\} | \text{BCS} \rangle \tag{331}$$

and

$$N(\omega a\omega' a';j)=\langle \mathrm{BCS}|\left\{\left[a_a^\dagger Q_\omega^\dagger\right]_j^\dagger,\left[a_{a'}^\dagger Q_{\omega'}^\dagger\right]_j\right\}|\mathrm{BCS}\rangle \tag{332}$$

where we have suppressed the quantum number m. For the first one we have the simple identity

$$\langle \mathrm{BCS}|\left\{a_a,\hat{H},a_{a'}^\dagger\right\}|\mathrm{BCS}\rangle = E_a\delta_{aa'}. \tag{333}$$

We can express the fourth one in terms of the matrix

$$K(\omega a\omega' a';j)=\hat{J}_\omega\hat{J}_{\omega'}\sum_b\left[\begin{Bmatrix} j_{a'} & j_b & J_\omega \\ j_{a'} & j & J_{\omega'}\end{Bmatrix}\overline{X}_{ba'}^{\omega}\overline{X}_{ba}^{\omega'}-\frac{\delta_{jj_b}}{\hat{j}^2}\overline{Y}_{ba}^{\omega}\overline{Y}_{ba'}^{\omega'}\right](\sigma_{ba}\sigma_{ba'})^{-1} \tag{334}$$

as

$$N(\omega a\omega' a';j)=\delta_{\omega\omega'}\delta_{aa'}+K(\omega a\omega' a';j), \tag{335}$$

which can in turn be used to express the second one as

$$\begin{aligned}&\langle \mathrm{BCS}|\left\{\left[a_a^\dagger Q_\omega^\dagger\right]_j^\dagger,\hat{H},\left[a_{a'}^\dagger Q_{\omega'}^\dagger\right]_j\right\}|\mathrm{BCS}\rangle=\frac{1}{2}\left(\Omega_\omega+E_a+\Omega_{\omega'}+E_{a'}\right)N(\omega a\omega' a';j)-\\&\frac{1}{2}\hat{J}_\omega\hat{J}_{\omega'}\sum_b\begin{Bmatrix} j_{a'} & j_b & J_\omega \\ j_{a'} & j & J_{\omega'}\end{Bmatrix}\left(\Omega_\omega+E_a+\Omega_{\omega'}+E_{a'}-2E_b\right)\overline{X}_{ba'}^{\omega}\overline{X}_{ba}^{\omega'}(\sigma_{ba}\sigma_{ba'})^{-1}-\\&\frac{1}{2}\hat{J}_\omega\hat{J}_{\omega'}\sum_b\frac{\delta_{jj_b}}{\hat{j}^2}\left(\Omega_\omega+E_a+\Omega_{\omega'}+E_{a'}+2E_b\right)\overline{Y}_{ba}^{\omega}\overline{Y}_{ba'}^{\omega'}(\sigma_{ba}\sigma_{ba'})^{-1}.\end{aligned} \tag{336}$$

For the third one, we have (with $j=j_{a'}$)

$$\begin{aligned}&\langle \mathrm{BCS}|\left\{\left[a_a Q_\omega\right]_j,\hat{H},a_{a'}^\dagger\right\}|\mathrm{BCS}\rangle=\frac{1}{3}\frac{\hat{J}_\omega}{\hat{j}_{a'}}\Bigg[\sum_{b\le b'}H_{\mathrm{pp}}(bb'aa'J_\omega)\left(u_bu_{b'}X_{bb'}^{\omega}-v_bv_{b'}Y_{bb'}^{\omega}\right)\sigma_{bb'}^{-1}\\&-\sum_{b\le b'}H_{\mathrm{hh}}(bb'aa'J_\omega)\left(v_bv_{b'}X_{bb'}^{\omega}-u_bu_{b'}Y_{bb'}^{\omega}\right)+\sum_{b\le b'}H_{\mathrm{ph}}(bb'aa'J_\omega)\left(u_bv_{b'}X_{bb'}^{\omega}-v_bu_{b'}Y_{bb'}^{\omega}\right)\\&-\sum_{b\le b'}H_{\mathrm{hp}}(bb'aa'J_\omega)\left(v_bu_{b'}X_{bb'}^{\omega}-u_bv_{b'}Y_{bb'}^{\omega}\right)\Bigg],\end{aligned} \tag{337}$$

where

$$H_{\mathrm{pp}}(bb'aa'J_\omega)=2v_bu_{b'}G(bb'aa'J_\omega),\quad H_{\mathrm{hh}}(bb'aa'J_\omega)=2u_bv_{b'}G(bb'aa'J_\omega), \tag{338}$$

$$H_{\rm ph}(bb'aa'J_\omega) = 2v_bv_{b'}F(bb'aa'J_\omega) + 2u_bu_{b'}F(b'baa'J_\omega)(-1)^{j_b+j_{b'}+J_\omega} \tag{339}$$

and

$$H_{\rm hp}(bb'aa'J_\omega) = 2u_bu_{b'}F(bb'aa'J_\omega) + 2v_bv_{b'}F(b'baa'J_\omega)(-1)^{j_b+j_{b'}+J_\omega}. \tag{340}$$

In the above expressions, the quantities

$$G(bb'aa'J_\omega) = -\frac{1}{2}\left[\mathcal{N}_{bb'}(J_\omega)\mathcal{N}_{aa'}(J_\omega)\right]^{-1}\langle bb';J_\omega|V|aa';J_\omega\rangle \tag{341}$$

and

$$F(b'baa'J_\omega) = -\frac{1}{2}\langle bb'^{-1};J_\omega|V_{\rm RES}|aa'^{-1};J_\omega\rangle \tag{342}$$

are the Baranger two-body matrix elements.

In the context of neutrino scattering off nuclei, the most interesting quantities derived from the nuclear model are the reduced one-body transition densities. We therefore present them here for the MQPM in the case of neutral current reactions involving proton-odd nuclei. These are taken directly from[53] with minor alterations. In the following we adopt the labels p and n to denote the two species of nucleons, and a and b to denote both species generally with the requirement, that in each expression the labels a and b denote a nucleon of the same species. With this in mind, we also define

$$\sigma_{ab} \equiv \sqrt{1+\delta_{ab}}. \tag{343}$$

In the MQPM, we have the cases of reduced one-body transition densities between two one-quasiparticle states, two quasiparticle-phonon states and between a one-quasiparticle state and a quasiparticle-phonon state. In the first case, we have

$$(n_f||\left[c_a^\dagger\tilde{c}_b\right]_\lambda||n_i) = \hat{\lambda}\left(u_au_b\delta_{an_f}\delta_{bn_i} + (-1)^{j_a+j_b-\lambda}v_av_b\delta_{an_i}\delta_{bn_f}\right). \tag{344}$$

In the last case we similarly have (with J_{ω_i} and J_{ω_f} denoting the angular momenta of the QRPA phonons)

$$(n_f||\left[c_n^\dagger\tilde{c}_{n'}\right]_\lambda||n_i\omega_i;J_i) = -\delta_{n_in_f}\delta_{\lambda J_{\omega_i}}(-1)^{j_{n_f}+J_i+\lambda}\hat{J}_i\sigma_{nn'}^{-1}\left(v_nu_{n'}\overline{X}^{\omega_i}_{nn'} + u_nv_{n'}\overline{Y}^{\omega_i}_{nn'}\right), \tag{345}$$

and

$$(n_f\omega_f; J_f||\left[c_n^\dagger \tilde{c}_{n'}\right]_\lambda ||n_i) = \delta_{n_i n_f}\delta_{\lambda J_{\omega_f}}\hat{J}_f\sigma^{-1}_{nn'}\left(u_n v_{n'}\overline{X}^{\omega_f}_{nn'} + v_n u_{n'}\overline{Y}^{\omega_f}_{nn'}\right), \tag{346}$$

for neutrons, and

$$\begin{aligned}(n_f||\left[c_p^\dagger \tilde{c}_{p'}\right]_\lambda ||n_i\omega_i; J_i) = (-1)^{j_{n_f}+J_i+\lambda+1}\hat{\lambda}\hat{J}_i\hat{J}_{\omega_i}\Bigg[\delta_{n_f n_i}\frac{\delta_{\lambda J_{\omega_i}}}{\hat{J}^2_{\omega_i}}\sigma^{-1}_{pp'}\Big(v_p u_{p'}\overline{X}^{\omega_i}_{pp'} + \\ u_p v_{p'}\overline{Y}^{\omega_i}_{pp'}\Big) + \left(\delta_{p'n_i}v_p u_{p'}\begin{Bmatrix} j_{n_f} & \lambda & J_i \\ j_{p'} & J_{\omega_i} & j_p\end{Bmatrix}\sigma^{-1}_{pn_f}\overline{X}^{\omega_i}_{pn_f} + \delta_{pn_f}\frac{\delta_{J_i j_{p'}}}{\hat{j}^2_{p'}}u_p v_{p'}\cdot \\ (-1)^{j_p+j_{p'}+\lambda}\sigma^{-1}_{p'n_i}\overline{Y}^{\omega_i}_{p'n_i}\right) - (-1)^{j_p+j_{p'}+\lambda}\Bigg(\delta_{pn_i}v_p u_{p'}\begin{Bmatrix} j_{n_f} & \lambda & J_i \\ j_p & J_{\omega_i} & j_{p'}\end{Bmatrix}\sigma^{-1}_{p'n_f}\overline{X}^{\omega_i}_{p'n_f} + \\ \delta_{p'n_f}\frac{\delta_{J_i j_p}}{\hat{j}^2_p}v_p u_{p'}(-1)^{j_p+j_{p'}+\lambda}\sigma^{-1}_{pn_i}\overline{Y}^{\omega_i}_{pn_i}\Bigg)\Bigg],\end{aligned} \tag{347}$$

and

$$\begin{aligned}(n_f\omega_f; J_f||\left[c_p^\dagger \tilde{c}_{p'}\right]_\lambda ||n_i) = \hat{\lambda}\hat{J}_f\hat{J}_{\omega_f}\Bigg[\delta_{n_f n_i}\frac{\delta_{\lambda J_{\omega_f}}}{\hat{J}^2_{\omega_f}}\sigma^{-1}_{pp'}\Big(u_p v_{p'}\overline{X}^{\omega_f}_{pp'} + v_p u_{p'}\overline{Y}^{\omega_f}_{pp'}\Big) + \\ \left(\delta_{p'n_f}u_p v_{p'}\begin{Bmatrix} J_f & \lambda & j_{n_i} \\ j_p & J_{\omega_f} & j_{p'}\end{Bmatrix}\sigma^{-1}_{pn_i}\overline{X}^{\omega_f}_{pn_i} + \delta_{pn_i}\frac{\delta_{J_f j_{p'}}}{\hat{j}^2_{p'}}v_p u_{p'}(-1)^{J_f+j_{n_i}+\lambda}\sigma^{-1}_{p'n_f}\overline{Y}^{\omega_f}_{p'n_f}\right) - \\ (-1)^{j_p+j_{p'}+\lambda}\Bigg(\delta_{pn_f}u_p v_{p'}\begin{Bmatrix} J_f & \lambda & j_{n_i} \\ j_{p'} & J_{\omega_f} & j_p\end{Bmatrix}\sigma^{-1}_{p'n_i}\overline{X}^{\omega_f}_{p'n_i} + \delta_{p'n_i}\frac{\delta_{J_f j_p}}{\hat{j}^2_p}v_p u_{p'}\cdot \\ (-1)^{j_{n_i}+J_f+\lambda}\sigma^{-1}_{pn_f}\overline{Y}^{\omega_f}_{pn_f}\Bigg)\Bigg]\end{aligned} \tag{348}$$

for protons. The second case can be expressed as

$$\begin{aligned}(n_f\omega_f; J_f||\left[c_a^\dagger \tilde{c}_b\right]_\lambda ||n_i\omega_i; J_i) = u_a u_b(n_f\omega_f; J_f||\left[a_a^\dagger \tilde{a}_b\right]_\lambda ||n_i\omega_i; J_i) + \\ (-1)^{j_a+j_b+\lambda}v_a v_b(n_f\omega_f; J_f||\left[a_b^\dagger \tilde{a}_a\right]_\lambda ||n_i\omega_i; J_i),\end{aligned} \tag{349}$$

where

$$(n_f\omega_f; J_f||\left[a_n^\dagger \tilde{a}_{n'}\right]_\lambda||n_i\omega_i; J_i) = \delta_{n_f n_i}\hat{\lambda}\hat{J}_{\omega_f}\hat{J}_{\omega_i}\hat{J}_f\hat{J}_i \begin{Bmatrix} \hat{J}_f & \lambda & \hat{J}_i \\ J_{\omega_i} & j_{n_f} & J_{\omega_f} \end{Bmatrix} \cdot$$
$$\sum_{b'}(-1)^{J_f+j_{n_f}+j_n+j_{b'}}\sigma^{-1}_{nb'}\sigma^{-1}_{n'b'}\Bigg(\begin{Bmatrix} J_{\omega_f} & \lambda & J_{\omega_i} \\ j_{n'} & j_{b'} & j_n \end{Bmatrix} \overline{X}^{\omega_f}_{nb'}\overline{X}^{\omega_i}_{n'b'} + \tag{350}$$
$$(-1)^\lambda \begin{Bmatrix} J_{\omega_f} & \lambda & J_{\omega_i} \\ j_n & j_{b'} & j_{n'} \end{Bmatrix} \overline{Y}^{\omega_f}_{n'b'}\overline{Y}^{\omega_i}_{nb'}\Bigg)$$

and

$$(n_f\omega_f; J_f||\left[a_p^\dagger \tilde{a}_{p'}\right]_\lambda||n_i\omega_i; J_i) = \hat{\lambda}\hat{J}_{\omega_f}\hat{J}_{\omega_i}\hat{J}_f\hat{J}_i\Bigg[\delta_{p'n_i}(-1)^{j_{n_f}+J_{\omega_f}+J_i+\lambda}\cdot$$
$$\begin{Bmatrix} J_i & J_f & \lambda \\ j_p & j_{p'} & J_{\omega_i} \end{Bmatrix}\sum_{b'}\sigma^{-1}_{pb'}\sigma^{-1}_{n_f b'}\Bigg(\begin{Bmatrix} J_f & J_{\omega_i} & j_p \\ j_{b'} & J_{\omega_f} & j_{n_f} \end{Bmatrix} \overline{X}^{\omega_f}_{pb'}\overline{X}^{\omega_i}_{n_f b'} - \frac{\delta_{j_{b'}J_f}}{\hat{j}^2_{b'}}\overline{Y}^{\omega_i}_{pb'}\overline{Y}^{\omega_f}_{n_f b'}\Bigg) -$$
$$\delta_{pn_f}(-1)^{J_{\omega_i}+j_{n_i}+j_p+j_{p'}+J_i+\lambda} \begin{Bmatrix} J_i & J_f & \lambda \\ j_p & j_{p'} & J_{\omega_f} \end{Bmatrix}\sum_{b'}\sigma^{-1}_{n_i b'}\sigma^{-1}_{p'b'}\Bigg(\begin{Bmatrix} J_i & J_{\omega_f} & j_{p'} \\ j_{b'} & J_{\omega_i} & j_{n_i} \end{Bmatrix} \overline{X}^{\omega_f}_{n_i b'}\overline{X}^{\omega_i}_{p'b'}$$
$$- \frac{\delta_{j_{b'}J_i}}{\hat{j}^2_{b'}}\overline{Y}^{\omega_i}_{pb'}\overline{Y}^{\omega_f}_{p'b'}\Bigg) + \delta_{n_i n_f} \begin{Bmatrix} \lambda & J_f & J_i \\ j_{n_f} & J_{\omega_i} & J_{\omega_f} \end{Bmatrix}\sum_{b'}(-1)^{j_p+j_{b'}+j_{n_f}+J_f}\sigma^{-1}_{pb'}\sigma^{-1}_{p'b'}\Bigg($$
$$\begin{Bmatrix} J_{\omega_f} & J_{\omega_i} & \lambda \\ j_{p'} & j_p & j_{b'} \end{Bmatrix}\overline{X}^{\omega_f}_{pb'}\overline{X}^{\omega_i}_{p'b'} + (-1)^\lambda \begin{Bmatrix} J_{\omega_i} & J_{\omega_f} & \lambda \\ j_{p'} & j_p & j_{b'} \end{Bmatrix}\overline{Y}^{\omega_i}_{pb'}\overline{Y}^{\omega_f}_{p'b'}\Bigg) + \sigma^{-1}_{pn_i}\sigma^{-1}_{p'n_f}\Bigg($$
$$(-1)^{J_{\omega_f}+J_{\omega_i}+j_{p'}+\lambda} \begin{Bmatrix} j_p & j_{n_i} & J_{\omega_f} \\ j_{p'} & J_{\omega_i} & j_{n_f} \\ \lambda & J_i & J_f \end{Bmatrix}\overline{X}^{\omega_f}_{pn_i}\overline{X}^{\omega_i}_{p'n_f} + (-1)^{j_p+J_f+\lambda}\frac{\delta_{j_{p'}J_f}\delta_{j_pJ_i}}{\hat{j}^2_{p'}\hat{j}^2_p}\overline{Y}^{\omega_i}_{pn_i}\overline{Y}^{\omega_f}_{p'n_f}\Bigg)\Bigg]$$
$$+ \delta_{pn_f}\delta_{p'n_i}\delta_{\omega_f\omega_i}\hat{J}_f\hat{J}_i\hat{\lambda}(-1)^{j_p+J_i+J_{\omega_f}+\lambda} \begin{Bmatrix} J_i & J_f & \lambda \\ j_p & j_{p'} & J_{\omega_f}. \end{Bmatrix}$$
(351)

The equations above hold when the initial and final states i and f are not the same. When $i = f$, equations 344, 345, 346, 347, 348 and 349 need to be modified by adding a term of $\delta_{ab}\delta_{\lambda 0}v_a^2\hat{j}_a\hat{J}_i$.

References

[1] C. Iliadis. *Nuclear Physics of the Stars*. Second, Revised and Enlarged Edition. Wiley-VCH, 2015.

[2] D. Clark and F. Stephenson. "The Historical Supernovae". In: *NATO Advanced Science Institutes (ASI) Series C*. Ed. by M. J. Rees and R. J. Stoneham. Vol. 90. NATO Advanced Science Institutes (ASI) Series C. Nov. 1982, pp. 355–370.

[3] K. Krane. *Introductory Nuclear Physics*. Wiley, 1987.

[4] S. Mertens. "Direct Neutrino Mass Experiments". In: *Journal of Physics: Conference Series* 718 (May 2016). ISSN: 1742-6596.

[5] K. Abe et al. *Constraint on the Matter-Antimatter Symmetry-Violating Phase in Neutrino Oscillations*. 2019. arXiv: 1910.03887 [hep-ex].

[6] E. Majorana and L. Maiani. "A symmetric theory of electrons and positrons". In: *Ettore Majorana Scientific Papers: On occasion of the centenary of his birth*. Ed. by G. F. Bassani. Berlin, Heidelberg: Springer Berlin Heidelberg, 2006, pp. 201–233. ISBN: 978-3-540-48095-2.

[7] A. G. Rosso et al. *Introduction to neutrino astronomy*. 2018. arXiv: 1806.06339 [astro-ph.HE].

[8] J. Suhonen and J. Toivanen. In: *Phys. Rev. C* 57 (1998), pp. 1237–1246.

[9] R. Broglia and V. Zelevinsky. *Fifty Years of Nuclear BCS: Pairing in Finite Systems*. World Scientific, 2013.

[10] J. Suhonen. *From Nucleons to Nucleus: Concepts of Microscopic Nuclear Theory*. Springer, 2007.

[11] J. Walecka. *Theoretical Nuclear and Subnuclear Physics*. Second Edition. Imperial College Press, World Scientific Publishing, 2004.

[12] Y. Nagashima. *Elementary Particle Physics, Volume 2: Foundations of the Standard Model*. Wiley-VCH, 2013.

[13] J. Sakurai and J. Napolitano. *Modern Quantum Mechanics*. Second Edition. Cambridge University Press, 2017.

[14] D. Tong. *Statistical Physics*. University of Cambridge Part II Mathematical Tripos. Lent Term, 2011 and 2012. 2011.

[15] F. Halzen and A. Martin. *Quarks and Leptons: An Introductory Course in Modern Particle Physics*. Wiley, 1984.

[16] R. Mehrem. *The Plane Wave Expansion, Infinite Integrals and Identities involving Spherical Bessel Functions*. 2009. arXiv: 0909.0494 [math-ph].

[17] D. Griffiths. *Introduction to Quantum Mechanics*. First Edition. Prentice Hall, 1994.

[18] M. Abramowitz and I. Stegun. *Handbook of Mathematical Functions with Formulas, Graphs, and Mathematical Tables*. Tenth Printing. National Bureau of Standards, 1972.

[19] V. Krainov, H. Reiss, and B. Smirnov. *Radiative Processes in Atomic Physics*. Wiley, 1997.

[20] A. Edmonds. *Angular Momentum in Quantum Mechanics*. Princeton University Press, 1957.

[21] T. Donnelly and R. Peccei. In: *Phys. Rep.* 50.1 (1979), pp. 1–85.

[22] J. Conway. *Functions of One Complex Variable*. Second Edition. Graduate Texts in Mathematics. Springer-Verlag, 1978.

[23] M. Reiher and A. Wolf. *Relativistic Quantum Chemistry: The Fundamental Theory of Molecular Science*. Wiley-VCH, 2009.

[24] E. Ydrefors et al. "Nuclear responses to supernova neutrinos for the stable molybdenum isotopes". In: *Neutrinos: Properties, Sources and Detection* (Jan. 2011), pp. 151–175.

[25] M. Baranger. In: *Phys. Rev.* 120 (1960), pp. 957–968.

[26] R. D. Woods and D. S. Saxon. "Diffuse Surface Optical Model for Nucleon-Nuclei Scattering". In: *Physical Review* 95 (July 1954), pp. 577–578. DOI: 10.1103/PhysRev.95.577.

[27] P. Ring and P. Schuck. *The Nuclear Many-Body Problem*. Study Edition. Springer, 2004.

[28] R. Adams and C. Essex. *Calculus: A Complete Course*. Eighth Edition. Pearson, 2013.

[29] J. Bjorken and S. Drell. *Relativistic Quantum Mechanics*. McGraw-Hill Book Company, 1964.

[30] W. Alberico, S. Bilenky, and C. Maieron. In: *Phys. Rep.* 358 (2002), pp. 227–308.

[31] W. Alberico et al. In: *Phys. Rev. C* 79 (2009), p. 065204.

[32] H. Budd, A. Bodek, and J. Arrington. *Modeling quasi-elastic form factors for electron and neutrino scattering*. 2003. arXiv: `hep-ex/0308005 [hep-ex]`.

[33] K. Holinde. In: *Phys. Rep.* 68 (1981), pp. 121–188.

[34] J. Katakura. In: *Nucl. Data Sheets* 112 (2011), pp. 495–854.

[35] J. Katakura and K. Kitao. In: *Nucl. Data Sheets* 97 (2002), pp. 765–926.

[36] A. Hashizume. In: *Nucl. Data Sheets* 112 (2011), pp. 1647–1831.

[37] Z. Elekes and J. Timar. In: *Nucl. Data Sheets* 129 (2005), pp. 191–436.

[38] J. Timar, Z. Elekes, and B. Singh. In: *Nucl. Data Sheets* 121 (2014), pp. 143–394.

[39] Y. Khazov, I. Mitropolsky, and A. Rodionov. In: *Nucl. Data Sheets* 107 (2006), pp. 2715–2930.

[40] Y. Khazov et al. In: *Nucl. Data Sheets* 104 (2005), pp. 497–790.

[41] Y. Khazov, A. Rodionov, and F. Kondev. In: *Nucl. Data Sheets* 112 (2011), pp. 855–1113.

[42] A. Sonzogni. In: *Nucl. Data Sheets* 103 (2004), pp. 1–182.

[43] B. Singh, A. Rodionov, and Y. Khazov. In: *Nucl. Data Sheets* 109 (2008), pp. 517–698.

[44] W. Almosly et al. In: *J. Phys. G: Nucl. Part. Phys.* 40 (2013), p. 095201.

[45] P. Pirinen. "Spin structure of the nucleon in the asymptotic limit". Master's thesis. University of Jyväskylä, Department of Physics, Oct. 2014.

[46] H. Janka and W. Hillebrandt. "Monte Carlo simulations of neutrino transport in type II supernovae." In: *Astron. Astrophys.* 78 (June 1989), pp. 375–397.

[47] M. Keil, G. Raffelt, and H. Janka. "Monte Carlo Study of Supernova Neutrino Spectra Formation". In: *The Astrophysical Journal* 590 (June 2003), pp. 971–991. DOI: 10.1086/375130. URL: https://doi.org/10.1086%2F375130.

[48] E. Ydrefors et al. "Detailed study of the neutral-current neutrino–nucleus scattering off the stable Mo isotopes". In: *Nucl. Phys. A* 896 (2012), pp. 1–23. ISSN: 0375-9474. DOI: https://doi.org/10.1016/j.nuclphysa.2012.10.001.

[49] P. Pirinen, J. Suhonen, and E. Ydrefors. "Charged-current neutrino-nucleus scattering off Xe isotopes". In: *Phys. Rev. C* 99 (Jan. 2019), p. 014320. DOI: 10.1103/PhysRevC.99.014320.

[50] J. Kostensalo, J. Suhonen, and K. Zuber. "Shell-model computed cross sections for charged-current scattering of astrophysical neutrinos off ^{40}Ar". In: *Phys. Rev. C* 97 (Mar. 2018), p. 034309. DOI: 10.1103/PhysRevC.97.034309.

[51] National Institute of Standards and Technology. *NIST Digital Library of Mathematical Functions*. https://dlmf.nist.gov/. Released date: 15.06.2020 Accessed: 17.07.2020.

[52] P. Pirinen. "Theoretical predictions of wimp-nucleus and neutrino-nucleus scattering in context of dark matter direct detection". PhD thesis. University of Jyväskylä, Department of Physics, Dec. 2018.

[53] E. Ydrefors. "Supernova-Neutrino Induced Reactions on Molybdenum via Neutral-Currents". PhD thesis. University of Jyväskylä, Department of Physics, Mar. 2012.

[54] A. Bohr and B. Mottelson. *Nuclear Structure*. World Scientific, 1969.